CONTENTS

Slovak Academy of Sciences Bratislava
Institute of Physics

Dissertation Thesis

2007

Cyril Adamuščín

Department of Theoretical Physics
Institute of Physics
Slovak Academy of Sciences, Bratislava

Thesis

Deuteron Structure in View of New JLab Proton Polarization Data and Unitary and Analytic Approach

March, 2007

Mgr. Cyril Adamuščín
Supervisor: RNDr. Stanislav Dubnička, DrSc.

DECLARATION

No portion of the work referred to in this Dissertation has been submitted in support of an application for another degree or qualication of this or any other University or other Institution of learning.

Cyril Adamuščín
Institute of Physics
Slovak Academy of Sciences
Bratislava, Slovakia
March, 2007

ACKNOWLEDGEMENTS

There are lots of people I would like to thank for helping me to make this thesis possible.

First of all, I would like to thank Dr. Stanislav Dubnička for being a patient supervisor and for supporting this work with his knowledge, ideas and criticism. I thank my temporary supervisor Dr. Egle Tomasi-Gustafsson for her endless support in both scientific and technical problems during my stay in Saclay. My gratitude also goes to Prof. Eduard Alexeevich Kuraev and Dr. Gennadiy I. Gakh for numerous enlightening discussions related to my thesis.

Also I would like to thank my colleagues Erik, Roman, Michal, René and Ján for their technical support for LaTeX, C programming, Linux, etc. But mainly for their moral support during my PhD studies.

My thanks go to all my friends for a lot of fun and for being patient during my particle physics monologs.

I am forever indebted to my parents and brothers for their understanding, patience and encouragement when it was most required. Finally, the ultimate thank-you for everything mentioned here and mainly for the greatest gift – love go to my beloved wife Beáta.

INTRODUCTION

Any atomic nucleus, including deuteron, is a compound of the protons and the neutrons. So it is obvious, that they should have some internal electromagnetic structure. In the middle 50' of the last century such internal structure was discovered even in the proton and the neutron. In the time of Hofstadter's [1] discovery of this non-point-like structure of the proton, there was no theory to explain this phenomenon and as a result in Quantum Electrodynamics (QED) it is impossible to describe electromagnetic current of the proton. That was the reason why it was parametrized as a sum of products of linearly independent vector covariants (constructed from fourmomenta and spin parameters of incoming and outgoing proton) and scalar functions of one variable – momentum squared to be transferred by a virtual photon ($Q^2 = -t$). These scalar functions are called electromagnetic form factors and more precisely, together with other types like weak and strange form factors, are defined in the first Chapter of this work.

Currently we know the reason of the non-point-like nature of the proton. It is (similarly to the nuclei) a compound of the quarks, which cause the internal electromagnetic structure of the proton. Also any other hadron has an internal electromagnetic structure caused by its quark origin and it can be phenomenologically described by its electromagnetic form factors.

We expect, that the behavior of these form factors from $-\infty$ to $+\infty$ on real axis will be predicted by the theory of quark-gluon interactions (Quantum Chromodynamics - QCD). But this theory is able to predict only asymptotic behavior of form factors in space-like region [2, 3]. In the time-like region, where form factors of hadrons are complex functions and they have complicated resonance behavior, QCD doesn't give any predictions up to now. As a consequence of this imperfection of QCD, phenomenological description of form factors of hadrons is still needed. The most famous of phenomeno-

logical models is Vector meson dominance model (VMD) [4, 5], which assumes virtual photon to change (with certain probability) into neutral vector-meson (ρ^0, ω, ϕ and their excitations), which decays into hadron-antihadron pair.

But also VMD model has some limitations. It violates an unitarity condition, which implies, that the imaginary part of the form factor is different from zero starting from the lowest branch point, what can not be fulfilled within VMD model. It has wrong asymptotic behavior and in the resonance region it gives infinity values of form factors.

All these disadvantages of VMD model can be solved within unitary and analytic models fulfilling all known properties of form factors, which are one of the main tools for the solution of the problems solved in this Dissertation Thesis.

The experimental data on the electromagnetic form factors are usually obtained from measurement of the angular distribution of the differential cross section in the elastic scattering and annihilation experiments. However, recent observations show importance of another source of information on electromagnetic form factors – polarization observables, which can be measured in processes with polarized particles. As we will show the polarization observables give more precise information on electromagnetic form factors and in case of particles with higher spin, like the deuteron, they are essential. Therefore next two Chapters are devoted to a brief review of polarization observables generally and four-component formalism in an investigation of the polarization phenomena of an electron-positron annihilation process into nucleon-antinucleon pairs.

Following Chapters are dedicated to a formulation of the proton electric form factor space-like behavior puzzle and subsequently to its phenomenological solution by exploiting the nonrelativistic impulse approximation of deuteron electromagnetic form factors.

In another Chapter processes of the nucleon-antinucleon annihilation into pion, nucleon and pair of leptons are investigated with the aim on an obtaining behaviors of the nucleon electromagnetic form factors in the unphysical region. In order to predict a behavior of corresponding cross sections, one is in need of an axial nucleon form factor. Therefore one Chapter describes also some model extension of the axial nucleon form factor into the time-like region.

In the last Chapter we study polarization observables in the electron-positron anni-

hilation into deuteron-antideuteron pair, which is the only possibility to obtain the first information on time-like behaviors of the deuteron electromagnetic form factors. With the aim on the estimating behaviors of the corresponding polarization observables, as well as behavior of the corresponding total cross section, the two-component and Unitary and Analytic models of the deuteron electromagnetic structure are elaborated earlier.

1. ELECTROWEAK FORM FACTORS OF HADRONS AND ATOMIC NUCLEI

1.1 Electromagnetic form factors

The idea of a form factor was firstly introduced in Quantum Mechanics, where the form factor represents correction of the scattering on a particle with spin 0 and internal charge distribution $\rho(\overrightarrow{r})$ to the Rutherford scattering on a point-like particle. For the form factor defined in this way the following formula is valid

$$F(\overrightarrow{p}, \overrightarrow{p}') = \int d^3r' e^{i(\overrightarrow{p}-\overrightarrow{p}').\overrightarrow{r}'} \rho(\overrightarrow{r}'), \tag{1.1}$$

where $\overrightarrow{p}, \overrightarrow{p}'$ are momenta of the incoming and outgoing particles and a differential cross section of scattering on a non-point-like particle is given by

$$\frac{d\sigma}{d\Omega} = \left(\frac{d\sigma}{d\Omega}\right)_R |F(\overrightarrow{p}, \overrightarrow{p}')|^2 ,$$

where $(d\sigma/d\Omega)_R$ is the differential cross section of the Rutherford scattering on the point-like particle. Also it is obvious that expression (1.1) for the form factor is a Fourier transformation of the charge distribution $\rho(\overrightarrow{r}')$ within the particle. Therefore it should be possible to obtain the charge distribution within the particle from the inverse Fourier transformation by measuring form factor.

In Quantum Field Theory a definition of the form factors is slightly different. As it was said in the Introduction, form factors are scalar functions of Q^2, which parametrize electromagnetic current of a hadron. The elastic electron scattering on a hadron $e^- h \to e^- h$ and annihilations $e^- e^+ \to h\overline{h}$ (see Fig. 1.1) are the most common processes, where electromagnetic structure of hadrons (h) is manifested. The corresponding amplitudes of these processes in the first order of the fine structure constant are

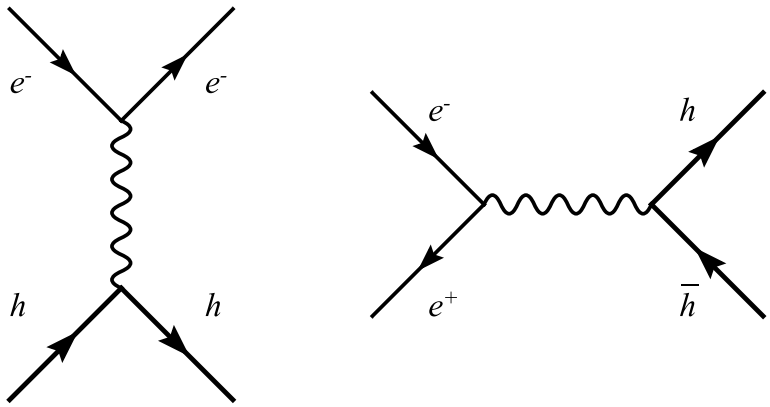

Fig. 1.1: Feynman diagrams for processes $e^- h \to e^- h$ and $e^- e^+ \to h\bar{h}$.

$$\mathcal{M}(e^- h \to e^- h) \approx \mathcal{M}^{\gamma}(s,t) = e^2 \overline{u}(k')\gamma_\mu u(k) \frac{g^{\mu\nu}}{q^2} \left\langle h, p \left| J_\nu^{EM} \right| h, p' \right\rangle$$

and

$$\mathcal{M}(e^- e^+ \to h\overline{h}) \approx \mathcal{M}^{\gamma}(t,s) = e^2 \overline{v}(k')\gamma_\mu u(k) \frac{g^{\mu\nu}}{q^2} \left\langle 0 \left| J_\nu^{EM} \right| \overline{h}, p; h, p' \right\rangle ,$$

where $g^{\mu\nu}/q^2$ is the virtual photon propagator and $\left\langle h, p \left| J_\nu^{EM} \right| h, p' \right\rangle , \left\langle 0 \left| J_\nu^{EM} \right| \overline{h}, p'; h, p \right\rangle$ are matrix elements of the electromagnetic current of the hadron, which can be written in the framework of QCD as

$$J_\nu^{EM} = \frac{2}{3}\overline{u}\gamma_\nu u - \frac{1}{3}\overline{d}\gamma_\nu d - \frac{1}{3}\overline{s}\gamma_\nu s.$$

But due to imperfections of the QCD and non-point-like nature of any hadron, we don't know the hadron electromagnetic current explicitly and we need to parametrize its matrix element. While the electromagnetic current is a relativistic covector, it can be parametrized as follows

$$\left\langle h, p \left| J_\mu^{EM} \right| h, p' \right\rangle = \sum_i R_\mu^i F_i(t), \tag{1.2}$$

where R_μ^i are all linearly independent relativistic covectors, constructed from fourmomenta and spin parameters of the hadron h and scalar functions $F_i(t)$ are electromagnetic form factors of the hadron. The number of linearly independent relativistic covectors depends on a spin of the hadron h.

In case of a spinless hadron $(\pi^{\pm}, K^0, K^{\pm})$ there are only 2 linearly independent covectors p_μ, p'_μ and Eq. (1.2) can be written as

$$\left\langle h, p \left| J_\mu^{EM} \right| h, p' \right\rangle = A.p_\mu + B.p'_\mu,$$

or

$$\left\langle h, p \left| J_\mu^{EM} \right| h, p' \right\rangle = F'.(p_\mu - p'_\mu) + F.(p_\mu + p'_\mu).$$

Both equations are equivalent, but the second one can be used together with Ward identity $q^\mu . \left\langle h, p \left| J_\mu^{EM} \right| h, p' \right\rangle = 0$ and we will obtain

$$q^\nu . \left\langle h, p \left| J_\nu^{EM} \right| h, p' \right\rangle = F'.q^2 + F.0 = 0 \Rightarrow F' = 0$$

because $(p^\mu + p'^\mu).(p_\mu - p'_\mu) = p^2 - p'^2 = 0$, whereas $|p_\mu| = \left|p'_\mu\right|$.

Now look over the scalar coefficient F. It should be a scalar function of scalar parameters, constructed from incoming and outgoing hadron's four momenta p and p' ($p^2, p'^2, p_\mu.p'^\mu$ and their linear combinations). Fortunately there is only one linearly independent scalar $p_\mu.p'^\mu$, because $p^2 = p'^2 = m^2$ are constants. Usually another linear combination $q^2 = (-Q^2 = t)$ is used and it is related to $p_\mu.p'^\mu$ in the following way

$$q^2 = (p - p')^2 = p^2 - 2p_\mu.p'^\mu + p'^2 = 2m^2 - 2p_\mu.p'^\mu.$$

Therefore the electromagnetic current of the spinless hadron can be parametrized as

$$\left\langle h, p \left| J_\mu^{EM} \right| h, p' \right\rangle = F(q^2).(p_\mu + p'_\mu), \tag{1.3}$$

where $F(q^2)$ is the electromagnetic form factor of hadron with spin 0 and it can be used to describe electromagnetic properties of such hadron.

In case of a spin 1/2 hadron $(p, n, H^3, He^3...)$ one can construct more relativistic covectors (or scalars) from bispinors $u, \overline{u'}$ (e.g. $\overline{u'}\gamma_\mu u$ or $\overline{u'}u$). Again, the number of linearly independent relativistic covectors can be reduced by using Dirac equation and Ward identity to 2 covectors and in a similar way we can show that there is only 1 linearly independent scalar (e.g. q^2). It means that matrix element of hadrons with spin=1/2 can be described by 2 form factors depending on q^2

$$\left\langle h, p' \left| J_\mu^{EM} \right| h, p \right\rangle = \frac{1}{2\pi^3} \overline{u}(p') \left[\gamma_\mu F_1(q^2) + \frac{1}{2m_h} \sigma_{\mu\nu} (p' - p)^\nu F_2(q^2) \right] u(p), \tag{1.4}$$

where $F_1(q^2), F_2(q^2)$ are called Dirac and Pauli form factors.

We can also choose another linear combination of these form factors, called Sachs electric and magnetic form factors $G_E(q^2), G_M(q^2)$, which are suitable in extracting of the experimental information on the hadron electromagnetic structure from measured cross sections

$$\begin{aligned}\frac{d\sigma^{lab}(e^-h \to e^-h)}{d\Omega} &= \frac{\alpha^2}{4E^2}\frac{\cos^2(\theta/2)}{\sin^4(\theta/2)}\frac{1}{1+\left(\frac{2E}{m_h}\right)\sin^2(\theta/2)} \\ &\times \left[\frac{G_E^2(q^2) - \frac{q^2}{4m_h^2}G_M^2(q^2)}{1-\frac{q^2}{4m_h^2}} - 2\frac{q^2}{4m_h^2}G_M^2(q^2)\tan^2(\theta/2)\right],\end{aligned}$$

where $\alpha = 1/137$, E is an incident electron energy, θ is an scattering angle and

$$\sigma_{tot}^{c.m.}(e^+e^- \to h\overline{h}) = \frac{4\pi\alpha^2\beta_h}{3t}\left[\left|G_M(q^2)\right|^2 + \frac{2m_h^2}{q^2}\left|G_E(q^2)\right|^2\right] \quad ; \quad \beta_h = \sqrt{1-\frac{4m_h^2}{q^2}}.$$

The Sachs form factors are related to Dirac and Pauli form factors as follows

$$G_E(q^2) = F_1(q^2) + \frac{q^2}{4m_p^2}F_2(q^2) \quad ; \quad G_M(q^2) = F_1(q^2) + F_2(q^2).$$

The Fourier transformation of the Sachs form factors in the Breit frame gives the charge and magnetization distribution inside the hadron.

Similarly in case of a spin 1 hadron (d, ρ, ω, ϕ) it is possible to show that the matrix element of the hadron electromagnetic current can be parametrized by three scalar functions of variable $t(= q^2)$

$$-\left\langle h,p\left|J_\mu^{EM}\right|h,p'\right\rangle = G_1(t)(\xi'^*.\xi)d_\mu + G_2(t)\left[\xi_\mu(\xi'^*.q) - \xi'^*_\mu(\xi.q)\right] - G_3(t)\frac{(\xi.q)(\xi'^*.q)}{2m_h^2}d_\mu, \tag{1.5}$$

where ξ, ξ' are polarization vectors of fourmomenta p_μ, p'_μ of the incoming and outgoing hadron h, which obey

$$\xi'.p' = 0 \ ; \ \xi.p = 0 \ ; \ \xi'^2 = -1 \ ; \ \xi^2 = -1 \ ; \ d_\mu = p'_\mu + p_\mu \ ; \ q_\mu = p'_\mu - p_\mu.$$

Again another linear combination of the form factors is used – $G_C(t), G_M t), G_Q(t)$, where $G_C(t)$ is the charge form factor, $G_M(t)$ is the magnetic form factor and $G_Q(t)$ is

the quadrupole form factor. They are related to $G_1(t), G_2(t), G_3(t)$ in the following way

$$\begin{aligned} G_M(t) &= G_2(t) \\ G_Q(t) &= G_1(t) - G_2(t) + (1+\eta)G_3(t) \\ G_C(t) &= G_1(t) + \frac{2}{3}\eta G_Q(t), \end{aligned} \tag{1.6}$$

where $\eta = -\frac{t}{4m_h^2}$.

However from measurement of the differential cross section of the $e^- h \to e^- h$ scattering with unpolarized particles one can obtain only structure functions $A(t)$ and $B(t)$ by using Rosenbluth separation of

$$\frac{d\sigma}{d\Omega} = \frac{\alpha^2 E' \cos^2(\theta/2)}{4E^3 \sin^4(\theta/2)}[A(t) + B(t)\tan^2(\theta/2)], \tag{1.7}$$

which are related to $G_C(t), G_M(t), G_Q(t)$ as

$$\begin{aligned} A(t) &= \frac{2}{3}\eta(1+\eta)G_M^2(t) + G_C^2(t) + \frac{8}{9}\eta^2 G_Q^2(t), \\ B(t) &= \frac{4}{3}\eta(1+\eta)^2 G_M^2(t). \end{aligned} \tag{1.8}$$

In addition it is possible to measure vector (e.g. p_x) and tensor (t_{2i}, where $i = 0, 1, 2$) polarization observables of spin 1 particle in space-like region, which give us additional information on the particle electromagnetic structure. The polarization of the outgoing hadron can be measured in a second, analyzing scattering. The cross section for the double scattering process can be written as

$$\begin{aligned} \frac{d\sigma}{d\Omega d\Omega_2} = \frac{d\sigma}{d\Omega d\Omega_2}\bigg|_0 \big[1 &+ \tfrac{3}{2}hp_x A_y \sin\phi_2 + \tfrac{1}{\sqrt{2}}t_{20}A_{zz} \\ &- \tfrac{2}{\sqrt{3}}t_{21}A_{xz}\cos\phi_2 + \tfrac{1}{\sqrt{3}}t_{22}(A_{xx} - A_{yy})\cos 2\phi_2\big], \end{aligned} \tag{1.9}$$

where $h = \pm 1/2$ is the polarization of the incoming electron beam, ϕ_2 the angle between the two scattering planes, and A_y and the A_{ij} are the vector and tensor analyzing powers of the second scattering. The polarization observables p_x, t_{2i} can be expressed by EM

FFs as

$$\begin{aligned} p_x &= -\frac{4}{3S}\left[\eta(1+\eta)\right]^{1/2} G_M (G_C + \tfrac{1}{3}\eta G_q)\tan\tfrac{1}{2}\theta \\ t_{20} &= -\frac{1}{\sqrt{2}S}\left[\tfrac{8}{3}\eta G_C G_Q + \tfrac{8}{9}\eta^2 G_Q^2 + \tfrac{1}{3}\eta\left[1+2(1+\eta)\tan^2\tfrac{1}{2}\theta\right] G_M^2\right] \\ t_{21} &= \frac{2\eta}{\sqrt{3}S}\left[\eta+\eta^2\sin^2\tfrac{1}{2}\theta\right]^{1/2} G_M G_Q \sin^{-1}\tfrac{1}{2}\theta \\ t_{22} &= -\frac{1}{2\sqrt{3}S}\eta G_M^2. \end{aligned} \tag{1.10}$$

Therefore the measurements of the hadron structure functions $A(t)$ and $B(t)$ and one additional hadron polarization observable in *ed* scattering allow us to extract values of all three spin 1 particle form factors in space-like region. In the case of deuteron the estimation of the polarization observable t_{20} is the most accurate and it is used together with the deuteron structure functions to extract the values of the deuteron form factors

$$\begin{aligned} G_M(t) &= \sqrt{\frac{3B(t)}{4\eta(1+\eta)}} \\ G_Q^2(t) &= \frac{\tilde{A}(t)\left(2+p\pm 2\sqrt{(1-p)(1+2p)}\right)}{4\eta^2} \\ G_C(t) &= \frac{9\tilde{A}(t)p - 4\eta^2 G_Q^2(t)}{6\eta G_Q(t)}, \end{aligned} \tag{1.11}$$

where

$$\tilde{A} = A - \frac{2}{3}\eta G_M^2 \quad ; \quad p = -\frac{\sqrt{2}(A+B\tan\frac{\theta}{2})t_{20} + \frac{(1+2(1+\eta)\tan^2\frac{\theta}{2})B}{4(1+\eta)}}{\tilde{A}}.$$

Values of the magnetic deuteron form factor are extracted from data on $B(t)$ structure function and values of charge and quadrupole form factors were extracted from $A(t), B(t), t_{20}$ for the values of variable t where t_{20} measurement are available, getting the values of $A(t)$ and $B(t)$ from an interpolation of the data on the differential cross section. The existing experimental data on *ed* scattering, differential cross section and the polarization observables, were collected in [6]. While the magnetic FF, $G_M(t)$, is directly related to $B(t)$, the extraction of the charge and quadrupole FFs requires the

solution of two quadratic equations, which may lead, in some cases, to two possible roots. Therefore, the date on $G_C(t)$ and $G_Q(t)$ consists of two different sets of solutions.

In case of strong interacting particles with spin greater than 1 the situation is even more complicated and up to now no general prescription for the parametrization of their matrix element of electromagnetic current exists.

1.2 Weak contribution to the hadron structure

According to Standard model there are 3 fundamental interactions in the Universe - electromagnetic, weak and strong (and 4th - gravity) force. Electromagnetic FFs describe structure of hadrons, given by strong forces, in the language of quantum electrodynamics (Fig.1.2a). In order to describe weak interaction effects, one need to introduce axial, pseudoscalar and eventually strange form factors of hadrons.

The weak interaction corresponds to the exchange of charged $W^{\pm}$-bosons (charged currents) and a neutral Z^0-boson (neutral current). The neutral current gives contribution (Fig.1.2b) to all processes discussed in this work, because the Z^0-boson has the same charge and spin as the photon. According to Standard model lepton EM current and the weak neutral current (NC) can be expressed as

$$\begin{aligned} EM &: \; l_\mu^{EM} = ieQ_l\bar{u}_l\gamma_\mu u_l = ieQ_l l_\mu \\ NC &: \; l_\mu^{NC} = ig\frac{M_Z}{4M_W}\left(g_V^f\bar{u}_l\gamma_\mu u_l + g_A^f\bar{u}_l\gamma_\mu\gamma_5 u_l\right) = ig\frac{M_Z}{4M_W}\left(g_V^f l_\mu + g_A^f l_{\mu 5}\right), \end{aligned} \tag{1.12}$$

where g and $e(=g\sin\theta_W)$ are weak and EM coupling strengths, Q_l is electromagnetic charge of the lepton, g_V^f, g_A^f are vector and axial-vector weak 'charges' of the fermion f (given in table 1.1) and M_Z, M_W are masses of Z^0 and $W^{\pm}$ bosons.

fermion	g_V^f	g_A^f
ν_e, ν_μ, ν_τ	1	-1
e^-, μ^-, τ^-	$-1+4\sin^2\theta_W$	1
u, c, t	$1-\frac{8}{3}\sin^2\theta_W$	-1
d, s, b	$-1+\frac{4}{3}\sin^2\theta_W$	1

Tab. 1.1: Standard model values for neutral current couplings of elementary fermions.

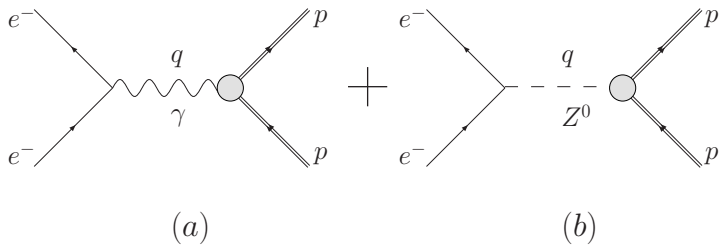

Fig. 1.2: Leading order amplitudes for scattering of electron on proton. (a) exchange of photon, (b) exchange of Z^0 boson.

On the other hand, hadronic currents can not be fully described within Standard model. As we know, EM hadronic current is a vector (J_μ^{EM}) and neutral hadronic current is composed from vector and axial-vector parts

$$J_\mu^{NC} = J_\mu^{NC,V} + J_{\mu 5}^{NC,A}. \tag{1.13}$$

Since hadrons are composed of quarks, the currents $J_\mu^{EM}, J_\mu^{NC,V}$ and $J_{\mu 5}^{NC,A}$ are the hadronic matrix elements of the electromagnetic, vector and axial-vector quark current operators

$$J_\mu^{EM} = \left\langle H \left| \hat{J}_\mu^{EM} \right| H \right\rangle , \quad J_\mu^{NC,V} = \left\langle H \left| \hat{J}_\mu^{NC,V} \right| H \right\rangle , \quad J_{\mu 5}^{NC,A} = \left\langle H \left| \hat{J}_{\mu 5}^{NC,A} \right| H \right\rangle , \tag{1.14}$$

where $|H\rangle$ is any hadronic state and

$$\hat{J}_\mu^{EM} = \sum_q Q_q \bar{u}_q \gamma_\mu u_q , \quad \hat{J}_\mu^{NC,V} = \sum_q g_V^q \bar{u}_q \gamma_\mu u_q , \quad \hat{J}_{\mu 5}^{NC,A} = \sum_q g_A^q \bar{u}_q \gamma_\mu \gamma_5 u_q, \tag{1.15}$$

where, in general, the expressions are summed over all quark flavors - u,d,s,c,b,t. However, we will assume that the structure of the hadronic states is dominated by the lighter quarks - q =u,d,s. The error introduced by neglecting the heavier quarks is expected to be of order 10^{-4} for vector currents ($\hat{J}_\mu^{EM}, \hat{J}_\mu^{NC,V}$) and 10^{-2} for axial-vector currents ($\hat{J}_{\mu 5}^{NC,A}$). Within such approximation one can decompose the current operators in terms of SU(3) octet and singlet currents

$$\hat{V}_\mu^{(a)} = \frac{1}{2}\bar{q}\lambda^a \gamma_\mu q , \quad \hat{A}_\mu^{(a)} = \frac{1}{2}\bar{q}\lambda^a \gamma_\mu \gamma_5 q , \quad q = \begin{pmatrix} u \\ d \\ s \end{pmatrix} , \tag{1.16}$$

where q represents the triplet of quarks, $\lambda^0 = \frac{2}{3}\hat{1}$ and the $\lambda^a, a = 1, ..., 8$ are the Gell-Mann SU(3) matrices. While neither EM current nor neutral current change the flavor of quarks, only SU(3) components without non diagonal terms ($a = 0, 3, 8$) can contribute to the EM and weak currents

$$\begin{aligned}
\hat{V}_\mu^{(0)} &= \frac{1}{3}(\bar{u}\gamma_\mu u + \bar{d}\gamma_\mu d + \bar{s}\gamma_\mu s)\ , \quad \hat{V}_\mu^{(3)} = \frac{1}{2}(\bar{u}\gamma_\mu u - \bar{d}\gamma_\mu d), \\
\hat{V}_\mu^{(8)} &= \frac{1}{2\sqrt{3}}(\bar{u}\gamma_\mu u + \bar{d}\gamma_\mu d - 2\bar{s}\gamma_\mu s), \\
\hat{A}_\mu^{(0)} &= \frac{1}{3}(\bar{u}\gamma_\mu\gamma_5 u + \bar{d}\gamma_\mu\gamma_5 d + \bar{s}\gamma_\mu\gamma_5 s)\ , \quad \hat{A}_\mu^{(3)} = \frac{1}{2}(\bar{u}\gamma_\mu\gamma_5 u - \bar{d}\gamma_\mu\gamma_5 d), \\
\hat{A}_\mu^{(8)} &= \frac{1}{2\sqrt{3}}(\bar{u}\gamma_\mu\gamma_5 u + \bar{d}\gamma_\mu\gamma_5 d - 2\bar{s}\gamma_\mu\gamma_5 s),
\end{aligned}$$

where, at the level of strong isospin, the 0th and the 8th SU(3) components are isoscalar operators and the 3rd SU(3) component is an isovector operator. Now we can use Eq. (1.15) and known EM charges of quarks to express the EM hadronic current as

$$\hat{J}_\mu^{EM} = \frac{2}{3}\bar{u}\gamma_\mu u - \frac{1}{3}\bar{d}\gamma_\mu d - \frac{1}{3}\bar{s}\gamma_\mu s, \tag{1.17}$$

which imply that the EM hadronic current can be expressed by using only the 3rd and the 8th SU(3) components as

$$\hat{J}_\mu^{EM} = \frac{1}{\sqrt{3}}\hat{V}_\mu^{(8)} + \hat{V}_\mu^{(3)}, \tag{1.18}$$

where $\hat{J}_\mu^{EM(T=0)} = \frac{1}{\sqrt{3}}\hat{V}_\mu^{(8)}$ is an isoscalar part of the hadronic current and $\hat{J}_\mu^{EM(T=1)} = \hat{V}_\mu^{(3)}$ is an isovector part of the hadronic current.

Since we want also to extract the strange contribution to the hadron structure, it is useful to note the relation between 2 isoscalar currents

$$\begin{aligned}
\hat{V}_\mu^{(0)} &= \frac{2}{\sqrt{3}}\hat{V}_\mu^{(8)} + \hat{V}_\mu^{(s)}\ , \quad \hat{A}_\mu^{(0)} = \frac{2}{\sqrt{3}}\hat{A}_\mu^{(8)} + \hat{A}_\mu^{(s)} \\
\hat{V}_\mu^{(s)} &= \bar{s}\gamma_\mu s\ , \quad \hat{A}_\mu^{(s)} = \bar{s}\gamma_\mu\gamma_5 s
\end{aligned} \tag{1.19}$$

By using these relations one can rewrite the weak neutral currents (1.15) as

$$\begin{aligned}
\hat{J}_\mu^{NC,V} &= \xi_V^{T=1}\hat{J}_\mu^{EM(T=1)} + \sqrt{3}\xi_V^{T=0}\hat{J}_\mu^{EM(T=0)} + \xi_V^{(0)}\hat{V}_\mu^{(s)}, \\
\hat{J}_{\mu 5}^{NC,A} &= \xi_A^{T=1}\hat{A}_\mu^{(3)} + \sqrt{3}\xi_A^{T=0}\hat{A}_\mu^{(8)} + \xi_A^{(0)}\hat{A}_\mu^{(s)},
\end{aligned} \tag{1.20}$$

where values of ξ couplings are obtained in the similar way as in the case of the EM hadronic current (1.17) and their values are given in Table1.2. An advantage of this approach is extracting of the strange contribution to the weak currents.

coupling	$\xi_V^{(0)}$	$\xi_V^{T=1}$	$\xi_V^{T=0}$
value	$g_V^u + g_V^d + g_V^s$	$g_V^u - g_V^d$	$\sqrt{3}(g_V^u + g_V^d)$
coupling	$\xi_A^{(0)}$	$\xi_A^{T=1}$	$\xi_A^{T=0}$
value	$g_A^u + g_A^d + g_A^s$	$g_A^u - g_A^d$	$\sqrt{3}(g_A^u + g_A^d)$

Tab. 1.2: Standard model values for neutral current couplings.

1.3 Axial and strange nucleon form factors

The nucleon matrix elements of the EM and the neutral hadronic currents (1.18,1.20) are restricted by Lorentz, parity and time invariance to the general forms

$$\begin{aligned}
\left\langle N(p')\middle|J_\mu^{EM}\middle|N(p)\right\rangle &= \bar{u}(p')\left[F_1(q^2)\gamma_\mu + i\frac{F_2(q^2)}{2m_N}\sigma_{\mu\nu}q^\nu\right]u(p)\\
\left\langle N(p')\middle|J_\mu^{NC,V}\middle|N(p)\right\rangle &= \bar{u}(p')\left[\tilde{F}_1(q^2)\gamma_\mu + i\frac{\tilde{F}_2(q^2)}{2m_N}\sigma_{\mu\nu}q^\nu\right]u(p)\\
\left\langle N(p')\middle|J_{\mu 5}^{NC,A}\middle|N(p)\right\rangle &= \bar{u}(p')\left[\tilde{G}_A(q^2)\gamma_\mu + \frac{\tilde{G}_P(q^2)}{m_N}q_\mu\right]\gamma_5 u(p),
\end{aligned} \tag{1.21}$$

where p', p are four momenta of incoming and outgoing nucleon, $q = p' - p$ is four momentum transferred, F_1, F_2 are usual EM Dirac and Pauli form factors, $\tilde{F}_1, \tilde{F}_2$ are their weak analogy and $\tilde{G}_A, \tilde{G}_P$ are axial and pseudoscalar form factors. Similarly to the definition of EM Sachs form factors, weak electric and magnetic form factors are defined as

$$\tilde{G}_E(q^2) = \tilde{F}_1(q^2) - \tau\tilde{F}_2(q^2)\,, \quad \tilde{G}_M(q^2) = \tilde{F}_1(q^2) + \tilde{F}_2(q^2), \tag{1.22}$$

Now if one defines the nucleon electric/magnetic isoscalar/isovector form factor as

$$\begin{aligned}
G_E^{T=1} &= \frac{1}{2}(G_E^p - G_E^n)\,, \quad G_E^{T=0} = \frac{1}{2}(G_E^p + G_E^n)\\
G_M^{T=1} &= \frac{1}{2}(G_M^p - G_M^n)\,, \quad G_M^{T=0} = \frac{1}{2}(G_M^p + G_M^n)
\end{aligned} \tag{1.23}$$

then, according to dependence of the weak hadronic vector neutral current (1.20) on isoscalar and isovector EM hadronic currents, weak electric and magnetic form factors can be written as

$$\tilde{G}_X^N = \sqrt{3}\xi_V^{T=0} G_X^{T=0} \pm \xi_V^{T=1} G_X^{T=1} + \xi_V^{(0)} G_X^{(s)} \ , \quad X = E, M \ , \ \ N = n, p, \tag{1.24}$$

where one use + for proton and − for neutron form factors. Also axial-vector form factors can be decomposed as

$$\tilde{G}_X^N = \sqrt{3}\xi_A^{(8)} G_X^{T=0} \pm \xi_A^{T=1} G_X^{(3)} + \xi_A^{(0)} G_X^{(s)} \ , \quad X = E, M \ , \ \ N = n, p. \tag{1.25}$$

As we can see now, the electroweak structure of the nucleon can be described by set of 10 form factors - $G_E^p, G_M^p, G_E^n, G_M^n, G_E^{(s)}, G_M^{(s)}, G_A^p, G_P^p, G_A^n, G_P^n$.

1.4 Measurement of the weak/strange structure of the nucleon

Up to now, the weak structure of the nucleon has been already measured by several different experimental methods.

Both axial and strange form factors of the nucleon can be determined from the measurement of (anti)neutrino scattering on protons ($\nu + p \rightarrow \nu + p$), from the measurement of pion electroproduction near threshold ($e + N_1 \rightarrow e + N_2 + \pi$) and from the measurement of asymmetry in parity violating elastic electron-nucleon scattering ($e + N \rightarrow e + N$). The normalization of the pseudoscalar form factor can be determined from the measurement of ordinary muon capture by proton ($\mu^- + p \rightarrow \nu_\mu + n$) and its behavior by radiative muon capture ($\mu^- + p \rightarrow \nu_\mu + n + \gamma$).

Let us take a look at the measurement of asymmetry in parity violating electron-proton (ep) scattering. In ep scattering both photon and Z^0 boson exchange enter the reaction and in principle ep scattering experiments probe both the electromagnetic and weak neutral currents. However the electromagnetic interaction is for $q^2 \ll M_Z^2$ several order of magnitudes stronger than weak interaction. In order to detect very small weak neutral current contribution to ep scattering one must use difference between electromagnetic and weak interaction - parity violation, which comes purely from weak interaction. It causes an asymmetry between differential cross sections for scattering of longitudinally polarized electrons parallel (+) and antiparallel (−) to their momenta,

because their nonzero difference means violation of parity. The exact definition of this parity violation (PV) asymmetry is

$$A_{LR} = \frac{\frac{d\sigma_+}{d\Omega} - \frac{d\sigma_-}{d\Omega}}{\frac{d\sigma_+}{d\Omega} + \frac{d\sigma_-}{d\Omega}} = A^0_{LR}\frac{W^{(PV)}(q^2,\varepsilon)}{F^2(q^2,\varepsilon)},$$
$$\varepsilon = \left[1 + 2(1+\tau)\tan^2\left(\frac{\theta}{2}\right)\right]^{-1}, \tag{1.26}$$

where $W^{(PV)}(q^2,\varepsilon)$ is the parity violating part of the differential cross section and can be evaluated from given forms of the proton neutral currents (1.21 ,1.22) and neglecting $\tilde{G}_P$ contribution as

$$\begin{aligned} W^{(PV)}(q^2,\varepsilon) = \; & - \; \frac{1}{8\pi(1+\tau)\varepsilon}\Big[g^e_A\left[\varepsilon G^p_E(q^2)\tilde{G}^p_E(q^2) + \tau G^p_M(q^2)\tilde{G}^p_M(q^2)\right] \\ & + \; g^e_V\sqrt{(1-\varepsilon^2)(1+\tau)\tau}G^p_M(q^2)\tilde{G}^p_A(q^2)\Big] \end{aligned} \tag{1.27}$$

the total form factor $F^2(q^2,\varepsilon)$ of proton equals

$$F^2_p(q^2,\varepsilon) = \frac{1}{4\pi(1+\tau)\varepsilon}\left(\varepsilon(G^p_E(q^2))^2 + \tau(G^p_M(q^2))^2\right) \tag{1.28}$$

and normalization $A^0_{LR} = q^2G_\mu/2\sqrt{2}\pi\alpha$, where G_μ is Fermi constant for muon decay. Inserting relations between NC and EM form factors (1.24) allows us to write the PV asymmetry for proton as

$$\begin{aligned} A_{LR}(ep) = \; & - \; A^0_{LR}\Big[\xi^p_V + \Big[\varepsilon G^p_E(\xi^n_V G^n_E + \xi^{(0)}_V G^{(s)}_E) + \tau G^p_M(\xi^n_V G^n_M + \xi^{(0)}_V G^{(s)}_M) \\ & - \; (1 - 4\sin^2\theta_W)\sqrt{(1-\varepsilon^2)(1+\tau)\tau}G^p_M\tilde{G}^p_A\Big] \\ & / \; 2\big[\varepsilon(G^p_E)^2 + \tau(G^p_M)^2\big]\Big], \end{aligned} \tag{1.29}$$

where definition of ξ^p_V, ξ^n_V couplings is

$$\xi^p_V = \frac{1}{2}(\xi^{T=1}_V + \sqrt{3}\xi^{T=0}_V)\,, \quad \xi^n_V = \frac{1}{2}(-\xi^{T=1}_V + \sqrt{3}\xi^{T=0}_V). \tag{1.30}$$

As we can see, PV asymmetry of ep scattering really depends on new form factors $G_E^{(s)}, G_M^{(s)}, G_A^p$. Together with experimental data on other observables measured in processes mentioned at the beginning of this section, it can be used to separate data on these form factors.

2. POLARIZATION OBSERVABLES - INTRODUCTION

2.1 Necessity of additional observables

The standard Rosenbluth separation method allows to extract only 2 independent real structure functions $A(t), B(t)$, from angular distribution of unpolarized differential cross section

$$\frac{d\sigma}{d\Omega} = \frac{\alpha^2 E' \cos^2(\theta/2)}{4E^3 \sin^4(\theta/2)}[A(q^2) + B(q^2)\tan^2(\theta/2)], \tag{2.1}$$

describing an elastic scattering of electrons on hadrons with arbitrary nonzero spin.

While electromagnetic form factors are real functions in space-like region and complex function in time-like region, 2 structure functions extracted from Rosenbluth separation are sufficient only for the full description of spin 1/2 hadrons in the space-like region. In order to describe structure of spin 1/2 hadrons in the time-like region one needs 2 additional real observables and for spin 1 particle one need 1 additional real observable in the space-like region resp. 4 additional observables in the time-like region.

The solution to this problem lies within the polarization observables, which describes dependence of the differential cross section on polarization of initial and final particles in a scattering or annihilation process.

2.2 Experiments with polarized particles

Nuclear scattering experiments in which polarization of one or more of the particles was known or measured have been performed since '50 of the previous century. In general there are 5 classes of such experiments:

- $a + b \rightarrow \vec{c} + d$ polarization experiments
- $a + \vec{b} \rightarrow c + d$ analysing power experiments
- $a + \vec{b} \rightarrow \vec{c} + d$ polarization transfer experiments
- $\vec{a} + \vec{b} \rightarrow c + d$ spin correlation (initial channel) experiments
- $a + b \rightarrow \vec{c} + \vec{d}$ spin correlation (final channel) experiments.

Experiments which involve polarized particles in the final channel imply usage of some device to measure the polarization of outgoing particles. It is usually done by observing an asymmetry of a latter scattering. Experiments with polarized particles in the initial channel measure effects like a modified differential cross section or a 'left-right' asymmetry. In this work we will discuss results of the nucleon polarization experiments from Jefferson Laboratory and the measurements of the deuteron polarization observables in the space-like region. We will also take a look on a possible measurements of the polarization observables in time-like region of the nucleon and the deuteron.

2.3 Formalism

In this section a formalism ([7]) for the description of a polarization phenomena will be shown on an example of spin 1/2 particles. Usually polarization observables are measured in scattering of polarized $e^{\pm}$ (resp. $\mu^{\pm}$) on hadrons (e.g. nucleons, deuteron) and a polarization of outgoing particles is measured by latter scattering.

According to Dirac theory a free electron/muon (ℓ) quantum state, with mass m_ℓ, 4-momentum p^μ and spin s^μ, is described by a wave function

$$\psi_{p,s}(x) = \frac{1}{(2\pi)^{3/2}} \sqrt{\frac{m_\ell}{p_0}} u(p,s) e^{-\mathrm{i}p.x}, \tag{2.2}$$

which satisfies the Dirac equation

$$(\mathrm{i}\gamma^\mu \partial_\mu - m_\ell)\psi_{p,s}(x) = 0 \tag{2.3}$$

and where $u(p,s)$ is a 4-component spinor of examined lepton, which satisfies

$$(\hat{p} - m_\ell)u(p,s) = 0. \tag{2.4}$$

The Dirac equation (2.4) can be easily solved in the rest frame of examined fermion, where $\tilde{p}_\mu = (m_\ell, 0)$, and solution in actual frame can be obtained by boost transformation. The Eq. (2.4) then becomes

$$(m_\ell \gamma_0 - m)u(\tilde{p}, \tilde{s}) = m_\ell \begin{pmatrix} -\mathbb{1} & \mathbb{1} \\ \mathbb{1} & -\mathbb{1} \end{pmatrix} u(\tilde{p}, \tilde{s}), \tag{2.5}$$

which has following solutions

$$u(\tilde{p}, \tilde{s}) = \sqrt{m_\ell} \begin{pmatrix} \zeta \\ \zeta \end{pmatrix}, \tag{2.6}$$

where ζ is 2-component Pauli spinor normalized to $\zeta^\dagger \zeta = 1$, which determines the spin orientation of the Dirac solution $u(\tilde{p}, \tilde{s})$ in terms of Pauli matrices.

Therefore a single spin 1/2 particle, in its rest frame, can be represented by a Pauli spinor

$$\zeta = \begin{pmatrix} a_1 \\ a_2 \end{pmatrix} \tag{2.7}$$

and an expectation value of an observable corresponding to a particular hermitian operator Ω is defined as

$$\langle \Omega \rangle = \zeta^\dagger \Omega \zeta = (a_1^* a_2^*) \begin{pmatrix} \Omega_{11} & \Omega_{12} \\ \Omega_{12}^* & \Omega_{22} \end{pmatrix} \begin{pmatrix} a_1 \\ a_2 \end{pmatrix} = |a_1|^2 \Omega_{11} + |a_2|^2 \Omega_{22} + 2\mathrm{Re}\Omega_{12} a_1 a_2^*. \tag{2.8}$$

Now it is convenient to define the density matrix

$$\rho = \zeta \zeta^\dagger = \begin{pmatrix} |a_1|^2 & a_1 a_2^* \\ a_2 a_1^* & |a_2|^2 \end{pmatrix}, \tag{2.9}$$

which simplifies Eq.(2.8) to

$$\langle \Omega \rangle = \mathrm{Tr}\rho\Omega. \tag{2.10}$$

In the case of a set of N particles, the average of the Ω expectation value in the set is

$$\overline{\langle \Omega \rangle} = \sum_{n=1}^{N} \zeta^{\dagger(n)} \Omega \zeta^{(n)}, \tag{2.11}$$

where the spinor for the nth particle is defined as

$$\zeta^{(n)} = \begin{pmatrix} a_1^{(n)} \\ a_2^{(n)} \end{pmatrix} \tag{2.12}$$

and Eq. (2.11) can be again written in terms of density matrix as

$$\overline{\langle\Omega\rangle} = \mathrm{Tr}\rho\Omega \qquad \rho = \frac{1}{N}\sum_{n=1}^{N}\zeta^{(n)}\zeta^{(n)\dagger} = \frac{1}{N}\begin{pmatrix} \sum_{n=1}^{N}|a_1^{(n)}|^2 & \sum_{n=1}^{N}a_1^{(n)}a_2^{(n)*} \\ \sum_{n=1}^{N}a_2^{(n)}a_1^{(n)*} & \sum_{n=1}^{N}|a_2^{(n)}|^2 \end{pmatrix}. \tag{2.13}$$

Due to the normalization, the expectation value of operator of the identity, represented by unit matrix $\mathbb{1}$, should equal 1

$$\overline{\langle\mathbb{1}\rangle} = \mathrm{Tr}\rho\mathbb{1} = \mathrm{Tr}\rho = \frac{1}{N}\sum_{n=1}^{N}(|a_1^{(n)}|^2 + |a_2^{(n)}|^2) = 1. \tag{2.14}$$

Now one can use this formalism to describe polarization states of a set of spin 1/2 particles. Orientation of a spin along x, y or z axis is specified by the usual Pauli spin operators σ_x, σ_y and σ_z

$$\sigma_x = \begin{pmatrix} 0 & 1 \\ 1 & 0 \end{pmatrix} \quad ; \quad \sigma_y = \begin{pmatrix} 0 & -\mathrm{i} \\ \mathrm{i} & 0 \end{pmatrix} \quad ; \quad \sigma_z = \begin{pmatrix} 1 & 0 \\ 0 & -1 \end{pmatrix}$$

and expectation values of the polarization along particular axis are

$$\begin{aligned} p_x &\equiv \overline{\langle\sigma_x\rangle} = \mathrm{Tr}\rho\sigma_x = \frac{2}{N}\sum_{n=1}^{N}\mathrm{Re}(a_1^{(n)}a_2^{(n)*}) \\ p_y &\equiv \overline{\langle\sigma_y\rangle} = \mathrm{Tr}\rho\sigma_y = \frac{2}{N}\sum_{n=1}^{N}\mathrm{Im}(a_1^{(n)}a_2^{(n)*}) \\ p_z &\equiv \overline{\langle\sigma_z\rangle} = \mathrm{Tr}\rho\sigma_z = \frac{1}{N}\sum_{n=1}^{N}(|a_1^{(n)}|^2 - |a_2^{(n)}|^2). \end{aligned} \tag{2.15}$$

These quantities are also called degrees of polarization.

While the spin 1/2 density matrix ρ is hermitian, it can be expanded in terms of the set of matrices $\mathbb{1}, \sigma_x, \sigma_y, \sigma_z$ as

$$\rho = \sum_{i=0}^{4} a_i\sigma_i, \tag{2.16}$$

where σ_i denotes identity and Pauli matrices and by using of definitions (2.15) and

$$\mathrm{Tr}\sigma_i\sigma_j = 2\delta_{ij}, \tag{2.17}$$

one finds that

$$2a_j = \mathrm{Tr}\rho\sigma_j = p_j. \tag{2.18}$$

Therefore the spin 1/2 density matrix can be written in terms of polarization expectation values as

$$\rho = \frac{1}{2}(\mathbb{1} + p_x\sigma_x + p_y\sigma_y + p_z\sigma_z). \tag{2.19}$$

In the simple case of a scattering with a spin structure $\frac{\vec{1}}{2} + 0 \rightarrow \frac{\vec{1}}{2} + 0$, we will show the dependence of differential cross section on polarization of spin 1/2 particles.

As far as quantum mechanics is a linear theory, the spinor that describes the outgoing spin 1/2 particle is related linearly to the spinor of the incoming spin 1/2 particle

$$\zeta_f = M\zeta_i, \tag{2.20}$$

where M is a 2×2 matrix whose elements are functions of relevant energies and angles of the reaction.

The density matrices of the initial and final states may be written according to (2.13) as

$$\rho_i = \frac{1}{N}\sum_{n=1}^{N}\zeta_i^{(n)}[\zeta_i^{(n)}]^\dagger \quad ; \quad \rho_f = \frac{1}{N}\sum_{n=1}^{N}\zeta_f^{(n)}[\zeta_f^{(n)}]^\dagger. \tag{2.21}$$

The trace of initial state density matrix is normalized to 1. On the other hand the trace of density matrix for the final state corresponds to differential cross section for the polarized beam

$$I(\theta,\phi) \sim \mathrm{Tr}\rho_f = \mathrm{Tr}M\rho_i M^\dagger, \tag{2.22}$$

where relation between ρ_f and ρ_i can be derived from Eqs. (2.20,2.21). The differential cross section of unpolarized beam, with density matrix

$$\rho_i = \frac{1}{2}\begin{pmatrix} 1 & 0 \\ 0 & 1 \end{pmatrix},$$

can be reduced to

$$I_0(\theta) \sim \frac{1}{2}\mathrm{Tr}MM^\dagger. \tag{2.23}$$

In order to calculate the expectation value of polarization of the scattered particles, one need to use modified density matrix ρ'_f normalized to 1

$$\rho'_f = \frac{\rho_f}{\mathrm{Tr}\rho_f},$$

which similarly to definitions (2.15) leads into

$$p'_k \equiv \overline{\langle \sigma'_k \rangle} = \frac{\mathrm{Tr}\rho_f \sigma'_k}{\mathrm{Tr}\rho_f}, \tag{2.24}$$

where k indicate the direction of outgoing particle polarization.

Now by substitution of the initial density matrix expansion (2.19) to the formula for differential cross section (2.22), one can easily derive

$$I(\theta, \phi) = \mathrm{Tr}M\rho_i M^\dagger = I_0(\theta) \left(1 + \sum_{j=1}^{3} p_j A_j(\theta) \right), \tag{2.25}$$

where

$$A_j(\theta) = \frac{\mathrm{Tr}M\sigma_j M^\dagger}{\mathrm{Tr}MM^\dagger} \tag{2.26}$$

is the analysing power of the reaction for the jth initial polarization component. Similarly one can derive an expression for differential cross section for the case when the polarization of outgoing spin 1/2 particles along k-axis is measured

$$p'_k I(\theta, \phi) = I_0(\theta) \left(P'_k(\theta) + \sum_{j=1}^{3} p_j K_j^k(\theta) \right), \tag{2.27}$$

where

$$P'_k(\theta) = \frac{\mathrm{Tr}MM^\dagger \sigma'_k}{\mathrm{Tr}MM^\dagger} \tag{2.28}$$

is the kth component of the polarization of outgoing particle produced by an unpolarized beam and

$$K_j^k(\theta) = \frac{\mathrm{Tr}M\sigma_j M^\dagger \sigma'_k}{\mathrm{Tr}MM^\dagger} \tag{2.29}$$

is the polarization transfer coefficient that relates the jth initial polarization component to the kth final polarization component. All off the polarization observables may vary between -1 and 1 for the present spin 1/2 case.

Actually the forms (2.25,2.27) for the differential cross sections are the most general forms allowed by the conservation of the angular momentum and in the concrete cases

(like the different spin structures of reaction) some of the polarization observables can become zero as we will see in next chapters concerning polarization observables.

Moreover the fermion spin state can be described also by the polarization 4-vector s^μ defined in the lepton rest frame, where $\tilde{p}^\mu = (m_\ell, 0)$, as $\tilde{s}^\mu = (0, \vec{\xi})$ where $\vec{\xi}$ is a unit 3-vector pointing in the direction of the electron spin. The polarization 4-vector s^μ in actual frame can be again obtained by Lorentz transformation of $\tilde{s}^\mu$. It satisfies following constraints

$$s \cdot p = 0 \quad s \cdot s = -1 \tag{2.30}$$

and it is related to $\vec{\xi}$ as

$$s^\mu = (s_0, \vec{s}) = \left(\frac{\vec{p} \cdot \vec{\xi}}{m_\ell}, \vec{\xi} + \frac{\vec{p}(\vec{p} \cdot \vec{\xi})}{m_\ell(m_\ell + p_0)} \right). \tag{2.31}$$

It can be used for the calculation of processes with polarized fermions, where

$$u\bar{u} = \frac{1}{2}(\hat{p} + m_\ell)(1 - \gamma_5 \hat{s}) \tag{2.32}$$

and antifermions, where

$$v\bar{v} = \frac{1}{2}(\hat{p} - m_\ell)(1 - \gamma_5 \hat{s}). \tag{2.33}$$

In the special case when s_μ describes fermion polarized along particular axis and degree of polarization λ (expectation value of the polarization) along this axis is lower than 1, expressions (2.32, 2.33) are modified to

$$u\bar{u} = \frac{1}{2}(\hat{p} + m_\ell)(1 - \lambda\gamma_5 \hat{s}).$$

3. POLARIZATION OBSERVABLES - EXAMPLE OF CALCULATION

3.1 Motivation

The aim of this Chapter is to give a pedagogical derivation of polarization observables for the annihilation reaction $e^+ + e^- \to N + \bar{N}$. The reaction mechanism is one photon + two photon exchange, the latter is described by an axial parametrization. After deriving the general expressions for the cross section of a binary process, the matrix element is written in terms of three complex amplitudes. The method to derive polarization observables is detailed and all expressions are given in terms of generalized form factors. The strategy for determining physical form factors in annihilation reactions in presence of two photon exchange is suggested, on the basis of model independent properties of the relevant observables.

3.2 Differential cross section

Let us define the cross section σ for a binary process

$$a(p_1) + b(p_2) \to c(p_3) + d(p_4), \tag{3.1}$$

where the momenta of the particles are indicated in parenthesis. The cross section σ characterizes the probability that a given process occurs. The number of final particles issued from a definite reaction is proportional to the number of incident particles N_B, the number of the target particles N_T and the constant of proportionality is the cross section:

$$N_F = \sigma N_B \times N_T. \tag{3.2}$$

The cross section can be viewed as an 'effective area' over which the incident particle reacts. Therefore, its dimension is cm^2, but more often barn (1 barn=10^{-28} m^2), or fm^2 (1 fm=10^{-15} m).

An useful quantity is the luminosity $\mathcal{L}$, defined as $\mathcal{L} = N_B\ [s^{-1}]N_T[cm^2]$. For simple counting estimations, $N_f = \sigma\mathcal{L}$. This is an operative definition, which is used in experimental physics.

On the other hand σ needs to be calculated theoretically for every type of process. The present derivation is done in a relativistic approach. This means that

1. The kinematics is relativistic;
2. The matrix element $\mathcal{M}$, which contains the dynamics of the reaction is a relativistic invariant. In general it is function of kinematical variables, also relativistic $\mathcal{M} = f(s,t,u)$;
3. σ has to be written in a relativistic invariant form;

The starting point is the following expression for the cross section

$$d\sigma = \frac{|\mathcal{M}|^2}{\mathcal{J}}(2\pi)^4\delta^{(4)}(p_1 + p_2 - p_3 - p_4)d\mathcal{P}, \tag{3.3}$$

which is composed by four terms:

1. The matrix element $\mathcal{M}$, which contains the dynamics of the reaction, and it is calculated following a model:
2. The flux of colliding particles $\mathcal{J}$;
3. The phase space for the final particles, $d\mathcal{P}$;
4. A term which insures the conservation of the four-momentum $\delta^{(4)}(p_1 + p_2 - p_3 - p_4)$ which is the product of four δ functions, because each component has to be conserved separately.

Let us calculate in detail each term.

3.2.1 Definition of flux

The flux is defined through the relative velocity of incoming and target particles:

$$\mathcal{I} = n_B n_T v_{rel}, \tag{3.4a}$$

$$\mathcal{I} = 4\sqrt{(p_1 \cdot p_2)^2 - M_1^2 M_2^2}, \tag{3.4b}$$

where $M_1(M_2)$ is the mass of the beam (target) particle, v_{rel} is the relative velocity between beam and target particles and the densities of the beam and target particles n_B, n_T are proportional to their energies as $n_i = 2E_i$.

Let us prove that the two expressions (3.4a) and (3.4b) are equivalent. It is more convenient to calculate $\mathcal{I}$ (Eq. 3.4) in the laboratory frame where the target is at rest:

$$p_1 = (E_1, \vec{p}_1), \;\; p_2 = (M_2, 0), \;\; |v_{rel}| = |\vec{v}_1 - \vec{v}_2| = \frac{|\vec{p}_1|}{E_1} \;\Rightarrow\; n_B = 2E_1, \; n_T = 2M_2. \tag{3.5}$$

Replacing the equalities (3.5) in Eq. (3.4a):

$$\mathcal{I} = 2E_1 2M_2 \frac{|\vec{p}_1|}{E_1} = 4M_2|\vec{p}_1|$$

and in Eq. (3.4b) :

$$(p_1 \cdot p_2)^2 - M_1^2 M_2^2 = M_2^2 E_1^2 - M_1^2 M_2^2 = M_2^2(E_1^2 - M_1^2) = M_2^2|\vec{p}_1|^2, \;\; \rightarrow \mathcal{I} = 4M_2|\vec{p}_1|$$

and the equalities (3.4) are proved. Moreover, we prove also that the flux does not depend on the reference frame, because it can be written in a Lorentz invariant form.

Let us consider the center of mass system (CMS):

$$p_1 = (E_1, \vec{k}), \; p_2 = (E_2, -\vec{k}), \; p_1 \cdot p_2 = E_1 E_2 + |\vec{k}|^2, \; M_1^2 = E_1^2 - |\vec{k}|^2, \; M_2^2 = E_2^2 - |\vec{k}|^2$$

and

$$\begin{aligned}(p_1 \cdot p_2)^2 - M_1^2 M_2^2 &= E_1^2 E_2^2 + 2E_1 E_2 |\vec{k}|^2 + |\vec{k}|^4 - E_1^2 E_2^2 + |\vec{k}|^2(E_1^2 + E_2^2) - |\vec{k}|^4 \\ &= |\vec{k}|^2(E_1 + E_2)^2 = |\vec{k}|^2 W^2. \end{aligned} \tag{3.6}$$

The flux, $\mathcal{I}$, can be written as

$$\mathcal{I} = 4|\vec{k}|W, \tag{3.7}$$

where $W = E_1 + E_2$ is the initial energy of the system in CMS.

3.2.2 Phase space

The phase space for a particle of energy E, mass M and four–momentum p (the number of states in the unit volume) can be written from quantum mechanics in an invariant form:

$$d\mathcal{P} = \int \frac{d^4p\ \delta(p^2 - M^2)}{(2\pi)^3}\Theta(E)$$

where the δ function insures that the particle is on mass shell and the step function $\Theta(E)$ insures that only the solution with positive energy is taken into account.

Explicating the term which depends on energy:

$$d^4p\ \delta(p^2 - M^2) = \delta^3\vec{p}dE\delta(E^2 - \vec{p}^2 - M^2).$$

and using the property of the δ function

$$\int \delta[f(x)]dx = \sum \frac{1}{|f'(x_i)|}, \tag{3.8}$$

(x_i are the roots of $f(x)$), with $f(E) = E^2 - \vec{p}^2 - M^2$, and $f'(E) = 2E$ one finds:

$$\int dE\delta(E^2 - \vec{p}^2 - M^2)\Theta(E) = \frac{1}{2E}.$$

For the considered reaction:

$$d\mathcal{P} = \frac{d^3\vec{p}_3}{(2\pi)^3 2E_3}\frac{d^3\vec{p}_4}{(2\pi)^3 2E_4}.$$

3.2.3 Calculation of the cross section

The total cross section can be written as:

$$\sigma = \frac{(2\pi)^4}{\mathcal{I}}\int |\mathcal{M}|^2\delta^{(4)}(p_1 + p_2 - p_3 - p_4)\frac{d^3\vec{p}_3}{(2\pi)^3 2E_3}\frac{d^3\vec{p}_4}{(2\pi)^3 2E_4}. \tag{3.9}$$

One can see that it corresponds to a six-fold differential, but four δ functions are equivalent to four integrations. So finally, for a binary process one is left with two independent variables, (E, θ) or (s, t). For three particles, one has nine differentials, four integrations i.e., five independent variables.

The term $\delta^{(4)}(p_1 + p_2 - p_3 - p_4)$ can be splitted into an energy and a space part: $\delta^{(4)}(p_1 + p_2 - p_3 - p_4) = \delta(E_1 + E_2 - E_3 - E_4)\delta^{(3)}(\vec{p}_1 + \vec{p}_2 - \vec{p}_3 - \vec{p}_4)$.

Note that

$$\int \delta^{(3)}(\vec{p}_1 + \vec{p}_2 - \vec{p}_3 - \vec{p}_4) d^3\vec{p}_4 = 1 \tag{3.10}$$

in any reference frame.

Let us use spherical coordinates in CMS ($p_3 = (E_3, \vec{p})$, $p_4 = (E_4, -\vec{p})$, $d^3\vec{p} = |\vec{p}|^2 d\Omega dp$)and consider the quantity $\mathcal{J}$:

$$\mathcal{J} = \delta(E_1 + E_2 - E_3 - E_4)\frac{d^3\vec{p}_3}{4E_3E_4} = \delta(W - E_3 - E_4)\frac{|\vec{p}|^2 d\Omega dp}{4E_3E_4}, \tag{3.11}$$

where

$$E_3^2 = M_3^2 + |\vec{p}|^2,\ E_4^2 = M_4^2 + |\vec{p}|^2 \rightarrow E_3 dE_3 = E_4 dE_4 = |\vec{p}| dp.$$

After integration, using the property (3.8):

$$\mathcal{J} = \int \delta(W - E_3 - E_4)\frac{dE_3 |\vec{p}| d\Omega}{4E_4} = \frac{|\vec{p}| d\Omega}{4E_4}\frac{1}{\left|\dfrac{d}{dE_3}(W - E_3 - E_4)\right|}, \tag{3.12}$$

where

$$\frac{d}{dE_3}(W - E_3 - E_4) = -1 - \frac{dE_4}{dE_3} = -1 - \frac{E_3}{E_4} = -\frac{W}{E_4} \tag{3.13}$$

and therefore

$$\mathcal{J} = \frac{|\vec{p}| d\Omega}{4W}. \tag{3.14}$$

Substituting Eqs. (3.7, 3.14) in Eq. (3.9) we find the general expression for the differential cross section of a binary process, in CMS:

$$\frac{d\sigma}{d\Omega} = \frac{|\mathcal{M}|^2 |\vec{p}|}{64\pi^2 W^2 |\vec{k}|}, \tag{3.15}$$

and for the total cross section:

$$\sigma = \int \frac{|\mathcal{M}|^2 |\vec{p}|}{64\pi^2 W^2 |\vec{k}|} d\Omega. \tag{3.16}$$

In case of elastic scattering, $|\vec{k}| = |\vec{p}|$, therefore:

$$\frac{d\sigma}{d\Omega}^{el} = \frac{|\mathcal{M}|^2}{64\pi^2 W^2} = |\mathcal{F}^{el}|^2 \tag{3.17}$$

with the elastic amplitude $\mathcal{F}^{el} = \dfrac{|\mathcal{M}|}{8\pi W}$.

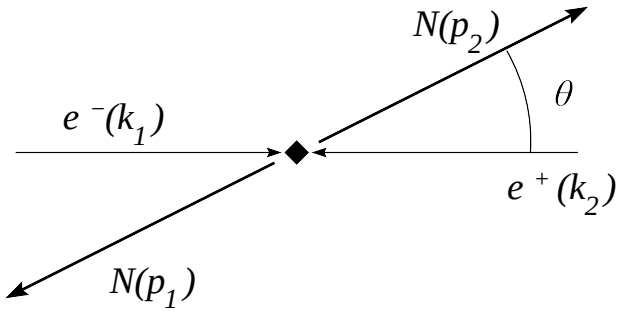

Fig. 3.1: Annihilation $e^- + e^+ \to \bar{N} + N$ in CMS system.

For the annihilation reaction considered here, $e^+ + e^- \to N + \bar{N}$, neglecting the mass of the electron, one has:

$$|\vec{k}| = \frac{W}{2},\ |\vec{p}| = \sqrt{E^2 - M^2} = E\sqrt{1 - M^2/E^2} = \frac{W}{2}\beta,$$

and

$$\frac{d\sigma}{d\Omega}^{ann} = \frac{|\mathcal{M}|^2\beta}{64\pi^2 q^2}, \tag{3.18}$$

where $\beta = \sqrt{1 - 4M^2/q^2}$ and $q^2 = s = (p_1 + p_2)^2$.

3.3 Axial parametrization of the matrix element

In presence of two photon exchange (TPE), the matrix element of the reaction $e^-(k_1) + e^+(k_2) \to \bar{N}(p_1) + N(p_2)$, can be parametrized by three complex amplitudes. In the present derivation we will use the following expression for the matrix element of this reaction, taking into account the TPE contribution,

$$\begin{aligned}\mathcal{M} \;=\; & -\frac{e^2}{q^2}\Big\{\bar{u}(-k_2)\gamma_\mu u(k_1)\bar{u}(p_2)\Big[\tilde{F}_1((k_1+k_2)^2,(k_1-p_1)^2)\gamma_\mu \\ & -\frac{\tilde{F}_2((k_1+k_2)^2,(k_1-p_1)^2)}{2m}\sigma_{\mu\nu}q_\nu\Big]u(-p_1) \\ & +\bar{u}(-k_2)\gamma_\mu\gamma_5 u(k_1)\bar{u}(p_2)\gamma_\mu\gamma_5 u(-p_1)A_N((k_1+k_2)^2,(k_1-p_1)^2)\Big\}, \end{aligned} \tag{3.19}$$

where m is nucleon mass, k_1 and k_2 are electron and positron four-momenta, p_1 and p_2 are antinucleon and nucleon four-momenta and $q = k_1 + k_2 = p_1 + p_2$. The first two

amplitudes contain the contributions of $1\gamma \bigotimes 2\gamma$ exchange, whereas the third amplitude is fully induced by 2γ exchange. A_N can be parametrized in different but equivalent ways. Here we use the axial parametrization that describes the exchange of a 1^+ particle. The spin and parity of the transition induced by TPE can be any, but the C-parity must be positive (whereas it is negative for 1γ exchange).

The three complex amplitudes, $\tilde{F}_{1N}, \tilde{F}_{2N}$ and A_N, which generally are functions of two independent kinematical variables, $(k_1+k_2)^2$ and $(k_1-p_1)^2$ fully describe the spin structure of the matrix element for the reaction $e^+ + e^- \to N + \bar{N}$ - for any number of exchanged virtual photons, because they contain C-odd and C-even terms.

This expression (3.19) holds under assumption of the P–invariance of the electromagnetic interaction and conservation of lepton helicity, which is correct for standard QED at the high energy, i.e., in zero electron mass limit. Note, however, that expression (3.19) is one of the many equivalent representations of the $e^+ + e^- \to N + \bar{N}$ reaction matrix element.

In the Born (1γ exchange) approximation these amplitudes reduce to:

$$\tilde{F}_1^{Born}((k_1+k_2)^2,(k_1-p_1)^2) = F_1(q^2), \quad \tilde{F}_2^{Born}(k_1+k_2)^2,(k_1-p_1)^2) = F_2(q^2),$$
$$A_N^{Born}((k_1+k_2)^2,(k_1-p_1)^2) = 0, \tag{3.20}$$

where $F_1(q^2)$ and $F_2(q^2)$ are the Dirac and Pauli nucleon electromagnetic form factors (FFs), respectively, and they are complex functions of the variable q^2. The complexity of FFs arises from the final–state strong interaction of the produced $N\bar{N}-$pair. In the following we use the standard magnetic $G_M(q^2)$ and charge $G_E(q^2)$ nucleon FFs which are related to FFs $F_1(q^2)$ and $F_2(q^2)$ as follows

$$G_M = F_1 + F_2,\ G_E = F_1 + \tau F_2,\ \tau = \frac{q^2}{4m^2} > 0. \tag{3.21}$$

By analogy with these relations, let us introduce a linear combinations of the $F_{1,2}(q^2,t)$ amplitudes which in the Born approximation correspond to the Sachs FFs G_M and G_E:

$$\begin{aligned} \tilde{G}_M((k_1+k_2)^2,(k_1-p_1)^2) &= \tilde{F}_1 + \tilde{F}_2, \\ \tilde{G}_E((k_1+k_2)^2,(k_1-p_1)^2) &= \tilde{F}_1 + \tau\tilde{F}_2. \end{aligned} \tag{3.22}$$

The matrix element (3.19) can be rewritten in terms of vector and axial electromagnetic

currents:

$$\mathcal{M} = -\frac{e^2}{q^2}\left(j_\mu^{(v)} J_\mu^{(v)} + j_\mu^{(a)} J_\mu^{(a)}\right), \tag{3.23}$$

where $j_\mu^{(v)}$, $j_\mu^{(a)}$ are vector and axial lepton currents and $J_\mu^{(v)}$, $J_\mu^{(a)}$ are vector and axial nucleon currents

$$j_\mu^{(v)} = \bar{u}(-k_2)\gamma_\mu u(k_1), \quad J_\mu^{(v)} = \bar{u}(p_2)\left[\tilde{F}_1\gamma_\mu - \frac{\tilde{F}_2}{2m}\sigma_{\mu\nu}q_\nu\right]u(-p_1),$$
$$j_\mu^{(a)} = \bar{u}(-k_2)\gamma_\mu\gamma_5 u(k_1), \quad J_\mu^{(a)} = \bar{u}(p_2)\gamma_\mu\gamma_5 u(-p_1)A_N,\ \sigma_{\mu\nu} = \frac{1}{2}[\gamma_\mu,\gamma_\nu]. \tag{3.24}$$

Then the differential cross section of the reaction $e^- + e^+ \to \bar{N} + N$ in CMS according to (3.18) can be written as

$$\begin{aligned}\frac{d\sigma}{d\Omega} &= \frac{\alpha^2\beta}{4q^6}\left(j_\mu^{(v)} J_\mu^{(v)} + j_\mu^{(a)} J_\mu^{(a)}\right)\left(j_\nu^{(v)} J_\nu^{(v)} + j_\nu^{(a)} J_\nu^{(a)}\right)^* \\ &= \frac{\alpha^2\beta}{4q^6}\left[L_{\mu\nu}^{(v)} H_{\mu\nu}^{(v)} + 2Re(L_{\mu\nu}^{(i)} H_{\mu\nu}^{(i)})\right],\ \alpha = \frac{e^2}{4\pi} = \frac{1}{137},\end{aligned}$$

where we neglected terms proportional to A_N^2 (since the amplitude A_N is entirely due to the TPE contribution, which is of the order of α). The 'vector' (v) and 'interference' (i) leptonic/hadronic tensors are defined as

$$L_{\mu\nu}^{(v)} = j_\mu^{(v)} j_\nu^{(v)*},\ L_{\mu\nu}^{(i)} = j_\mu^{(a)} j_\nu^{(v)*},\ H_{\mu\nu}^{(v)} = J_\mu^{(v)} J_\nu^{(v)*},\ H_{\mu\nu}^{(i)} = J_\mu^{(a)} J_\nu^{(v)*}. \tag{3.25}$$

Note that the term proportional to the Dirac-like FF, $\tilde{F}_1$, in the expression for the nucleon vector current, $J_\mu^{(v)}$, (3.24) is gauge invariant, when both particles $(N, \bar{N})$ are on mass shell. The second term proportional to the Pauli-like FF, $\tilde{F}_2$, is always gauge invariant:

$$(\sigma_{\mu\nu}q_\nu)q_\mu = \frac{1}{2}(\gamma_\mu\gamma_\nu - \gamma_\nu\gamma_\mu)q_\nu q_\mu = \frac{1}{2}(\hat{q}\hat{q} - \hat{q}\hat{q}) = 0.$$

It is possible to find other forms of the nucleon vector current $J_\mu^{(v)}$, which are equivalent only for on-shell particles. In our case nucleons are the final particles, therefore they are on-shell.

Let us show that for on-shell nucleons the expression for the $J_\mu^{(v)}$ (3.24) can be simplified by using Dirac equations[1] for particles (nucleon - p_2) and antiparticles (antinucleon

[1] It is correct only when nucleon and antinucleon are on mass shell (real particles), i.e., they satisfy the Dirac equation.

- p_1)

$$\begin{aligned} \bar{u}(p_2)(\hat{p}_2 - m) = 0 \quad &\Rightarrow \quad \bar{u}(p_2)\hat{p}_2 = \bar{u}(p_2)m \\ (\hat{p}_1 + m)u(-p_1) = 0 \quad &\Rightarrow \quad \hat{p}_1 u(-p_1) = -u(-p_1)m \end{aligned}$$

and the properties of Dirac matrices : $\{\gamma_\mu, \gamma_\nu\} = 2g_{\mu\nu}$, where $g_{\mu\nu}$ is the metric tensor of the Minkowski spacetime, $\hat{a}\hat{b} + \hat{b}\hat{a} = 2ab$, $\hat{a}\gamma_\mu + \gamma_\mu\hat{a} = 2a_\mu$, where a and b are four vectors.

Let us develop the term accompanying $\tilde{F}_2$:

$$\begin{aligned} \bar{u}(p_2)\sigma_{\mu\nu}q_\nu u(-p_1) &= \frac{1}{2}\bar{u}(p_2)\left(\gamma_\mu\gamma_\nu - \gamma_\nu\gamma_\mu\right)q_\nu u(-p_1) = \frac{1}{2}\bar{u}(p_2)\left(\gamma_\mu\hat{q} - \hat{q}\gamma_\mu\right)u(-p_1) \\ &= \frac{1}{2}\bar{u}(p_2)\left[\gamma_\mu(\hat{p}_1 + \hat{p}_2) - (\hat{p}_1 + \hat{p}_2)\gamma_\mu\right]u(-p_1) \\ &= \frac{1}{2}\bar{u}(p_2)\left[\gamma_\mu(-m + \hat{p}_2) - (\hat{p}_1 + m)\gamma_\mu\right]u(-p_1) \\ &= \frac{1}{2}\bar{u}(p_2)\left[-2m\gamma_\mu + (\gamma_\mu\hat{p}_2 - \hat{p}_1\gamma_\mu)\right]u(-p_1) \\ &= \frac{1}{2}\bar{u}(p_2)\left[-2m\gamma_\mu + (2p_{2\mu} - \hat{p}_2\gamma_\mu - 2p_{1\mu} + \gamma_\mu\hat{p}_1)\right]u(-p_1) \\ &= \frac{1}{2}\bar{u}(p_2)\left[-4m\gamma_\mu + 2(p_2 - p_1)_\mu\right]u(-p_1). \end{aligned} \tag{3.26}$$

Replacing in the expression for $J_\mu^{(v)}$, Eq. (3.24):

$$\begin{aligned} J_\mu^{(v)} &= \bar{u}(p_2)\left[(\tilde{F}_1 + \tilde{F}_2)\gamma_\mu - \frac{\tilde{F}_2}{2m}(p_2 - p_1)_\mu\right]u(-p_1) \\ &= \bar{u}(p_2)\left[\left(\tilde{F}_1 + \tilde{F}_2\right)\gamma_\mu - \frac{\tilde{F}_2}{m}P_\mu\right]u(-p_1), \end{aligned} \tag{3.27}$$

where $P = (p_2 - p_1)/2$ and $\tilde{F}_1$, $\tilde{F}_2$ can be substituted by generalized magnetic and charge nucleon FFs, Eq. (3.22):

$$J_\mu^{(v)} = \bar{u}(p_2)\left[\tilde{G}_{M,N}(q^2,t)\gamma_\mu - \frac{\tilde{G}_{M,N}(q^2,t) - \tilde{G}_{E,N}(q^2,t)}{m(1-\tau)}P_\mu\right]u(-p_1). \tag{3.28}$$

For simplicity, we will use in our calculations:

$$\frac{\tilde{G}_{M,N} - \tilde{G}_{E,N}}{m(1-\tau)} = G_{2N}. \tag{3.29}$$

3.4 Lepton and hadron tensors

We give a detailed derivation of the tensors, in particular of the lepton tensor, by explicating the matrix components.

3.4.1 Lepton tensors

The calculation of the leptonic tensors leads to the calculation of a trace. Let us give the explicit derivation. From Eqs. (3.24,3.25), the expression for the 'vector part' of the leptonic tensor is:

$$L_{\mu\nu}^{(v)} = \bar{u}(-k_2)\gamma_\mu u(k_1)\left[\bar{u}(-k_2)\gamma_\nu u(k_1)\right]^* . \tag{3.30}$$

Using the definition $\bar{u}(-k_2) = u^\dagger(-k_2)\gamma_4 = u^*(-k_2)\gamma_4$ and the following properties of the γ matrices: $\gamma_4^* = \gamma_4$, $(\gamma_4)_{ij} = (\gamma_4)_{ji}$, $(\gamma_4)_{kl}(\gamma_4)_{lm} = \delta_{km}$, the complex conjugated term can be written as

$$[\bar{u}(-k_2)\gamma_\nu u(k_1)]^* = [u^*(-k_2)\gamma_4\gamma_\nu u(k_1)]^* = u(-k_2)\gamma_4^*\gamma_\nu^* u^*(k_1). \tag{3.31}$$

In component form (with spinor indices):

$$\begin{aligned} u_i(-k_2)(\gamma_4^*)_{ij}(\gamma_\nu^*)_{jk}u^*(k_1)_k &= u(-k_2)_i(\gamma_4)_{ij}(\gamma_\nu^*)_{jk}\delta_{km}u^*(k_1)_m \\ &= u(-k_2)_i(\gamma_4)_{ij}(\gamma_\nu^*)_{jk}(\gamma_4)_{kl}(\gamma_4)_{lm}u^*(k_1)_m \\ &= u_m^*(k_1)(\gamma_4)_{ml}(\gamma_4)_{lk}(\gamma_\nu^\dagger)_{kj}(\gamma_4)_{ji}u_i(-k_2) \\ &= \bar{u}(k_1)\gamma_4\gamma_\nu^\dagger\gamma_4 u(-k_2) = \bar{u}(k_1)\gamma_\nu u(-k_2). \end{aligned}$$

Therefore

$$[\bar{u}(-k_2)\gamma_\nu u(k_1)]^* = \bar{u}(k_1)\gamma_\nu u(-k_2). \tag{3.32}$$

This result will be used all along the paper, with other terms between bispinors (γ_ν, $\gamma_\nu\gamma_5$, P_ν).

Let us write the tensor (3.30) in component form

$$\begin{aligned} L_{\mu\nu}^{(v)} &= \bar{u}_i(-k_2)(\gamma_\mu)_{ij}u(k_1)_j\bar{u}_a(k_1)(\gamma_\nu)_{ab}u_b(-k_2) \\ &= u_b(-k_2)\bar{u}_i(-k_2)(\gamma_\mu)_{ij}u_j(k_1)\bar{u}_a(k_1)(\gamma_\nu)_{ab} \\ &= (\rho_2)_{bi}(\gamma_\mu)_{ij}(\rho_1)_{ja}(\gamma_\nu)_{ab} = Tr[u(-k_2)\bar{u}(-k_2)\gamma_\mu u(k_1)\bar{u}(k_1)\gamma_\nu], \end{aligned} \tag{3.33}$$

where we applied the property that a product of matrices is a matrix and the first and last indices coincide: $Tr\mathrm{A} = \sum_b \mathrm{A}_{bb}$. The density matrices $\rho = u(p)\bar{u}(p)$ for polarized and unpolarized particles and antiparticles are given in the Table 3.1.

	particle	antiparticle
unpolarized	$\hat{p} + m$	$\hat{p} - m$
polarized	$(\hat{p} + m)\frac{1}{2}(1 - \gamma_5 \hat{s})$	$(\hat{p} - m)\frac{1}{2}(1 - \gamma_5 \hat{s})$

Tab. 3.1: The density matrices for polarized/unpolarized particles and antiparticles.

The polarization four-vector s is related to the unit vector along polarization of the particle in its rest system, $\vec{\xi}$ by

$$s_0 = \frac{1}{m}\vec{p}\cdot\vec{\xi}\,;\ \vec{s} = \vec{\xi} + \frac{\vec{p}(\vec{p}\cdot\vec{\xi})}{m(m+E)}. \tag{3.34}$$

Let us consider firstly unpolarized incoming positron and longitudinally polarized incoming electron. In this case the leptonic vector tensor, can be written as

$$L^{(v)}_{\mu\nu} = Tr\left[(\hat{k}_2 - m_e)\gamma_\mu(\hat{k}_1 + m_e)\frac{1}{2}(1 - \gamma_5\hat{s})\gamma_\nu\right] = L^{(v)}_{\mu\nu}(0) + L^{(v)}_{\mu\nu}(S) \tag{3.35}$$

and expanded as a sum over polarization states.

The unpolarized lepton tensor : $L^{(v)}_{\mu\nu}(0)$

Let us extract the part of the leptonic vector tensor which does not depend on polarization:

$$L^{(v)}_{\mu\nu}(0) = \frac{1}{2}Tr\left[(\hat{k}_2 - m_e)\gamma_\mu(\hat{k}_1 + m_e)\gamma_\nu\right] = \frac{1}{2}\left[Tr(\hat{k}_2\gamma_\mu\hat{k}_1\gamma_\nu) - m_e^2 Tr\left(\gamma_\mu\gamma_\nu\right)\right].$$

Using the rules for calculating the traces of Dirac matrices : $Tr\gamma_\mu\gamma_\nu = 4g_{\mu\nu}$ and $Tr\gamma_\rho\gamma_\mu\gamma_\sigma\gamma_\nu = 4(g_{\rho\mu}g_{\sigma\nu} + g_{\mu\sigma}g_{\nu\rho} - g_{\sigma\rho}g_{\mu\nu})$ one finds:

$$L^{(v)}_{\mu\nu}(0) = 2\left(k_{1\nu}k_{2\mu} + k_{1\mu}k_{2\nu} - k_1.k_2 g_{\mu\nu} - m_e^2 g_{\mu\nu}\right) = -q^2 g_{\mu\nu} + 2\left(k_{1\nu}k_{2\mu} + k_{1\mu}k_{2\nu}\right), \tag{3.36}$$

where we used identity

$$q^2 = (k_1 + k_2)^2 = k_1^2 + 2k_1k_2 + k_2^2 = 2(m_e^2 + k_1k_2) \Rightarrow k_1k_2 + m_e^2 = \frac{q^2}{2}. \tag{3.37}$$

The tensor describing an unpolarized electron is symmetric.

The polarized lepton tensor : $L^{(v)}_{\mu\nu}(S)$

For the polarized part of the lepton tensor one has

$$\begin{aligned} L^{(v)}_{\mu\nu}(S) &= -\frac{1}{2}Tr\left[(\hat{k}_2 - m_e)\gamma_\mu(\hat{k}_1 + m_e)\gamma_5\hat{s}\gamma_\nu\right] \\ &= -\frac{1}{2}m_e\left\{Tr\left[\gamma_5\hat{k}_2\gamma_\mu\hat{s}\gamma_\nu\right] - Tr\left[\gamma_5\gamma_\mu\hat{k}_1\hat{s}\gamma_\nu\right]\right\} \\ &= 2m_e i\left\langle k_2\mu s\nu\right\rangle - 2m_e i\left\langle \mu k_1 s\nu\right\rangle = 2m_e i\left\langle \mu\nu sq\right\rangle, \end{aligned} \tag{3.38}$$

where we used the notation

$$Tr(\gamma_5\gamma_\mu\gamma_\nu\gamma_\rho\gamma_\sigma) = -4i\varepsilon_{\mu\nu\rho\sigma} = -4i\left\langle \mu\nu\rho\sigma\right\rangle,$$

and the properties of permutations of Dirac matrices. The greek letters μ, ν are used for the uncontracted indices of the antisymmetric tensor $\varepsilon_{\mu\nu\rho\sigma}$.

One can check that the tensor $L^{(v)}_{\mu\nu}(S)$ (3.38) has the following property, which follows from current conservation:

$$q_\mu \cdot L^{(v)}_{\mu\nu}(S) = \varepsilon_{\mu\nu\sigma\rho}s_\sigma q_\rho q_\mu = 0$$

as it is the product of an antisymmetric tensor ($\varepsilon_{\mu\nu\sigma\rho}$) times a symmetric tensor $q_\rho q_\mu$.

When the electron is longitudinally polarized ($\vec{\xi} \parallel \vec{k}_1 \rightarrow \vec{\xi}\cdot\vec{k}_1 = |\vec{k}_1| = \sqrt{E^2 - m_e^2} \approx E$), the components of the polarization vector s_μ (Eq. 3.34) become

$$s_0 = \frac{E}{m_e}\ ;\ \vec{s} = \vec{\xi}\left(1 + \frac{|\vec{k}_1|^2}{m_e(m_e+E)}\right) = \vec{\xi}\left(1 + \frac{E^2 - m_e^2}{m_e(E+m_e)}\right) = \vec{\xi}\frac{E}{m_e},\ \text{i.e.,}\ s_\mu = \lambda_e\frac{k_{1\mu}}{m_e}, \tag{3.39}$$

where the helicity λ_e takes the values $= \pm 1$ if $\vec{\xi}$ is parallel or antiparallel to $\vec{k}_1$. One can see that the longitudinally polarized part of 'vector' lepton tensor (3.38) is not suppressed by the electron mass and it can be written as:

$$L^{(v)}_{\mu\nu}(S) = 2i\lambda_e\left\langle \mu\nu k_1 q\right\rangle. \tag{3.40}$$

Notice that the transversal component of the vector polarization remains unchanged and should be evaluated from (3.38).

The unpolarized lepton tensor : $L^{(i)}_{\mu\nu}(0)$

According to (3.24) and (3.25)

$$L^{(i)}_{\mu\nu} = \bar{u}(-k_2)\gamma_\mu\gamma_5 u(k_1)\left[\bar{u}(-k_2)\gamma_\nu u(k_1)\right]^* = \bar{u}(-k_2)\gamma_\mu\gamma_5 u(k_1)\bar{u}(k_1)\gamma_\nu u(-k_2),$$

resp.

$$\begin{aligned} L^{(i)}_{\mu\nu} &= Tr\left[u(-k_2)\bar{u}(-k_2)\gamma_\mu\gamma_5 u(k_1)\bar{u}(k_1)\gamma_\nu\right] \\ &= Tr\left[(\hat{k}_2 - m_e)\gamma_\mu\gamma_5(\hat{k}_1 + m_e)\frac{1}{2}(1-\gamma_5\hat{s})\gamma_\nu\right]. \end{aligned} \tag{3.41}$$

Again it can be divided to polarized and unpolarized part. For the unpolarized part

$$L^{(i)}_{\mu\nu}(0) = \frac{1}{2}Tr\left[(\hat{k}_2 - m_e)\gamma_\mu\gamma_5(\hat{k}_1 + m_e)\gamma_\nu\right] = \frac{1}{2}Tr\left[\gamma_5\hat{k}_2\gamma_\mu\hat{k}_1\gamma_\nu\right], \tag{3.42}$$

which can be expressed as

$$L^{(i)}_{\mu\nu}(0) = \frac{1}{2}(-4i)\varepsilon_{\rho\mu\sigma\nu}k_{2\rho}k_{1\sigma} = 2i\left\langle\mu\nu k_2 k_1\right\rangle. \tag{3.43}$$

The polarized lepton tensor : $L^{(i)}_{\mu\nu}(S)$

The polarized part of $L^{(i)}_{\mu\nu}$ is written as:

$$\begin{aligned} L^{(i)}_{\mu\nu}(S) &= -\frac{1}{2}Tr\left[(\hat{k}_2 - m_e)\gamma_\mu\gamma_5(\hat{k}_1 + m_e)\gamma_5\hat{s}\gamma_\nu\right] \\ &= -\frac{1}{2}Tr\left[(\hat{k}_2 - m_e)\gamma_\mu m_e\hat{s}\gamma_\nu\right] + \frac{1}{2}Tr\left[(\hat{k}_2 - m_e)\gamma_\mu\hat{k}_1\hat{s}\gamma_\nu\right], \end{aligned} \tag{3.44}$$

where we used $\gamma_5^2 = 1$. Eq. (3.44) can be simplified to

$$\begin{aligned} L^{(i)}_{\mu\nu}(S) &= -\frac{m_e}{2}\left[Tr(\hat{k}_2\gamma_\mu\hat{s}\gamma_\nu) - Tr(\gamma_\mu\hat{k}_1\hat{s}\gamma_\nu)\right] \\ &= -2m_e\left[k_{2\mu}s_\nu + k_{2\nu}s_\mu - k_2\cdot s g_{\mu\nu} - k_{1\mu}s_\nu + k_{1\nu}s_\mu - k_1\cdot s g_{\mu\nu}\right]. \end{aligned}$$

In case of longitudinally polarized electron beam, with the help of Eq. (3.39), this expression simplifies to:

$$L^{(i)}_{\mu\nu}(S) = \lambda_e[q^2 g_{\mu\nu} - 2(k_{2\mu}k_{1\nu} + k_{2\nu}k_{1\mu})]. \tag{3.45}$$

Lepton tensor summary

The leptonic tensors for the case of longitudinally polarized electrons

$$L^{(v)}_{\mu\nu} = -q^2 g_{\mu\nu} + 2(k_{1\mu}k_{2\nu} + k_{1\nu}k_{2\mu}) + 2i\lambda_e \langle \mu\nu k_1 q \rangle \quad (3.46)$$

$$L^{(i)}_{\mu\nu} = 2i \langle \mu\nu k_2 k_1 \rangle + \lambda_e[q^2 g_{\mu\nu} - 2(k_{1\mu}k_{2\nu} + k_{1\nu}k_{2\mu})], \quad (3.47)$$

where λ_e is the degree of the electron longitudinal polarization. We will consider that the lepton is fully polarized, i.e., $|\lambda_e| = 1$, but it shows explicitly which part of the leptonic tensor depends on polarization of the incoming electron.

3.4.2 Hadron tensors

According to the definitions (3.25) and (3.28), $H^{(v)}_{\mu\nu}$ can be expressed as

$$\begin{aligned} H^{(v)}_{\mu\nu} &= \bar{u}(p_2)\left[G_M\gamma_\mu - G_2 P_\mu\right] u(-p_1)\left[\bar{u}(p_2)\left[G_M\gamma_\nu - G_2 P_\nu\right] u(-p_1)\right]^* \\ &= \bar{u}(p_2)\left[G_M\gamma_\mu - G_2 P_\mu\right] u(-p_1)\bar{u}(-p_1)\left[G^*_M\gamma_\nu - G^*_2 P_\nu\right] u(p_2) \\ &= Tr\left[u(p_2)\bar{u}(p_2)\left[G_M\gamma_\mu - G_2 P_\mu\right] u(-p_1)\bar{u}(-p_1)\left[G^*_M\gamma_\nu - G^*_2 P_\nu\right]\right]. \end{aligned} \quad (3.48)$$

Generally, taking into account the polarization states of the produced nucleon and antinucleon, the hadronic tensor can be written as the sum of three contributions

$$H_{\mu\nu} = H_{\mu\nu}(0) + H_{\mu\nu}(s_1) + H_{\mu\nu}(s_1, s_2), \quad (3.49)$$

where the tensor $H_{\mu\nu}(0)$ describes the production of unpolarized particles, the tensor $H_{\mu\nu}(s_1)$ describes the production of polarized nucleon or antinucleon and the tensor $H_{\mu\nu}(s_1, s_2)$ corresponds to the production of both polarized particles (N and $\bar{N}$).

According to this notation and using the expressions of the density matrices from Table 3.1, Eq. (3.48) can be written as:

$$H^{(v)}_{\mu\nu} = Tr\left\{(\hat{p}_2 + m)\left[\tilde{G}_M\gamma_\mu - G_2 P_\mu\right](\hat{p}_1 - m)\frac{1}{2}(1 - \gamma_5\hat{s}_1)\left[\tilde{G}^*_M\gamma_\nu - G^*_2 P_\nu\right]\right\}, \quad (3.50)$$

which can be considered as a sum of polarized and unpolarized parts (similarly to the leptonic tensor), $s_{1\mu}$ is the polarization four-vector of the antinucleon.

The unpolarized hadron tensor : $H^{(v)}_{\mu\nu}(0)$

The unpolarized part of $H^{(v)}_{\mu\nu}$ can be extracted from (3.50)

$$\begin{aligned} H^{(v)}_{\mu\nu}(0) &= \frac{1}{2}Tr\left[(\hat{p}_2+m)\left(\tilde{G}_M\gamma_\mu - G_2P_\mu\right)(\hat{p}_1-m)\left(\tilde{G}^*_M\gamma_\nu - G^*_2P_\nu\right)\right] \\ &= \frac{1}{2}\Big[\tilde{G}_M\tilde{G}^*_M Tr(\hat{p}_2\gamma_\mu\hat{p}_1\gamma_\nu) + m\tilde{G}_M G^*_2P_\nu Tr(\hat{p}_2\gamma_\mu) + G_2G^*_2P_\mu P_\nu Tr(\hat{p}_2\hat{p}_1) \\ &+ m\tilde{G}^*_M G_2P_\mu Tr(\hat{p}_2\gamma_\nu) - m\tilde{G}_M G^*_2P_\nu Tr(\gamma_\mu\hat{p}_1) - m^2\tilde{G}_M\tilde{G}^*_M Tr(\gamma_\mu\gamma_\nu) \\ &- m\tilde{G}^*_M G_2P_\mu Tr(\hat{p}_1\gamma_\nu) - m^2G_2G^*_2P_\mu P_\nu Tr\hat{1}\Big] \end{aligned}$$

where we omit the terms containing an odd number of γ matrices, since their trace vanishes, and further simplify as:

$$\begin{aligned} H^{(v)}_{\mu\nu}(0) &= 2\Big[|\tilde{G}_M|^2(p_{1\mu}p_{2\nu} + p_{1\nu}p_{2\mu} - (p_1p_2+m^2)g_{\mu\nu}) \\ &+ P_\mu P_\nu\big(|G_2|^2(p_1p_2-m^2) + 4mRe\tilde{G}_MG^*_2\big)\Big]. \end{aligned}$$

Now we can apply following identities

$$p_1p_2 + m^2 = \frac{q^2}{2}\ ;\ p_1p_2 - m^2 = 2m^2(\tau-1)\ ;\ p_{1\mu}p_{2\nu} + p_{1\nu}p_{2\mu} = \frac{q_\mu q_\nu}{2} - 2P_\mu P_\nu \qquad (3.51)$$

to obtain

$$H^{(v)}_{\mu\nu}(0) = H_1\tilde{g}_{\mu\nu} + H_2P_\mu P_\nu, \qquad (3.52)$$

where $\tilde{g}_{\mu\nu} = g_{\mu\nu} - q_\mu q_\nu/q^2$ and

$$\begin{aligned} H_1 &= -q^2|\tilde{G}_M|^2 \qquad (3.53) \\ H_2 &= 4\left[m^2|G_2|^2(\tau-1) - |\tilde{G}_M|^2 + 2mRe(\tilde{G}_MG^*_2)\right]. \end{aligned}$$

The formula for H_2 can be rewritten in terms of G_M and G_E

$$H_2 = \frac{4}{\tau-1}\left[|\tilde{G}_E|^2 - \tau|\tilde{G}_M|^2\right]. \qquad (3.54)$$

The polarized hadron tensor : $H^{(v)}_{\mu\nu}(s_1)$

The polarized part of $H^{(v)}_{\mu\nu}$ (also from (3.50))

$$\begin{aligned} H^{(v)}_{\mu\nu}(s_1) &= -\frac{1}{2}Tr\left[(\hat{p}_2+m)\left(\tilde{G}_M\gamma_\mu - G_2P_\mu\right)(\hat{p}_1-m)\gamma_5\hat{s}_1\left(\tilde{G}^*_M\gamma_\nu - G^*_2P_\nu\right)\right] \\ &= \frac{1}{2}\Big[Tr(\hat{p}_2\tilde{G}_M\gamma_\mu\hat{p}_1\gamma_5\hat{s}_1G^*_2P_\nu) + Tr(\hat{p}_2\tilde{G}_M\gamma_\mu m\gamma_5\hat{s}_1\tilde{G}^*_M\gamma_\nu) \\ &+ Tr(\hat{p}_2G_2P_\mu\hat{p}_1\gamma_5\hat{s}_1\tilde{G}^*_M\gamma_\nu) - Tr(m\tilde{G}_M\gamma_\mu\hat{p}_1\gamma_5\hat{s}_1\tilde{G}^*_M\gamma_\nu) \\ &= \frac{1}{2}\Big[-\tilde{G}_MG^*_2P_\nu Tr(\gamma_5\hat{p}_2\gamma_\mu\hat{p}_1\hat{s}_1) + m|\tilde{G}_M|^2Tr(\gamma_5\hat{p}_2\gamma_\mu\hat{s}_1\gamma_\nu) \\ &+ \tilde{G}^*_MG_2P_\mu Tr(\gamma_5\hat{p}_2\hat{p}_1\hat{s}_1\gamma_\nu) - m|\tilde{G}_M|^2Tr(\gamma_5\gamma_\mu\hat{p}_1\hat{s}_1\gamma_\nu)\Big] \end{aligned}$$

can be simplified

$$\begin{aligned} H^{(v)}_{\mu\nu}(s_1) &= 2i\Big[\tilde{G}_MG^*_2P_\nu\left\langle p_2\mu p_1s_1\right\rangle + m|\tilde{G}_M|^2(\left\langle\mu p_1s_1\nu\right\rangle - \left\langle p_2\mu s_1\nu\right\rangle) \\ &- \tilde{G}^*_MG_2P_\mu\left\langle p_2p_1s_1\nu\right\rangle\Big] \\ &= 2i\Big[(\tilde{G}_MG^*_2)^*P_\mu\left\langle\nu p_2p_1s_1\right\rangle - \tilde{G}_MG^*_2P_\nu\left\langle\mu p_2p_1s_1\right\rangle + m|\tilde{G}_M|^2\left\langle\mu\nu qs_1\right\rangle\Big], \end{aligned}$$

or alternatively in terms of $\tilde{G}_M$ and $\tilde{G}_E$

$$\begin{aligned} H^{(v)}_{\mu\nu}(s_1) &= \frac{2}{m(\tau-1)}\Big[im^2(\tau-1)|\tilde{G}_M|^2\left\langle\mu\nu qs_1\right\rangle \\ &+ iRe(\tilde{G}_M(\tilde{G}_E-\tilde{G}_M)^*)(P_\mu\left\langle\nu p_2p_1s_1\right\rangle - P_\nu\left\langle\mu p_2p_1s_1\right\rangle) \\ &+ Im(\tilde{G}_M\tilde{G}^*_E)(P_\mu\left\langle\nu p_2p_1s_1\right\rangle + P_\nu\left\langle\mu p_2p_1s_1\right\rangle)\Big], \end{aligned} \tag{3.55}$$

where we used $Im|G_M|^2 = 0$ and identity

$$Re(A)(P_\mu Q_\nu - P\nu Q_\mu) - iIm(A)(P_\mu Q_\nu + P\nu Q_\mu) = A^*P_\mu Q_\nu - AP_\nu Q_\mu,$$

which can be easily proved. Notice, that the first 2 terms in equation (3.55) are anti-symmetric and the third (last) term is symmetric with aspect to the exchange $\mu \leftrightarrow \nu$.

The unpolarized hadron tensor : $H^{(i)}_{\mu\nu}(0)$

Using the definitions (3.25) and (3.28)

$$\begin{aligned} H^{(i)}_{\mu\nu} &= \bar{u}(p_2)\gamma_\mu\gamma_5u(-p_1)A_N\left[\bar{u}(p_2)(\tilde{G}_M\gamma_\nu - G_2P_\nu)u(-p_1)\right]^* \\ &= Tr\left[(\hat{p}_2+m)\gamma_\mu\gamma_5A_N(\hat{p}_1-m)\frac{1}{2}(1-\gamma_5\hat{s}_1)(\tilde{G}^*_M\gamma_\nu - G^*_2P_\nu)\right], \end{aligned} \tag{3.56}$$

which gives for the unpolarized part

$$\begin{aligned} H^{(i)}_{\mu\nu}(0) &= \frac{1}{2}Tr\left[(\hat{p}_2+m)\gamma_\mu\gamma_5 A_N(\hat{p}_1-m)(\tilde{G}^*_M\gamma_\nu - G^*_2P_\nu)\right] \\ &= \frac{1}{2}A_N\tilde{G}^*_M Tr[\gamma_5\hat{p}_2\gamma_\mu\hat{p}_1\gamma_\nu] = 2iA_N\tilde{G}^*_M\left\langle\mu\nu p_2 p_1\right\rangle. \end{aligned} \tag{3.57}$$

The polarized hadron tensor : $H^{(i)}_{\mu\nu}(s_1)$

The polarized part of $H^{(i)}_{\mu\nu}$ follows from Eq. (3.56)

$$\begin{aligned} H^{(i)}_{\mu\nu}(s_1) &= -\frac{1}{2}Tr\left[(\hat{p}_2+m)\gamma_\mu\gamma_5 A_N(\hat{p}_1-m)\gamma_5\hat{s}_1(\tilde{G}^*_M\gamma_\nu - G^*_2P_\nu)\right] \\ &= \frac{1}{2}A_N\Big[Tr[(\hat{p}_2+m)\gamma_\mu m\hat{s}_1(\tilde{G}^*_M\gamma_\nu - G^*_2P_\nu)] \\ &+ Tr[(\hat{p}_2+m)\gamma_\mu\hat{p}_1\hat{s}_1(\tilde{G}^*_M\gamma_\nu - G^*_2P_\nu)]\Big] \\ &= \frac{1}{2}A_N\Big[-m^2G^*_2P_\nu Tr[\gamma_\mu\hat{s}_1] + m\tilde{G}^*_M Tr[\hat{p}_2\gamma_\mu\hat{s}_1\gamma_\nu] \\ &- G^*_2P_\nu Tr[\hat{p}_2\gamma_\mu\hat{p}_1\hat{s}_1] + m\tilde{G}^*_M Tr[\gamma_\mu\hat{p}_1\hat{s}_1\gamma_\nu]\Big] \end{aligned} \tag{3.58}$$

and by applying rules for traces we get

$$\begin{aligned} H^{(i)}_{\mu\nu}(s_1) &= 2A_N\Big[-m^2G^*_2P_\nu s_{1\mu} - G^*_2P_\nu(p_{2\mu}p_1\cdot s_1 + p_{1\mu}p_2\cdot s_1 - p_1\cdot p_2 s_{1\mu}) \\ &+ m\tilde{G}^*_M(p_{2\mu}s_{1\nu} + p_{2\nu}s_{1\mu} - p_2\cdot s_1 g_{\mu\nu} + p_{1\mu}s_{1\nu} - p_{1\nu}s_{1\mu} + p_1\cdot s_1 g_{\mu\nu})\Big], \end{aligned} \tag{3.59}$$

where

$$s_1\cdot p_1 = 0\,;\; s_1\cdot p_2 = s_1\cdot q,$$

while $s_{1\mu}$ is polarization four-vector of the antinucleon. Using Eq. (3.51) it can be simplified (3.59) to

$$\begin{aligned} H^{(i)}_{\mu\nu}(s_1) &= 2A_N\Big[2m^2(\tau-1)G^*_2P_\nu s_{1\mu} - G^*_2P_\nu p_{1\mu}s_1\cdot q - m\tilde{G}^*_M q\cdot s_1 g_{\mu\nu} \\ &+ m\tilde{G}^*_M(p_{2\mu}s_{1\nu} + p_{2\nu}s_{1\mu} + p_{1\mu}s_{1\nu} - p_{1\nu}s_{1\mu})\Big], \end{aligned} \tag{3.60}$$

which can be rewritten in terms of the generalized Sachs FFs as

$$\begin{aligned} H^{(i)}_{\mu\nu}(s_1) &= mA_N\Big[-2q\cdot s_1\tilde{G}^*_M g_{\mu\nu} - \frac{2q\cdot s_1}{m^2(1-\tau)}(\tilde{G}_M-\tilde{G}_E)^* p_{1\mu}P_\nu \\ &+ (\tilde{G}_M+\tilde{G}_E)^*(s_{1\mu}p_{2\nu} + s_{1\nu}p_{2\mu}) + (\tilde{G}_M-\tilde{G}_E)^*(s_{1\mu}p_{1\nu} + s_{1\nu}p_{1\mu}) \\ &- (\tilde{G}_M+\tilde{G}_E)^*(s_{1\mu}p_{1\nu} - s_{1\nu}p_{1\mu}) - (\tilde{G}_M-\tilde{G}_E)^*(s_{1\mu}p_{2\nu} - s_{1\nu}p_{2\mu})\Big], \end{aligned} \tag{3.61}$$

where we can distinguish two antisymmetric terms and three symmetric terms *(and the term proportional to $p_{1\mu}P_\nu$)* :

$$2p_{1\mu}P_\nu = p_{1\mu}P_\nu + p_{1\nu}P_\mu + p_{1\mu}P_\nu - p_{1\nu}P_\mu.$$

3.5 Differential cross section

The differential cross section can be written as the sum of unpolarized and polarized terms, corresponding to the different polarization states and polarization direction of the incident and scattered particles. In our case we consider just polarization of the outgoing antinucleon and longitudinal polarization of the incoming electron (with the degree of polarization λ_e).

$$\frac{d\sigma}{d\Omega} = \frac{d\sigma_{un}}{d\Omega}\left[1 + P_y\xi_y + \lambda_e P_x\xi_x + \lambda_e P_z\xi_z\right]. \tag{3.62}$$

3.5.1 Unpolarized differential cross section

The unpolarized differential cross section can be written as

$$\frac{d\sigma_{un}}{d\Omega} = \frac{\alpha^2\beta}{4q^6}\left[L^{(v)}_{\mu\nu}(0)H^{(v)}_{\mu\nu}(0) + 2Re(L^{(i)}_{\mu\nu}(0)H^{(i)}_{\mu\nu}(0))\right] = \frac{\alpha^2\beta}{4q^2}D,$$

where $\beta = \sqrt{1-4m^2/q^2}$ is nucleon velocity in CMS and

$$D = \frac{1}{q^4}\left[L^{(v)}_{\mu\nu}(0)H^{(v)}_{\mu\nu}(0) + 2Re(L^{(i)}_{\mu\nu}(0)H^{(i)}_{\mu\nu}(0))\right]. \tag{3.63}$$

Let us calculate the first term of D. According to Eqs. (3.36) and (3.52)

$$\begin{aligned} L^{(v)}_{\mu\nu}(0)H^{(v)}_{\mu\nu}(0) &= \left[-q^2 g_{\mu\nu} + 2\left(k_{1\nu}k_{2\mu} + k_{1\mu}k_{2\nu}\right)\right] \times \left[H_1\tilde{g}_{\mu\nu} + H_2 P_\mu P_\nu\right] \\ &= -H_1 q^2(4 - \frac{q^2}{q^2}) - H_2 q^2 P^2 + 4H_1\left(k_1.k_2 - \frac{(k_1.q)(k_2.q)}{q^2}\right) \\ &+ 4H_2(k_1.P)(k_2.P), \end{aligned} \tag{3.64}$$

where $k_1.k_2 = k_1.q = k_2.q = q^2/2$ and

$$P^2 = \frac{(m^2 - p_1.p_2)}{2} = \frac{m^2 - (E^2 - \vec{p}_1.\vec{p}_2)}{2} = m^2 - E^2 = m^2(1-\tau), \tag{3.65}$$

where $E^2 = q^2/4$ and $m^2 = E^2 - \vec{p}_1^{\,2}$.

Let us define a coordinate frame in CMS of the reaction $e^+ + e^- \to N + \bar{N}$ in such a way that the z axis is directed along the three-momentum of the antinucleon ($\vec{p}_1$). Therefore, the components of four-momenta can be written as

$$\begin{aligned} p_1 = (E, 0, 0, |\vec{p}_1|) \quad &; \quad k_1 = (E, -|\vec{k}_1|\sin\theta, 0, |\vec{k}_1|\cos\theta) \\ p_2 = (E, 0, 0, -|\vec{p}_1|) \quad &; \quad k_2 = (E, |\vec{k}_1|\sin\theta, 0, -|\vec{k}_1|\cos\theta) \\ q = (2E, 0, 0, 0) \quad &; \quad P = (0, 0, 0, -|\vec{p}_1|), \end{aligned} \tag{3.66}$$

where $|\vec{k}_1| = E = m\sqrt{\tau}$, $|\vec{p}_1| = \sqrt{E^2 - m^2} = m\sqrt{\tau - 1}$ and θ is the angle between electron and detected antinucleon momenta. These identities and definitions lead to

$$\begin{aligned} L^{(v)}_{\mu\nu}(0) H^{(v)}_{\mu\nu}(0) &= 2q^4 |\tilde{G}_M|^2 + 4m^2 q^2 (|\tilde{G}_E|^2 - \tau |\tilde{G}_M|^2) \\ &- \frac{16}{\tau - 1} (|\tilde{G}_E|^2 - \tau |\tilde{G}_M|^2) |\vec{k}_1|^2 |\vec{p}_1|^2 \cos^2\theta \\ &= q^4 \left[|\tilde{G}_M|^2 + \frac{1}{\tau} |\tilde{G}_E|^2 - \frac{1}{\tau} (|\tilde{G}_E|^2 - \tau |\tilde{G}_M|^2) \cos^2\theta \right] \\ &= q^4 \left[|\tilde{G}_M|^2 (1 + \cos^2\theta) + \frac{1}{\tau} |\tilde{G}_E|^2 \sin^2\theta \right]. \end{aligned} \tag{3.67}$$

The second term of D can be written according to Eqs. (3.43) and (3.57) as

$$L^{(i)}_{\mu\nu}(0) H^{(i)}_{\mu\nu}(0) = 2i \langle \mu\nu k_2 k_1 \rangle \times 2i A_N \tilde{G}^*_M \langle \mu\nu p_2 p_1 \rangle ,$$

which can be written as (see appendix)

$$\begin{aligned} L^{(i)}_{\mu\nu}(0) H^{(i)}_{\mu\nu}(0) &= -4 A_N \tilde{G}^*_M 2 \left((k_2.p_1)(k_1.p_2) - (k_2.p_2)(k_1.p_1) \right) \\ &= q^4 \left[-2 A_N \tilde{G}^*_M \frac{1}{\tau} \sqrt{\tau(\tau - 1)} \cos\theta \right]. \end{aligned} \tag{3.68}$$

Finally we get the following expression for D

$$D = |\tilde{G}_M|^2 (1 + \cos^2\theta) + \frac{1}{\tau} |\tilde{G}_E|^2 \sin^2\theta - \frac{4}{\tau} \sqrt{\tau(\tau - 1)} \cos\theta \, Re \tilde{G}_M A^*_N. \tag{3.69}$$

3.5.2 Single spin polarization observables, antiproton polarization P_y

P_y is a single-spin polarization observable, which appears in the Born approximation in the $e^- + e^+ \to N + \bar{N}$ process with one polarized particle - the antinucleon ($\bar{N}$), which

is polarized along the y-axis. It is shown below, that this observable doesn't depend on polarization of electron. Polarization of antinucleon along y-axis means, that its polarization unit vector $\vec{\xi}$ has only y-component ($\vec{\xi} = (0,1,0)$). This leads to following properties of antinucleon s_{1y} (3.34), (3.66)

$$\vec{p_1} \cdot \vec{\xi} = 0 \Rightarrow s_{10} = 0\,;\ \vec{s}_{1y} = \vec{\xi} = (0,1,0). \tag{3.70}$$

The general expression for P_y is

$$\begin{aligned} P_y &= \frac{\alpha^2\beta}{4q^6}\left[L^{(v)}_{\mu\nu}H^{(v)}_{\mu\nu}(s_{1y}) + 2Re(L^{(i)}_{\mu\nu}H^{(i)}_{\mu\nu}(s_{1y}))\right] \Big/ \frac{d\sigma_{un}}{d\Omega} \\ &= \frac{1}{Dq^4}\left[L^{(v)}_{\mu\nu}H^{(v)}_{\mu\nu}(s_{1y}) + 2Re(L^{(i)}_{\mu\nu}H^{(i)}_{\mu\nu}(s_{1y}))\right], \end{aligned} \tag{3.71}$$

which can be divided into two parts - with unpolarized electron and with polarized electron

$$\begin{aligned} P_y &= \frac{1}{Dq^4}\left[L^{(v)}_{\mu\nu}(0)H^{(v)}_{\mu\nu}(s_{1y}) + 2Re(L^{(i)}_{\mu\nu}(0)H^{(i)}_{\mu\nu}(s_{1y}))\right] \\ &+ \frac{1}{Dq^4}\left[L^{(v)}_{\mu\nu}(S)H^{(v)}_{\mu\nu}(s_{1y}) + 2Re(L^{(i)}_{\mu\nu}(S)H^{(i)}_{\mu\nu}(s_{1y}))\right]. \end{aligned}$$

At first we will prove, that longitudinally polarized electron doesn't contribute to polarization observable P_y. The first term of the polarized electron part equals (3.40), (3.55) for $\lambda_e = 1$:

$$\begin{aligned} L^{(v)}_{\mu\nu}(S)H^{(v)}_{\mu\nu}(s_{1y}) &= 2i\,\langle\mu\nu k_1 q\rangle \times \frac{2}{m(\tau-1)}\Big[im^2(\tau-1)|\tilde{G}_M|^2\,\langle\mu\nu q s_{1y}\rangle \\ &+ iRe(\tilde{G}_M(\tilde{G}_E - \tilde{G}_M)^*)(P_\mu\,\langle\nu p_2 p_1 s_{1y}\rangle - P_\nu\,\langle\mu p_2 p_1 s_{1y}\rangle) \\ &+ Im(\tilde{G}_M\tilde{G}^*_E)(P_\mu\,\langle\nu p_2 p_1 s_{1y}\rangle + P_\nu\,\langle\mu p_2 p_1 s_{1y}\rangle)\Big]. \end{aligned}$$

The lepton tensor is antisymmetric, therefore its product with the third (symmetric) part of the hadron tensor vanishes. The first product is proportional to

$$\langle\mu\nu k_1 q\rangle \times \langle\mu\nu q s_{1y}\rangle = 2(k_1\cdot s_{1y}\ q^2 - k_1\cdot q\ s_{1y}\cdot q) = 0, \tag{3.72}$$

where we used (3.66, 3.70) $k_1.s_{1y} = s_{1y}.q = 0$. The second product is proportional to

$$\begin{aligned} &\langle\mu\nu k_1 q\rangle \times (P_\mu\,\langle\nu p_2 p_1 s_{1y}\rangle - P_\nu\,\langle\mu p_2 p_1 s_{1y}\rangle) = -2\,\langle\nu P k_1 q\rangle\,\langle\nu p_2 p_1 s_{1y}\rangle \\ &= -2\big[P\cdot p_2(k_1\cdot s_{1y}\ q\cdot p_1 - k_1\cdot p_1\ q\cdot s_{1y}) + P\cdot p_1(k_1\cdot p_2\ q\cdot s_{1y} - k_1\cdot s_{1y}\ q\cdot p_2) \\ &+ P\cdot s_{1y}(k_1\cdot p_1\ q\cdot p_2 - k_1\cdot p_2\ q\cdot p_1)\big] = 0, \end{aligned} \tag{3.73}$$

where again Eqs. (3.66, 3.70) was used ($P \cdot s_{1y} = q \cdot s_{1y} = k_1 \cdot s_{1y} = 0$).

The second part of the polarized electron part of P_y (3.45), (3.61)

$$\begin{aligned} & L^{(i)}_{\mu\nu}(s) H^{(i)}_{\mu\nu}(s_{1y}) = \left[q^2 g_{\mu\nu} - 2(k_{2\mu}k_{1\nu} + k_{2\nu}k_{1\mu})\right] \times \\ \times \quad & mA_N \Big[-2q \cdot s_{1y} \tilde{G}^*_M g_{\mu\nu} - \frac{2q.s_{1y}}{m^2(1-\tau)} (\tilde{G}_M - \tilde{G}_E)^* p_{1\mu} P_\nu \\ + \quad & (\tilde{G}_M + \tilde{G}_E)^* (s_{1y\mu} p_{2\nu} + s_{1y\nu} p_{2\mu}) + (\tilde{G}_M - \tilde{G}_E)^* (s_{1y\mu} p_{1\nu} + s_{1y\nu} p_{1\mu}) \\ - \quad & (\tilde{G}_M + \tilde{G}_E)^* (s_{1y\mu} p_{1\nu} - s_{1y\nu} p_{1\mu}) - (\tilde{G}_M - \tilde{G}_E)^* (s_{1y\mu} p_{2\nu} - s_{1y\nu} p_{2\mu}) \Big], \end{aligned}$$

where taking into account that $q \cdot s_{1y} = 0$ and that the product of a symmetric tensor ($L^{(i)}_{\mu\nu}$) and an antisymmetric tensor is zero leads to

$$\begin{aligned} L^{(i)}_{\mu\nu}(s_1) H^{(i)}_{\mu\nu}(s_{1y}) &= 2q^2 m A_N \Big[\tilde{(G_M + G_E)}^* s_{1y} \cdot p_2 + (\tilde{G}_M - \tilde{G}_E)^* s_{1y} \cdot p_1 \Big) \\ &- 4m A_N \big((\tilde{G}_M + \tilde{G}_E)^* (k_2 \cdot s_{1y}\ k_1 \cdot p_2 + k_1 \cdot s_{1y}\ k_2 \cdot p_2) \\ &+ (\tilde{G}_M - \tilde{G}_E)^* (k_2.s_{1y}\ k_1 \cdot p_1 + k_1 \cdot s_{1y}\ k_2 \cdot p_1) \big) = 0, \end{aligned} \tag{3.74}$$

while $k_2 \cdot s_{1y} = k_1 \cdot s_{1y} = p_1 \cdot s_{1y} = p_2 \cdot s_{1y} = 0$.

Therefore, the polarization observable P_y depends only on the unpolarized part

$$P_y = \frac{1}{Dq^4} \left[L^{(v)}_{\mu\nu}(0) H^{(v)}_{\mu\nu}(s_{1y}) + 2Re(L^{(i)}_{\mu\nu}(0) H^{(i)}_{\mu\nu}(s_{1y})) \right]. \tag{3.75}$$

With the help of Eqs. (3.36, 3.55), the first term is equal to

$$\begin{aligned} L^{(v)}_{\mu\nu}(s) H^{(v)}_{\mu\nu}(s_{1y}) &= \left[-q^2 g_{\mu\nu} + 2\left(k_{1\nu}k_{2\mu} + k_{1\mu}k_{2\nu}\right) \right] \\ &\times \frac{2}{m(\tau-1)} \Big[im^2(\tau-1) |\tilde{G}_M|^2 \langle \mu\nu q s_{1y} \rangle \\ &+ iRe(\tilde{G}_M (\tilde{G}_E - \tilde{G}_M)^*) (P_\mu \langle \nu p_2 p_1 s_{1y} \rangle - P_\nu \langle \mu p_2 p_1 s_{1y} \rangle) \\ &+ Im(\tilde{G}_M \tilde{G}^*_E) (P_\mu \langle \nu p_2 p_1 s_{1y} \rangle + P_\nu \langle \mu p_2 p_1 s_{1y} \rangle) \Big]. \end{aligned}$$

As $L^{(v)}_{\mu\nu}(0)$ is a symmetric tensor it gives non-zero product only with the last (symmetric) part of $H^{(v)}_{\mu\nu}(s_{1y})$

$$\begin{aligned} L^{(v)}_{\mu\nu}(0) H^{(v)}_{\mu\nu}(s_{1y}) &= \left[-q^2 g_{\mu\nu} + 2\left(k_{1\nu}k_{2\mu} + k_{1\mu}k_{2\nu}\right) \right] \\ &\times \frac{2}{m(\tau-1)} \Big[Im(\tilde{G}_M \tilde{G}^*_E) (P_\mu \langle \nu p_2 p_1 s_{1y} \rangle + P_\nu \langle \mu p_2 p_1 s_{1y} \rangle) \Big] \\ &= \frac{2Im(\tilde{G}_M \tilde{G}^*_E)}{m(\tau-1)} \left[-q^2 \langle p_2 p_2 p_1 s_{1y} \rangle + q^2 \langle p_1 p_2 p_1 s_{1y} \rangle \right. \\ &+ \left. 4k_1 \cdot P \langle k_2 p_2 p_1 s_{1y} \rangle + 4k_2 \cdot P \langle k_1 p_2 p_1 s_{1y} \rangle \right], \end{aligned}$$

where $\langle p_2 p_2 p_1 s_{1y}\rangle = \langle p_1 p_2 p_1 s_{1y}\rangle = 0$, because they are antisymmetric with two equal components.

The computation of $\langle k_2 p_2 p_1 s_{1y}\rangle$ and $\langle k_1 p_2 p_1 s_{1y}\rangle$ is more complicated and for the first time we will make it in detail. Let us recall the definition of

$$\langle k_2 p_2 p_1 s_1\rangle = \varepsilon_{\mu\nu\rho\sigma} k_{2\mu} p_{2\nu} p_{1\rho} s_{1y\sigma},\ \ \mu,\nu,\rho,\sigma = 0...3. \tag{3.76}$$

We get non-zero result only if indices μ,ν,ρ,σ are different from each other (due to antisymmetric ε-tensor property) and components $k_{2\mu}, p_{2\nu}, p_{1\rho}, s_{1y\sigma}$ are non-zero for the given index. Notice, that in case of P_y polarization four-vector s_{1y} has only one (y) non-zero component (3.70), so in the equation (3.76) $\sigma = 2$. On the other hand four-momentum k_2 is the only one with non-zero x-component and therefore $\mu = 1$. At last p_1 and p_2 have two nonzero components, what leads into (with $\varepsilon_{1230} = 1$)

$$\begin{aligned}
\varepsilon_{1\nu\rho 2} k_{2x} p_{2\nu} p_{1\rho} s_{1yy} &= -\varepsilon_{1032} k_{2x} p_{20} p_{1z} - \varepsilon_{1302} k_{2x} p_{2z} p_{10} \\
&= k_{2x} p_{20} p_{1z} - k_{2x} p_{2z} p_{10} = 2E|\vec{k}_1||\vec{p}_1|\sin\theta \\
&= \frac{q^2}{2} m\sqrt{\tau-1}\sin\theta.
\end{aligned} \tag{3.77}$$

For the $\langle k_1 p_2 p_1 s_{1y}\rangle$ we obtain a similar result

$$\langle k_1 p_2 p_1 s_{1y}\rangle = -\frac{q^2}{2} m\sqrt{\tau-1}\sin\theta.$$

and according to Eq. (3.66) $k_1 \cdot P = -k_2 \cdot P = m^2\sqrt{\tau(\tau-1)}\cos\theta$, which all together give a result

$$\begin{aligned}
L^{(v)}_{\mu\nu}(0) H^{(v)}_{\mu\nu}(s_{1y}) &= \frac{8}{m(\tau-1)} Im(\tilde{G}_M \tilde{G}^*_E) q^2 m^3 (\tau-1)\sqrt{\tau}\sin\theta\cos\theta \\
&= 8m^2 q^2 Im(\tilde{G}_M \tilde{G}^*_E)\sqrt{\tau}\sin\theta\cos\theta.
\end{aligned} \tag{3.78}$$

With the help of Eqs. (3.43, 3.61), the second term of Eq. (3.75) is equal to

$$\begin{aligned}
& L^{(i)}_{\mu\nu}(0) H^{(i)}_{\mu\nu}(s_{1y}) = 2i\,\langle \mu\nu k_2 k_1\rangle \times \\
\times\ & mA_N\Big[-2q\cdot s_{1y}\tilde{G}^*_M \tilde{G}\mu\nu - \frac{2q\cdot s_{1y}}{m^2(1-\tau)}(\tilde{G}_M - \tilde{G}_E)^* p_{1\mu} P_\nu \\
+\ & (\tilde{G}_M + \tilde{G}_E)^*(s_{1y\mu} p_{2\nu} + s_{1y\nu} p_{2\mu}) + (\tilde{G}M - \tilde{G}_E)^*(s_{1y\mu} p_{1\nu} + s_{1y\nu} p_{1\mu}) \\
-\ & (\tilde{G}_M + \tilde{G}E)^*(s_{1y\mu} p_{1\nu} - s_{1y\nu} p_{1\mu}) - (\tilde{G}_M - \tilde{G}_E)^*(s_{1y\mu} p_{2\nu} - s_{1y\nu} p_{2\mu})\Big],
\end{aligned}$$

where $q \cdot s_{1y} = 0$ and antisymmetric $L^{(i)}_{\mu\nu}(0)$ gives zero product with symmetric parts of $H^{(i)}_{\mu\nu}(s_{1y})$

$$\begin{aligned} L^{(i)}_{\mu\nu}(0)H^{(i)}_{\mu\nu}(s_{1y}) &= -2imA_N \langle \mu\nu k_2 k_1 \rangle \Big[(\tilde{G}_M + \tilde{G}_E)^*(s_{1y\mu}p_{1\nu} - s_{1y\nu}p_{1\mu}) \\ &+ (\tilde{G}_M - \tilde{G}_E)^*(s_{1y\mu}p_{2\nu} - s_{1y\nu}p_{2\mu}) \Big] \\ &= -4imA_N \Big[\tilde{G}^*_M(\langle s_{1y}p_1k_2k_1\rangle + \langle s_{1y}p_2k_2k_1\rangle) \\ &+ \tilde{G}^*_E(\langle s_{1y}p_1k_2k_1\rangle - \langle s_{1y}p_2k_2k_1\rangle) \Big] \end{aligned}$$

and

$$\begin{aligned} \langle s_{1y}p_1k_2k_1\rangle + \langle s_{1y}p_2k_2k_1\rangle &= \langle s_{1y}qk_2k_1\rangle = 0 \\ \langle s_{1y}p_1k_2k_1\rangle - \langle s_{1y}p_2k_2k_1\rangle &= -2\langle s_{1y}Pk_2k_1\rangle . \end{aligned}$$

Therefore

$$L^{(i)}_{\mu\nu}(0)H^{(i)}_{\mu\nu}(s_{1y}) = 8imA_N\tilde{G}^*_E \langle s_{1y}Pk_2k_1\rangle ,$$

where (similar to previous derivation)

$$\begin{aligned} \varepsilon_{23\mu\nu}s_{yy}P_z k_{2\mu}k_{1\nu} &= -\varepsilon_{2301}(-|\vec{p}_1|)k_{20}k_{1x} - \varepsilon_{2310}(-|\vec{p}_1|)k_{2x}k_{10} \\ &= 2m^3\tau\sqrt{\tau-1}\sin\theta. \end{aligned}$$

So the second term of Eq. (3.75) is

$$L^{(i)}_{\mu\nu}(0)H^{(i)}_{\mu\nu}(s_{1y}) = 16im^4A_N\tilde{G}^*_E\tau\sqrt{\tau-1}\sin\theta \tag{3.79}$$

and finally for P_y (3.78, 3.79) we get

$$\begin{aligned} P_y &= \frac{2\sin\theta}{D\sqrt{\tau}}\Big[Im(\tilde{G}_M\tilde{G}^*_E)\cos\theta + \sqrt{\frac{\tau-1}{\tau}}Re[iA_N\tilde{G}^*_E]\Big] \\ &= \frac{2\sin\theta}{D\sqrt{\tau}}\Big[Im(\tilde{G}_M\tilde{G}^*_E)\cos\theta + \sqrt{\frac{\tau-1}{\tau}}Im[A^*_N\tilde{G}_E]\Big]. \end{aligned} \tag{3.80}$$

3.5.3 P_x

P_x is a double-spin polarization observable: the polarization of the incoming electron is necessary, in order to obtain a polarization of the outgoing antinucleon along the x-axis.

The definition of the polarization observable P_x is similar to P_y (3.71)

$$P_x = \frac{1}{Dq^4}\left[L^{(v)}_{\mu\nu}H^{(v)}_{\mu\nu}(s_{1x}) + 2Re(L^{(i)}_{\mu\nu}H^{(i)}_{\mu\nu}(s_{1x}))\right], \tag{3.81}$$

where, according to definition (3.34), the four-vector s_{1x} is

$$\vec{\xi} = (1,0,0) \Rightarrow s_{x0} = 0\,;\ \vec{s}_{1x} = (1,0,0). \tag{3.82}$$

For the derivation of P_x we can use the same arguments as for P_y, with the following specificities:

- k_1, k_2 are not perpendicular to s_{1x} and $k_1 \cdot s_{1x} = -k_2 \cdot s_{1x} = |\vec{k}_1|\sin\theta$.
- the fully contracted terms $\langle....\rangle$, which contain only s, k_1, k_2, p_1, p_2, q, P are vanishing, because these four-vectors have zero y-component.

The first property can be used in steps (3.72, 3.73, 3.74) and, as a consequence, the polarized electron part of P_x is not vanishing. The second property can be used in the derivation of unpolarized electron part of P_x, where similarly to P_y, the only 'non-zero' terms are proportional to $\langle....\rangle$ terms, which are zero for P_x. Therefore unpolarized electron process doesn't contribute to P_x.

Let us repeat steps (3.72, 3.73) for P_x

$$\langle\mu\nu k_1 q\rangle \times \langle\mu\nu q s_{1x}\rangle = 2(k_1\cdot s_{1x}\ q^2 - k_1\cdot q\ s_{1x}\cdot q) = 2k_1\cdot s_{1x}\ q^2 = 2m\sqrt{\tau}q^2\sin\theta,$$

where $s_{1x}\cdot q = 0$. And

$$\begin{aligned}\langle\mu\nu k_1 q\rangle \ \times\ & (P_\mu\langle\nu p_2 p_1 s_{1x}\rangle - P_\nu\langle\mu p_2 p_1 s_{1x}\rangle) = -2\big[P\cdot p_2(k_1\cdot s_{1x}\ q\cdot p_1 - k_1\cdot p_1\ q\cdot s_{1x})\\ +\ & P\cdot p_1(k_1\cdot p_2\ q\cdot s_{1x} - k_1\cdot s_{1x}\ q\cdot p_2) + P\cdot s_{1x}(k_1\cdot p_1\ q\cdot p_2 - k_1\cdot p_2\ q\cdot p_1)\big]\\ =\ & 2\big[P\cdot p_1\ k_1\cdot s_{1x}\ q\cdot p_2 - P\cdot p_2\ k_1\cdot s_{1x}\ q\cdot p_1\big] = 2q^2m^3(\tau-1)\sqrt{\tau}\sin\theta,\end{aligned}$$

where $s_{1x}\cdot q = s_{1x}\cdot P = 0$. These differences lead to

$$\begin{aligned}L^{(v)}_{\mu\nu}(s)H^{(v)}_{\mu\nu}(s_{1x}) &= -8m^2q^2\sqrt{\tau}\sin\theta\big[|\tilde{G}_M|^2 + Re(\tilde{G}_M(\tilde{G}_E - \tilde{G}_M)^*)\big]\\ &= -8m^2q^2\sqrt{\tau}\sin\theta Re(\tilde{G}_M\tilde{G}^*_E)\end{aligned} \tag{3.83}$$

And step (3.74)

$$\begin{aligned} L^{(i)}_{\mu\nu}(s)H^{(i)}_{\mu\nu}(s_{1x}) &= 2q^2 mA_N\big((\tilde{G}_M+\tilde{G}_E)^* s_{1x}\cdot p_2+(\tilde{G}_M-\tilde{G}_E)^* s_{1x}\cdot p_1\big) \\ &- 4mA_N\big[(\tilde{G}_M+\tilde{G}_E)^*(k_2\cdot s_{1x}\ k_1\cdot p_2+k_1\cdot s_{1x}\ k_2\cdot p_2) \\ &+ (\tilde{G}_M-\tilde{G}_E)^*(k_2\cdot s_{1x}\ k_1\cdot p_1+k_1\cdot s_{1x}\ k_2\cdot p_1)\big] \\ &= 0-4mA_N\big[(\tilde{G}_M+\tilde{G}_E)^* k_1\cdot s_{1x}\ p_2(k_2-k_1) \\ &+ (\tilde{G}_M-\tilde{G}_E)^* k_1\cdot s_{1x}\ p_1(k_2-k_1)\big] \\ &= 16m^4\tau\sqrt{\tau-1}\cos\theta\sin\theta A_N\tilde{G}^*_E. \end{aligned} \tag{3.84}$$

The results (3.83, 3.84) lead to final formula for P_x

$$P_x=-\frac{2\sin\theta}{D\sqrt{\tau}}\left[Re(\tilde{G}_M\tilde{G}^*_E)-\sqrt{\frac{\tau-1}{\tau}}\cos\theta Re(A_N\tilde{G}^*_E)\right]. \tag{3.85}$$

3.5.4 The component P_z

P_z is the polarization of the outgoing antinucleon along the z-axis. It is a double spin polarization observable, induced by the polarization of incoming electron. The definition of P_z is (similarly to P_y):

$$P_z=\frac{1}{Dq^4}\left[L^{(v)}_{\mu\nu}H^{(v)}_{\mu\nu}(s_{1z})+2Re(L^{(i)}_{\mu\nu}H^{(i)}_{\mu\nu}(s_{1z}))\right],$$

where s_{1z} is the polarization four-vector with components (similar to longitudinal polarization of electron, Eq. (3.39))

$$\vec{\xi}=(0,0,1)\Rightarrow s_{z0}=\frac{|\vec{p}_1|}{m}=\sqrt{\tau-1}\,;\ \vec{s}_{1z}=(0,0,\frac{E}{m})=(0,0,\sqrt{\tau}). \tag{3.86}$$

As we can see s_{1z} doesn't have y-component, what implies (similar as for P_x) that the unpolarized electron part doesn't contribute to P_z

$$P_z=\frac{1}{Dq^4}\left[L^{(v)}_{\mu\nu}(S)H^{(v)}_{\mu\nu}(s_{1z})+2Re(L^{(i)}_{\mu\nu}(S)H^{(i)}_{\mu\nu}(s_{1z}))\right]. \tag{3.87}$$

The first part of Eq. (3.87) comes from Eqs. (3.40, 3.55)

$$\begin{aligned} L^{(v)}_{\mu\nu}(S)H^{(v)}_{\mu\nu}(s_{1z}) &= 2i\langle\mu\nu k_1 q\rangle\times\frac{2}{m(\tau-1)}\Big[im^2(\tau-1)|\tilde{G}_M|^2\langle\mu\nu q s_{1z}\rangle \\ &+ iRe(\tilde{G}_M(\tilde{G}_E-\tilde{G}_M)^*)(P_\mu\langle\nu p_2 p_1 s_{1z}\rangle-P_\nu\langle\mu p_2 p_1 s_{1z}\rangle) \\ &+ Im(\tilde{G}_M\tilde{G}^*_E)(P_\mu\langle\nu p_2 p_1 s_{1z}\rangle+P_\nu\langle\mu p_2 p_1 s_{1z}\rangle)\Big], \end{aligned}$$

where antisymmetric leptonic tensor gives vanish with symmetric parts of hadronic tensor

$$L^{(v)}_{\mu\nu}(S)H^{(v)}_{\mu\nu}(s_{1z}) = 2i\,\langle\mu\nu k_1 q\rangle \times \frac{2}{m(\tau-1)}\Big[im^2(\tau-1)|\tilde{G}_M|^2\,\langle\mu\nu q s_{1z}\rangle + iRe(\tilde{G}_M(\tilde{G}_E-\tilde{G}_M)^*)(P_\mu\,\langle\nu p_2 p_1 s_{1z}\rangle - P_\nu\,\langle\mu p_2 p_1 s_{1z}\rangle)\Big], \tag{3.88}$$

where

$$\langle\mu\nu k_1 q\rangle \times \langle\mu\nu q s_{1z}\rangle = 2(k_1\cdot s_{1z}\; q^2 - q\cdot s_{1z}\; k_1\cdot q) = -2mq^2\tau\cos\theta \tag{3.89}$$

and

$$\begin{aligned}&\langle\mu\nu k_1 q\rangle \times (P_\mu\,\langle\nu p_2 p_1 s_{1z}\rangle - P_\nu\,\langle\mu p_2 p_1 s_{1z}\rangle) = -2\,\langle\mu P k_1 q\rangle \times \langle\mu p_2 p_1 s_{1z}\rangle\\ &= -2\Big[P\cdot p_2(k_1\cdot s_{1z}\; q\cdot p_1 - k_1\cdot p_1\; q\cdot s_{1z}) + P\cdot p_1(k_1\cdot p_2\; q\cdot s_{1z} - k_1\cdot s_{1z}\; q\cdot p_2)\\ &+P\cdot s_{1z}(k_1\cdot p_1\; q\cdot p_2 - k_1\cdot p_2\; q\cdot p_1)\Big] = 0,\end{aligned} \tag{3.90}$$

where we used notations (3.66) and (3.86). Now we can use Eqs. (3.89, 3.90) in Eq. (3.88)

$$L^{(v)}_{\mu\nu}(S)H^{(v)}_{\mu\nu}(s_{1z}) = 2q^4|\tilde{G}_M|^2\cos\theta \tag{3.91}$$

The second part of (3.87) is according to (3.45, 3.61)

$$\begin{aligned}&L^{(i)}_{\mu\nu}(S)H^{(i)}_{\mu\nu}(s_{1z}) = \Big[q^2 g_{\mu\nu} - 2(k_{2\mu}k_{1\nu} + k_{2\nu}k_{1\mu})\Big]\times\\ &\times mA_N\Big[-2q.s_{1z}\tilde{G}^*_M g_{\mu\nu} - \frac{2q.s_{1z}}{m^2(1-\tau)}(\tilde{G}_M-\tilde{G}_E)^* p_{1\mu}P_\nu\\ &+(\tilde{G}_M+\tilde{G}_E)^*(s_{z\mu}p_{2\nu}+s_{z\nu}p_{2\mu}) + (\tilde{G}_M-\tilde{G}_E)^*(s_{z\mu}p_{1\nu}+s_{z\nu}p_{1\mu})\\ &-(\tilde{G}_M+\tilde{G}_E)^*(s_{z\mu}p_{1\nu}-s_{z\nu}p_{1\mu}) - (\tilde{G}_M-\tilde{G}_E)^*(s_{z\mu}p_{2\nu}-s_{z\nu}p_{2\mu})\Big],\end{aligned}$$

where the symmetric leptonic tensor vanish when multiplied with the antisymmetric part of hadronic tensor

$$\begin{aligned}&L^{(i)}_{\mu\nu}(S)H^{(i)}_{\mu\nu}(s_{1z}) = \Big[q^2 g_{\mu\nu} - 2(k_{2\mu}k_{1\nu} + k_{2\nu}k_{1\mu})\Big]\times\\ &\times mA_N\Big[-2q.s_{1z}\tilde{G}^*_M g_{\mu\nu} - \frac{2q.s_{1z}(\tilde{G}_M-\tilde{G}_E)^*}{m^2(1-\tau)}p_{1\mu}P_\nu\\ &+(\tilde{G}_M+\tilde{G}_E)^*(s_{z\mu}p_{2\nu}+s_{z\nu}p_{2\mu}) + (\tilde{G}_M-\tilde{G}_E)^*(s_{z\mu}p_{1\nu}+s_{z\nu}p_{1\mu})\Big]\end{aligned} \tag{3.92}$$

and after multiplication we get

$$
\begin{aligned}
& L^{(i)}_{\mu\nu}(S) H^{(i)}_{\mu\nu}(s_{1z}) = \\
& = \; 2q^2 m A_N \Big[-3q.s_{1z}\tilde{G}^*_M - \frac{q.s_{1z}(\tilde{G}_M - \tilde{G}_E)^*}{m^2(1-\tau)} p_1.P + 2\tilde{G}^*_E s_{1z}.P \Big] \\
& + 4m A_N \Big[2q.s_{1z}\tilde{G}^*_M k_1.k_2 + \frac{q.s_{1z}(\tilde{G}_M - \tilde{G}_E)^*}{m^2(1-\tau)} (p_1.k_1 \; P.k_2 + p_1.k_2 \; P.k_1) \\
& - (\tilde{G}_M + \tilde{G}_E)^* (s_{1z}.k_2 \; p_2.k_1 + s_{1z}.k_1 \; p_2.k_2) \\
& - (\tilde{G}_M - \tilde{G}_E)^* (s_{1z}.k_2 \; p_1.k_1 + s_{1z}.k_1 \; p_1.k_2) \Big].
\end{aligned}
\tag{3.93}
$$

Now from Eqs. (3.66) and (3.86) the following expression is obtained:

$$
L^{(i)}_{\mu\nu}(S) H^{(i)}_{\mu\nu}(s_{1z}) = -q^4 A_N \tilde{G}^*_M \sqrt{\frac{\tau - 1}{\tau}} (1 + \cos^2\theta). \tag{3.94}
$$

Substituting Eqs. (3.91, 3.94) into Eq. (3.87), we obtain the final formula for P_z

$$
P_z = \frac{2}{D} \Big[|\tilde{G}_M|^2 \cos\theta - Re(A_N \tilde{G}^*_M) \sqrt{\frac{\tau - 1}{\tau}} (1 + \cos^2\theta) \Big]. \tag{3.95}
$$

4. VECTOR MESON DOMINANCE MODEL AND ITS EXTENSION WITH CORRECT ASYMPTOTIC BEHAVIOR

4.1 Vector meson dominance model

While Quantum Chromodynamics failed in a description of electromagnetic form factors of hadrons (mainly in the resonance region), a phenomenological model of hadron form factors is needed. The best-known phenomenological model of the electromagnetic form factors of hadrons is the vector meson dominance (VMD) model. This model was constructed [4, 5] in order to describe the non-trivial resonance behavior of $\sigma(e^-e^+ \rightarrow \text{hadrons})$, caused by creation of unstable vector mesons. Vector meson dominance model assumes that under a certain probability the virtual photon transforms into a vector meson, which interacts with the hadron, as it is shown in Fig.2.1. While there are more than one vector meson we need to include contributions from all possible vector mesons. In this way we will obtain following parametrization of the electromagnetic form factor of the hadron

$$F(t) = \sum_{v}^{n} \frac{f_{v\overline{h}h}}{f_v} \frac{m_v^2}{m_v^2 - t}, \tag{4.1}$$

where $t = -Q^2$, $f_{vh\overline{h}}, f_v$ are coupling constants for (vector meson-hadrons) and (vector meson-photon), n is the number of vector mesons with photon quantum numbers and m_v is the vector meson mass.

However, while VMD model explains resonance behavior of form factors, it is only a rough approximation of the interaction between hadrons and photons and it has several limitations. In general it has wrong asymptotic behavior $F(t)_{|t|\rightarrow\infty} \sim t^{-1}$, while it

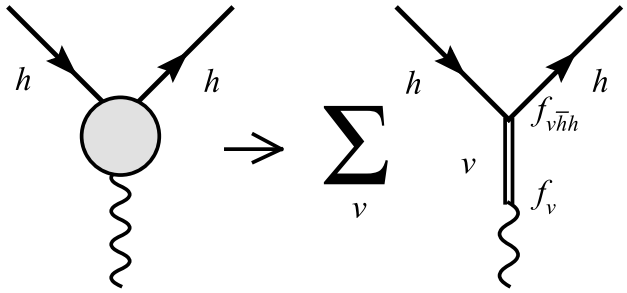

Fig. 4.1: Interaction of photon with hadrons can be approximated as sum of all possible processes, where photon transforms to vector meson, which strongly interacts with hadrons.

should be $F(t)_{|t|\to\infty} \sim t^{1-n_q}$, where n_q is number of constituent quarks in considered hadron [2, 3]. Also the VMD parametrization of a form factor diverges to the infinity for $t \to m_v^2$. This problem can be solved by introducing non-zero widths of vector mesons ($m_v \to m_v - i\Gamma_v$), but it violates unitarity condition of form factors.

Solution of the first problem will be shown in the next section, where asymptotic condition $F(t)_{|t|\to\infty} \sim t^{1-n_q}$ and normalization of form factor will be used to derive VMD model with correct asymptotic behavior [8, 9].

All other problems of VMD model are solved within Unitary and Analytic model, which fulfills all known properties of electromagnetic form factors.

4.2 Two sets of algebraic equations for the coupling constants ratios

As it was said at the end of the previous section the asymptotic behavior of any electromagnetic form factor of any hadron is known from Quantum chromodynamics [2, 3] and it should be

$$F(t)_{|t|\to\infty} \sim t^{1-n_q}, \tag{4.2}$$

where n_q is the number of constituent quarks in the hadron. Fortunately it is possible to obtain such behavior in VMD model for specific values of ratios of coupling constants $\left(\frac{f_{vh\overline{h}}}{f_v}\right)$.

Now we will introduce the technique of obtaining such ratios of coupling constants.

We can rearrange VMD parametrization (2.1) to common denominator

$$F(t) = \frac{A_0 + A_1.t + ... + A_{n-1.}t^{n-1}}{(m_1^2 - t)(m_2^2 - t)...(m_n^2 - t)},$$

where coefficients A_i can be written as

$$\begin{aligned}
A_{n-1} &= (-1)^{n-1} \sum_{v=1}^{n} m_v^2 a_v \\
A_{n-2} &= (-1)^{n-2} \sum_{v=1}^{n} m_v^2 a_v \sum_{\substack{i=1 \\ i \neq v}}^{n} m_i^2 \\
A_{n-3} &= (-1)^{n-3} \sum_{v=1}^{n} m_v^2 a_v \sum_{\substack{i_1, i_2 = 1 \\ i_1 < i_2 \\ i_r \neq v}}^{n} m_{i_1}^2 m_{i_2}^2 \\
&... \\
A_{n-p} &= (-1)^{n-p} \sum_{v=1}^{n} m_v^2 a_v \sum_{\substack{i_1, i_2, ..., i_{p-1} = 1 \\ i_1 < i_2 < ... < i_{p-1} \\ i_r \neq v}}^{n} m_{i_1}^2 m_{i_2}^2 ... m_{i_{p-1}}^2 \\
&... \\
A_0 &= \sum_{v=1}^{n} m_v^2 a_v \sum_{\substack{i_1, i_2, ..., i_{n-1} = 1 \\ i_1 < i_2 < ... < i_{n-1}, i_r \neq v}}^{n} m_{i_1}^2 m_{i_2}^2 ... m_{i_{n-1}}^2,
\end{aligned} \tag{4.3}$$

where m_v's are masses of vector mesons and $a_v = \frac{f_{vh\bar{h}}}{f_v}$ are ratios of the coupling constants. If we assume that asymptotic behavior of the form factor equals

$$F(t)_{|t| \to \infty} \sim t^{-m},$$

in order to fulfill it, the coefficients $A_{n-1}, A_{n-2}, ..., A_{n+1-m}$ should equal zero. In this way we can derive following asymptotic conditions for ratios of the coupling constants

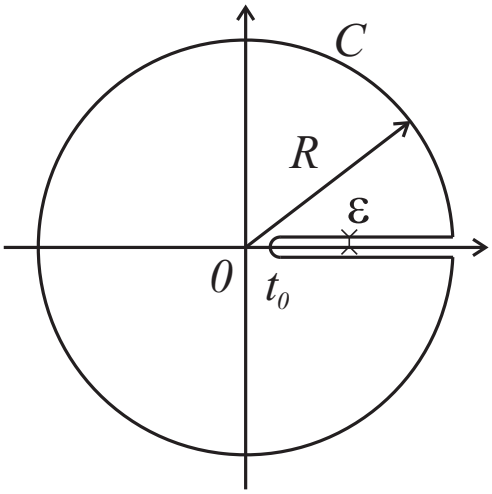

Fig. 4.2: Any hadron form factor is an analytic function inside the region bounded by the curve C.

a_j

$$\begin{aligned}
\sum_{v=1}^{n} m_v^2 a_v &= 0 \\
\sum_{v=1}^{n} m_v^2 a_v \sum_{\substack{i=1 \\ i\neq v}}^{n} m_i^2 &= 0 \\
\sum_{v=1}^{n} m_v^2 a_v \sum_{\substack{i_1,i_2=1 \\ i_1<i_2 \\ i_r\neq v}}^{n} m_{i_1}^2 m_{i_2}^2 &= 0 \qquad (4.4) \\
&\ldots \\
\sum_{v=1}^{n} m_v^2 a_v \sum_{\substack{i_1,i_2,\ldots,i_{m-2}=1 \\ i_1<i_2<\ldots<i_{m-2} \\ i_r\neq v}}^{n} m_{i_1}^2 m_{i_2}^2 \ldots m_{i_{m-2}}^2 &= 0.
\end{aligned}$$

As we can see, the set of equations (2.4) derived in this way is quite complicated. But there is also another set of equations for ratios of coupling constants derived from analytic properties of form factor, which is analytic function in the whole complex t-plane besides the cut from the square-root branch point corresponding to the lowest threshold (t_0) to $+\infty$.

As consequence of these analytic properties and the Cauchy theorem the line integral

along the curve C from Fig. 4.2 equals

$$\oint_C F(t)dt = 0. \tag{4.5}$$

The integral (4.5) can be splitted into four parts

$$\oint_{C_R} F(t)dt + \int_{-\infty}^{t_0} F(t - i\varepsilon)dt + \oint_{C_{\varepsilon/2}} F(t)dt + \int_{t_0}^{\infty} F(t + i\varepsilon)dt = 0, \tag{4.6}$$

where $\varepsilon > 0, \varepsilon \to 0$ and $R \to \infty$, what implies that the first and the third integral in Eq. (4.6) equal zero. This can be easily verified.

To compute the first integral, we will use known asymptotic behavior of the form factor $F(t)$

$$\lim_{R\to\infty} F(t) = \frac{1}{t^m} \Longrightarrow \oint_{C_R} F(t)dt \to \oint_{C_R} \frac{1}{t^m}dt \quad \text{for} \quad R \to \infty.$$

We need to transform t to the polar coordinates R, ϕ, where R has constant value

$$t = R.e^{i\phi} \Rightarrow \oint_{C_R} \frac{1}{(R.e^{i\phi})^m} d(R.e^{i\phi}) = \int_0^{2\pi} \frac{1}{(R.e^{i\phi})^m} R.e^{i\phi}.i.d\phi$$

and we get

$$\oint_{C_R} F(t)dt \to \frac{i}{R^{m-1}} \int_0^{2\pi} e^{i(1-m)\phi} d\phi,$$

which fulfills the following relation

$$\lim_{R\to\infty} \frac{i}{R^{m-1}} \int_0^{2\pi} e^{i(1-m)\phi} d\phi = 0, \quad \text{because} \quad \lim_{R\to\infty} \frac{1}{R^{m-1}} = 0. \tag{4.7}$$

Regarding the third integral, the function $F(t)$ is analytic in the neighborhood of the point t_0 ($U(t_0)$), what means, that it is also bounded in $U(t_0)$

$$\exists A \in \mathcal{R}; |F(t)| \leq A \quad \text{for} \quad \forall t \in U(t_0),$$

so absolute value of the third integral is lower than

$$\left| \oint_{C_{\varepsilon/2}} F(t)dt \right| \leq \oint_{C_{\varepsilon/2}} |F(t)|\, dt \leq \oint_{C_{\varepsilon/2}} A dt \leq \pi\varepsilon A,$$

where $\varepsilon \to 0$. Therefore also the third integral converges to zero

$$\lim_{\varepsilon\to 0}\left|\oint_{C_{\varepsilon/2}} F(t)dt\right| = 0 \Longrightarrow \lim_{\varepsilon\to 0}\oint_{C_{\varepsilon/2}} F(t)dt = 0. \tag{4.8}$$

Remaining parts of (4.6) can be adjusted by the Schwarz reflection principle

$$F_h^*(t) = F_h(t^*) \Rightarrow F(t+i\varepsilon) - F(t-i\varepsilon) = 2ImF(t+i\varepsilon) \tag{4.9}$$

to the final formula

$$\int_{t_0}^{\infty} ImF(t)dt = 0, \tag{4.10}$$

which is known as the superconvergence sum rule for imaginary part of the form factor. Moreover the same algorithm (as in (4.6)) can be used also for the multiples $t.F, t^2.F, ..., t^{m-2}.F$, but not for the higher powers of t, because the following condition must be fulfilled

$$\lim_{R\to\infty}\frac{1}{R^{m-1}}R^k = \lim_{R\to\infty}\frac{1}{R^{m-k-1}} = 0 \Rightarrow m-k-1 \geq 1 \Rightarrow k \leq m-2. \tag{4.11}$$

In this way we will obtain a set of integral superconvergence sum rules for the imaginary part of the form factor

$$\begin{aligned}
\int_{t_0}^{\infty} ImF(t)dt &= 0 \\
\int_{t_0}^{\infty} t.ImF(t)dt &= 0 \\
&\ldots \\
\int_{t_0}^{\infty} t^{m-2}.ImF(t)dt &= 0.
\end{aligned} \tag{4.12}$$

Now we can approximate the imaginary part of the form factor by using δ-function in the following way

$$ImF_h(t) = \sum_i^n a_i\delta(t-m_i^2)m_i^2. \tag{4.13}$$

And we will get another set of equations for the ratios of coupling constants by substi-

tuting this approximation (4.13) to the set (4.12)

$$\begin{aligned} \sum_{v=1}^{n} m_v^2 a_v &= 0 \\ \sum_{v=1}^{n} m_v^4 a_v &= 0 \\ &\dots \\ \sum_{v=1}^{n} m_v^{2(m-1)} a_v &= 0, \end{aligned} \tag{4.14}$$

where coefficients m_v^{2k} are simply even powers of masses of vector mesons.

This set of equations for a_v is much more simple than (4.4) and it can be solved quite easily. Unfortunately derivation of the second set (4.14) is doubtful, because the analytic properties of the form factor are utilized, which, however, are not present in VMD model (4.1) and therefore we still must use the first set of equations (4.4). On the other hand, as we will show in the next section, both sets of equations (4.4, 4.14) are equivalent and we can use any of them to derive a general solution for the ratios of coupling constants a_v.

4.3 The proof of equivalence of two sets of algebraic equations for the ratios of coupling constants

The equivalence of these sets of equations (4.4, 4.14) will be proved by showing, that it is possible to rearrange the first set of equations (4.4) to the second set (4.14). It will be shown by a mathematical induction. Idea of such proof will be shown on the example of the first two equations from both sets.

Example:

We would like to show, that if the first equation from the set (4.4 or 4.14) is valid

$$\sum_{v=1}^{n} m_v^2 a_v = 0, \tag{4.15}$$

the second equation from the set (4.4) could be rearranged to the second equation from

the set (4.14)

$$\sum_{j=1}^{n} m_j^2 a_j \sum_{\substack{i=1 \\ i\neq j}}^{n} m_i^2 = 0 \Leftrightarrow \sum_{j=1}^{n} m_j^4 a_j = 0.$$

Notice, that equation on the left side (from the set (4.4)) contains terms $m_i^2 m_j^2 a_j$ except the case $i = j$ (because of the condition under the sign for the second sum). If we add missing terms ($i = j$) to the both sides of this equation, we will obtain

$$\begin{aligned} \sum_{j=1}^{n} m_j^2 a_j \sum_{\substack{i=1 \\ i\neq j}}^{n} m_i^2 + \sum_{j=1}^{n} m_j^4 a_j &= \sum_{j=1}^{n} m_j^4 a_j \\ \sum_{j=1}^{n} m_j^2 a_j \sum_{i=1}^{n} m_i^2 &= \sum_{j=1}^{n} m_j^4 a_j. \end{aligned}$$

Now we have two separate sums and from condition (4.15), it is clear that left side of equation equals zero

$$0 = \sum_{j=1}^{n} m_j^4 a_j,$$

what is exactly the second equation from the set (4.14).

Proof:

The first step of the mathematical induction is fulfilled, because the first equations of our sets are the same. Now we need to show, that if the first $(p-1)$ equations from both sets are equivalent, also the first p equations from both sets are equivalent.

In other words, we need to show that if first $(p-1)$ equations from the second set is valid

$$\sum_{j=1}^{n} m_j^2 a_j = 0 \ ; \ \sum_{j=1}^{n} m_j^4 a_j = 0 \ ; \ \ldots \ ; \ \sum_{j=1}^{n} m_j^{2p-2} a_j = 0, \tag{4.16}$$

then also following equivalence is valid

$$\sum_{j=1}^{n} m_j^2 a_j \sum_{\substack{i_1,i_2,\ldots,i_{p-1}=1 \\ i_1<i_2<\ldots<i_{p-1} \\ i_r\neq j}}^{n} m_{i_1}^2 m_{i_2}^2 \ldots m_{i_{p-1}}^2 = 0 \Leftrightarrow \sum_{j=1}^{n} m_j^{2p} a_j = 0, \tag{4.17}$$

where the equation on the left side is the p-th equation from the first set and the equation on the right side is the p-th equation from the second set. Notice, that the

second sum in the equation on the left side contains terms $m_{i_1}^2 m_{i_2}^2 ... m_{i_{p-1}}^2$ and there are all combinations without repetition of m_i^2 except ones containing m_j^2 (because of the condition $i_r \neq j$). Analogous to the example, we can add the missing terms to the both sides of the p-th equation. It can be easily verified that the missing terms are

$$\sum_{j=1}^{n} m_j^2 a_j \sum_{\substack{i_1,i_2,...,i_{p-2}=1 \\ i_1<i_2<...<i_{p-2} \\ i_r \neq j}}^{n} m_{i_1}^2 m_{i_2}^2 ... m_{i_{p-2}}^2 m_j^2. \tag{4.18}$$

After adding them to the both sides of the p-th equation we will receive on the left side

$$\sum_{j=1}^{n} m_j^2 a_j \sum_{\substack{i_1,i_2,...,i_{p-1}=1 \\ i_1<i_2<...<i_{p-1} \\ i_r \neq j}}^{n} m_{i_1}^2 m_{i_2}^2 ... m_{i_{p-1}}^2 + \sum_{j=1}^{n} m_j^2 a_j \sum_{\substack{i_1,i_2,...,i_{p-2}=1 \\ i_1<i_2<...<i_{p-2} \\ i_r \neq j}}^{n} m_{i_1}^2 m_{i_2}^2 ... m_{i_{p-2}}^2 m_j^2 = (*) \tag{4.19}$$

and thanks to the commutability of the multiplication, we can rearrange squared masses in the product $m_{i_1}^2 m_{i_2}^2 ... m_{i_{p-2}}^2 m_j^2$ to be ascending ordered ($i_1 < i_2 < ...$). In this way we can sum (4.19)

$$(*) = \sum_{j=1}^{n} m_j^2 a_j \sum_{\substack{i_1,i_2,...,i_{p-1}=1 \\ i_1<i_2<...<i_{p-1}}}^{n} m_{i_1}^2 m_{i_2}^2 ... m_{i_{p-1}}^2, \tag{4.20}$$

where the sums can be summed separately and we know from (4.16) that $\sum_{j=1}^{n} m_j^2 a_j = 0$, which means that $(*) = 0$. But on the right side of the equation we still have terms (4.18),

$$0 = \sum_{j=1}^{n} m_j^2 a_j \sum_{\substack{i_1,i_2,...,i_{p-2}=1 \\ i_1<i_2<...<i_{p-2} \\ i_r \neq j}}^{n} m_{i_1}^2 m_{i_2}^2 ... m_{i_{p-2}}^2 m_j^2,$$

which can be rearranged

$$0 = \sum_{j=1}^{n} m_j^4 a_j \sum_{\substack{i_1,i_2,...,i_{p-2}=1 \\ i_1<i_2<...<i_{p-2} \\ i_r \neq j}}^{n} m_{i_1}^2 m_{i_2}^2 ... m_{i_{p-2}}^2. \tag{4.21}$$

In this way we reduced the number of squared masses in product $m_{i_1}^2 m_{i_2}^2 ... m_{i_{p-2}}^2$ under the second sum from $p-1$ to $p-2$ and we raised the power of the term under the first sum by 2 ($m_j^2 a_j \rightarrow m_j^4 a_j$).

Now it is obvious that the same technique can be repeated $(p-1)$ times (with one difference - we need to use others equations from the premise (4.16)), because we assume the first $(p-1)$ equations from both sets to be equivalent. If we use this technique $(p-2)$ times we will obtain condition

$$\sum_{j=1}^{n} m_j^{2p-2} a_j \sum_{\substack{i=1 \\ i_r \neq j}}^{n} m_i^2 = 0, \tag{4.22}$$

where the "missing" terms are

$$\sum_{j=1}^{n} m_j^{2p-2} a_j m_j^2.$$

If we add them to the both sides of (4.22), we will get

$$\begin{aligned} \sum_{j=1}^{n} m_j^{2p-2} a_j \sum_{\substack{i=1 \\ i_r \neq j}}^{n} m_i^2 + \sum_{j=1}^{n} m_j^{2p-2} a_j m_j^2 &= \sum_{j=1}^{n} m_j^{2p-2} a_j m_j^2 \\ \sum_{j=1}^{n} m_j^{2p-2} a_j \sum_{i=1}^{n} m_i^2 &= \sum_{j=1}^{n} m_j^{2p} a_j. \end{aligned} \tag{4.23}$$

Now it is sufficient to use the last of the assumed equations (4.16)

$$\begin{aligned} 0. \sum_{i=1}^{n} m_i^2 &= \sum_{j=1}^{n} m_j^{2p} a_j \\ \sum_{j=1}^{n} m_j^{2p} a_j &= 0, \end{aligned} \tag{4.24}$$

which was to be demonstrated.

4.4 Modified vector meson dominance model with the correct asymptotic behavior

Now we can use even the second set of equations despite the fact, that it was derived by using wrong assumptions for the form factor

$$\begin{aligned} \sum_{v=1}^{n} m_v^2 a_v &= 0 \\ \sum_{v=1}^{n} m_v^4 a_v &= 0 \\ &\dots \\ \sum_{v=1}^{n} m_v^{2(m-1)} a_v &= 0. \end{aligned} \tag{4.25}$$

and normalization of the form factor

$$\sum_{v=1}^{n} a_v = F_0 \tag{4.26}$$

to derive [8] modified VMD model with the correct normalization and asymptotic behavior. While we obtained m equations, it is obvious, that there must be at least m vector mesons to fulfill asymptotic and normalization conditions.

In general case, when $n > m$

$$\begin{aligned} F_h(t) &= F_0 \frac{\prod_{v=1}^{m} m_v^2}{\prod_{v=1}^{m}(m_v^2 - t)} - \sum_{k=m+1}^{n} \frac{\prod_{v=1}^{m} m_v^2}{\prod_{v=1}^{m}(m_v^2 - t)} a_k + \\ &+ \sum_{k=m+1}^{n} \left[\sum_{i=1}^{m} \frac{m_k^2}{m_k^2 - t} \frac{\prod_{v=1, v\neq i}^{m} m_v^2}{\prod_{v=1, v\neq i}^{m}(m_v^2 - t)} \frac{\prod_{v=1, v\neq i}^{m}(m_v^2 - m_k^2)}{\prod_{v=1, v\neq i}^{m}(m_v^2 - m_i^2)} \right] a_k. \end{aligned} \tag{4.27}$$

In special case, when $n = m$

$$F_h(t) = F_0 \frac{\prod_{v=1}^{m} m_v^2}{\prod_{v=1}^{m}(m_v^2 - t)}. \tag{4.28}$$

This model automatically fulfills the asymptotic and normalization conditions and in addition it has less free parameters, while m parameters can be obtained from Eqs. (4.25, 4.26).

5. UNITARY AND ANALYTIC MODEL OF HADRON ELECTROMAGNETIC STRUCTURE

In this Chapter we will present a construction of the model which reflects all known properties of electromagnetic form factors of hadrons and is known as Unitary and Analytic (U&A) model of electromagnetic structure of hadron.

At first, we review all known properties of any hadron electromagnetic form factor $F(t)$.

- Any electromagnetic form factor $F(t)$ is normalized at $t = 0$

$$F(0) = F_0 \tag{5.1}$$

  e.g. proton electric form factor is normalized at $t = 0$ as

$$G_E^p(0) = 1$$

- $F(t)$ can be considered as a complex function of a complex variable. It is an analytic function in the whole complex t-plane besides the cut from the lowest branch point to $+\infty$ [10]

- A discontinuity across the latter cut is given by unitarity condition

$$\frac{1}{2i}\left\{\left\langle h\overline{h}\left|J_\mu^{EM}(0)\right|0\right\rangle - \left\langle 0\left|J_\mu^{EM}(0)\right|h\overline{h}\right\rangle^*\right\} = \sum_n \left\langle h\overline{h}\left|T^+\right|n\right\rangle \left\langle n\left|J_\mu^{EM}(0)\right|0\right\rangle, \tag{5.2}$$

  where $|n\rangle$ represents an intermediate state (allowed by conservation laws) and T^+ is an operator of the amplitude from the intermediate state $|n\rangle$ to $h\overline{h}$ state.

- To every intermediate state $|n\rangle$ corresponds a branch point at the value of t, which is equal to squared sum of masses of the corresponding particles, e.g. for intermediate state $|\pi^+\pi^-\rangle$ is corresponding branch point at $t = (2m_\pi)^2$.

- The consequence of the Hermitivity of J_μ^{EM}

$$(J_\mu^{EM})^+ = J_\mu^{EM} \tag{5.3}$$

  is the reality of $F(t)$ on real axis from $-\infty$ to t_0.

- By application of the Schwarz reflection principle to $F(t)$ in the complex t-plane the reality condition

$$F^*(t) = F(t^*) \tag{5.4}$$

  is obtained, which gives a relation between values of $F(t)$ on the upper $(t + i\varepsilon)$ and lower $(t - i\varepsilon)$ boundary of the cut ($t > t_0$ and $\varepsilon \ll 1$) in the form as follows

$$F^*(t + i\varepsilon) = F(t - i\varepsilon) \tag{5.5}$$

- As a consequence of the reality condition (5.4) to every resonance pole also a complex conjugate pole has to exist.

- The asymptotic behavior of the hadron form factors was predicted by quark counting rules [11, 12] as

$$F(t)_{|t|\to\infty} \sim t^{1-n_q}, \tag{5.6}$$

  and this prediction was confirmed by pQCD for particles with spin 0, 1/2, 1 up to the logarithmic corrections [2, 3].

To our knowledge there are no other general properties of hadron form factors $F(t)$ to be known for the time being. In order to construct such Unitary and Analytic model we need to

1. Apply the following nonlinear transformation

$$t = t_0 - \frac{4(t_{in} - t_0)}{[1/W(t) - W(t)]^2}, \tag{5.7}$$

where t_0 is the square-root branch point corresponding to the lowest threshold and t_{in} is an effective square-root branch point simulating contributions of all other relevant thresholds given by unitarity condition. This transformation automatically generates the relations

$$m_v^2 = t_0 + \frac{4(t_{in} - t_0)}{[1/W_{v0} - W_{v0}]^2} \tag{5.8}$$

and

$$0 = t_0 + \frac{4(t_{in} - t_0)}{[1/W_N - W_N]^2}, \tag{5.9}$$

where W_{v0} and W_N are values of $W(t)$ in $t = m_v^2$ and $t = 0$, respectively.

2. Use relations between W_{v0} and W_{v0}^*.

3. Introduce instability of the resonance (vector meson) by its non-zero width $\Gamma_v \neq 0$.

The application of (5.7-5.9) to common expressions in formulas (4.27, 4.28)

$$\frac{m_v^2}{(m_v^2 - t)} \quad ; \quad \frac{(m_v^2 - m_k^2)}{(m_v^2 - m_i^2)}$$

leads to the following factorized forms

$$\begin{aligned} \frac{m_v^2}{m_v^2 - t} &= \frac{m_v^2 - 0}{m_v^2 - t} = \left(\frac{1 - W(t)^2}{1 - W_N^2}\right)^2 \\ &\times \frac{(W_N - W_{v0})\,(W_N + W_{v0})\,(W_N - 1/W_{v0})\,(W_N + 1/W_{v0})}{(W(t) - W_{v0})\,(W(t) + W_{v0})\,(W(t) - 1/W_{v0})\,(W(t) + 1/W_{v0})} \end{aligned} \tag{5.10}$$

and

$$\begin{aligned} \frac{m_v^2 - m_k^2}{m_j^2 - m_i^2} &= \frac{(m_v^2 - 0) - (m_k^2 - 0)}{(m_j^2 - 0) - (m_i^2 - 0)} = \\ &= \left[\frac{(W_N - W_{v0})(W_N + W_{v0})(W_N - 1/W_{v0})(W_N + 1/W_{v0})}{(W_{v0} - 1/W_{v0})^2} - \right. \\ &\left. - \frac{(W_N - W_{k0})(W_N + W_{k0})(W_N - 1/W_{k0})(W_N + 1/W_{k0})}{(W_{k0} - 1/W_{k0})^2}\right] \Bigg/ \\ &\left[\frac{(W_N - W_{j0})(W_N + W_{j0})(W_N - 1/W_{j0})(W_N + 1/W_{j0})}{(W_{j0} - 1/W_{j0})^2} - \right. \\ &\left. - \frac{(W_N - W_{i0})(W_N + W_{i0})(W_N - 1/W_{i0})(W_N + 1/W_{i0})}{(W_{i0} - 1/W_{i0})^2}\right]. \end{aligned} \tag{5.11}$$

Also we can prove that relation between W_{v0} and W^*_{v0} is

$$\begin{array}{lll} \text{a)} \quad \text{if} \quad m_v^2 - \Gamma_v^2/4 \;<\; t_{in} & \Rightarrow & W_{v0} = -W^*_{v0} \\ \\ \text{b)} \quad \text{if} \quad m_v^2 - \Gamma_v^2/4 \;>\; t_{in} & \Rightarrow & W_{v0} = 1/W^*_{v0}, \end{array} \tag{5.12}$$

which in the case a) leads the expressions (5.10, 5.11) to the forms

$$\begin{aligned} \frac{m_v^2}{m_v^2 - t} \;&=\; \left(\frac{1 - W(t)^2}{1 - W_N^2}\right)^2 \\ &\times \frac{(W_N - W_{v0})\,(W_N - W^*_{v0})\,(W_N - 1/W_{v0})\,(W_N - 1/W^*_{v0})}{(W(t) - W_{v0})\,(W(t) - W^*_{v0})\,(W(t) - 1/W_{v0})\,(W(t) - 1/W^*_{v0})} \end{aligned} \tag{5.13}$$

and

$$\begin{aligned} \frac{m_v^2 - m_k^2}{m_j^2 - m_i^2} \;&=\; \left[\frac{(W_N - W_{v0})(W_N - W^*_{v0})(W_N - 1/W_{v0})(W_N - 1/W^*_{v0})}{-(W_{v0} - 1/W_{v0})(W^*_{v0} - 1/W^*_{v0})} - \right. \\ &\left. - \frac{(W_N - W_{k0})(W_N - W^*_{k0})(W_N - 1/W_{k0})(W_N - 1/W^*_{k0})}{-(W_{k0} - 1/W_{k0})(W^*_{k0} - 1/W^*_{k0})}\right] \Bigg/ \\ &\left[\frac{(W_N - W_{j0})(W_N - W^*_{j0})(W_N - 1/W_{j0})(W_N - 1/W^*_{j0})}{-(W_{j0} - 1/W_{j0})(W^*_{j0} - 1/W^*_{j0})} - \right. \\ &\left. - \frac{(W_N - W_{i0})(W_N - W^*_{i0})(W_N - 1/W_{i0})(W_N - 1/W^*_{i0})}{-(W_{i0} - 1/W_{i0})(W^*_{i0} - 1/W^*_{i0})}\right] \\ &=\; \frac{C_a(W_{v0}) - C_a(W_{k0})}{C(W_{j0}) - C_a(W_{i0})} \end{aligned} \tag{5.14}$$

and in the case b) it leads to the forms

$$\begin{aligned} \frac{m_v^2}{m_v^2 - t} \;&=\; \left(\frac{1 - W(t)^2}{1 - W_N^2}\right)^2 \\ &\times \frac{(W_N - W_{v0})\,(W_N - W^*_{v0})\,(W_N + W_{v0})\,(W_N + W^*_{v0})}{(W(t) - W_{v0})\,(W(t) - W^*_{v0})\,(W(t) + W_{v0})\,(W(t) + W^*_{v0})} \end{aligned} \tag{5.15}$$

and

$$\begin{aligned}\frac{m_v^2-m_k^2}{m_j^2-m_i^2} &= \left[\frac{(W_N-W_{v0})(W_N-W_{v0}^*)(W_N+W_{v0})(W_N+W_{v0}^*)}{-(W_{v0}-1/W_{v0})(W_{v0}^*-1/W_{v0}^*)}-\right.\\ &\left.-\frac{(W_N-W_{k0})(W_N-W_{k0}^*)(W_N+W_{k0})(W_N+W_{k0}^*)}{-(W_{k0}-1/W_{k0})(W_{k0}^*-1/W_{k0}^*)}\right]\Bigg/\\ &\left[\frac{(W_N-W_{j0})(W_N-W_{j0}^*)(W_N+W_{j0})(W_N+W_{j0}^*)}{-(W_{j0}-1/W_{j0})(W_{j0}^*-1/W_{j0}^*)}-\right.\\ &\left.-\frac{(W_N-W_{i0})(W_N-W_{i0}^*)(W_N+W_{i0})(W_N+W_{i0}^*)}{-(W_{i0}-1/W_{i0})(W_{i0}^*-1/W_{i0}^*)}\right]\\ &= \frac{C_b(W_{v0})-C_b(W_{k0})}{C_b(W_{j0})-C_b(W_{i0})}. \end{aligned} \tag{5.16}$$

Now we can see that the expressions (5.14, 5.16) are always real, because W_N is a real number and it means that each bracket is multiplied by its complex conjugate. At the same way it can be shown that the expressions (5.13, 5.15) are real, while $W(t)$ is a real number, what is fulfilled for $t < t_0$. As a consequence of this property of Unitary and Analytic model also electromagnetic form factors are real numbers for $t < t_0$, where t_0 is the lowest threshold in investigated form factor.

At the end we need to introduce non-zero width of the resonance by a substitution

$$m_v^2 \to (m_v - i\Gamma_v/2)^2,$$

which formally means that in the expressions (5.13-5.16) we will use W_v instead of W_{v0}. Finally in the case a) we get

$$\begin{aligned}\frac{m_v^2}{m_v^2-t} &= \left(\frac{1-W(t)^2}{1-W_N^2}\right)^2 \frac{(W_N-W_v)\,(W_N-W_v^*)\,(W_N-1/W_v)\,(W_N-1/W_v^*)}{(W(t)-W_v)\,(W(t)-W_v^*)\,(W(t)-1/W_v)\,(W(t)-1/W_v^*)}\\ &= \left(\frac{1-W(t)^2}{1-W_N^2}\right)^2 L(W_v) \end{aligned} \tag{5.17}$$

and

$$\frac{m_v^2-m_k^2}{m_j^2-m_i^2} = \frac{C_a(W_v)-C_a(W_k)}{C_a(W_j)-C_a(W_i)}. \tag{5.18}$$

And in the case b) we get

$$\begin{aligned}\frac{m_v^2}{m_v^2-t} &= \left(\frac{1-W(t)^2}{1-W_N^2}\right)^2 \frac{(W_N-W_v)\,(W_N-W_v^*)\,(W_N+W_v)\,(W_N+W_v^*)}{(W(t)-W_v)\,(W(t)-W_v^*)\,(W(t)+W_v)\,(W(t)+W_v^*)} \\ &= \left(\frac{1-W(t)^2}{1-W_N^2}\right)^2 H(W_v) \end{aligned} \tag{5.19}$$

and

$$\frac{m_v^2-m_k^2}{m_j^2-m_i^2} = \frac{C_b(W_v)-C_b(W_k)}{C_b(W_j)-C_b(W_i)}. \tag{5.20}$$

Now we can use this forms of expressions (5.17-5.20) in the modified VMD parametrization of electromagnetic form factors (4.27, 4.28) to obtain general unitary and analytic parametrization of electromagnetic form factors

$$\begin{aligned}F_h(t) &= \left(\frac{1-W(t)^2}{1-W_N^2}\right)^{2m} \left[\left(F_0-\sum_{k=m+1}^{n} a_k\right)\prod_{v=1}^{m} LH(W_v) + \right. \\ &\left. + \sum_{k=m+1}^{n} LH(W_k)\left[\sum_{i=1}^{m}\prod_{v=1,v\neq i}^{m}\left\{LH(W_v)\frac{C(W_v)-C(W_k)}{C(W_v)-C(W_i)}\right\}\right] a_k\right] \end{aligned} \tag{5.21}$$

and a special unitary and analytic parametrization of electromagnetic form factors (in the case $n = m$)

$$F_h(t) = F_0\left(\frac{1-W(t)^2}{1-W_N^2}\right)^{2m}\prod_{v=1}^{m} LH(W_v), \tag{5.22}$$

where $LH(W_x)$ equals $L(W_x)$ respectively $H(W_x)$, when the resonance vector meson x fulfills condition a), respectively b). The same is valid for $C(W_x)$ and $C_a(W_x)$, respectively $C_b(W_x)$.

Unitary and analytic parametrization (5.21, 5.22) constructed in this way will be used in next Chapters to describe electromagnetic structure of nucleons and deuteron.

5.1 Necessity of more vector mesons

According to Eq. (5.22) one can guess the minimal number of vector mesons needed for constructing an unitary and analytic model of a given hadron, which fulfills a predicted asymptotic behavior of its electromagnetic form factors. For instance, a form factor $F(t)$ with given asymptotic behavior

$$F(t) \sim t^{-m}_{|t|\to-\infty}$$

can be parametrized within a unitary and analytic model by using m vector mesons.

However in the case when experimental data on electromagnetic form factors of an examined particle show an existence of one or several nodes, this result should be modified due to inability of (5.22) to reproduce zero, as it will be shown in this section. Moreover the value of $t = t_{node}$, where FF equals zero with sufficient precision, can be used as another condition and reduce number of free parameters of the model.

In case of the special parametrization (5.22) (when $n = m$)

$$F(t) = F_0 \left(\frac{1 - X(t)^2}{1 - X_N^2} \right)^{2m} \prod_{v=1}^{m} LH(X_v),$$

where $LH(X_v)$ equals

$$\begin{aligned} &\text{in case of: } m_v^2 - \Gamma_v^2/4 < t_{in} \\ &LH(X_v) = \frac{(X_N - X_v)(X_N - X_v^*)(X_N - 1/X_v)(X_N - 1/X_v^*)}{(X(t) - X_v)(X(t) - X_v^*)(X(t) - 1/X_v)(X(t) - 1/X_v^*)} \\ &\text{in case of: } m_v^2 - \Gamma_v^2/4 > t_{in} \\ &LH(W_v) = \frac{(X_N - X_v)(X_N - X_v^*)(X_N + X_v)(X_N + X_v^*)}{(X(t) - X_v)(X(t) - X_v^*)(X(t) + X_v)(X(t) + X_v^*)} \end{aligned}$$

and

$$X(t) = i \frac{\sqrt{\left(\frac{t_{in}-t_0}{t_0}\right)^{1/2} + \left(\frac{t-t_0}{t_0}\right)^{1/2}} - \sqrt{\left(\frac{t_{in}-t_0}{t_0}\right)^{1/2} - \left(\frac{t-t_0}{t_0}\right)^{1/2}}}{\sqrt{\left(\frac{t_{in}-t_0}{t_0}\right)^{1/2} + \left(\frac{t-t_0}{t_0}\right)^{1/2}} + \sqrt{\left(\frac{t_{in}-t_0}{t_0}\right)^{1/2} - \left(\frac{t-t_0}{t_0}\right)^{1/2}}}, \tag{5.23}$$

While $F(t)$ is the product of several terms, $F(t) = 0$ only if the nominator of at least 1 term equals 0. However the nominator of $LH(X_v)$ has constant value as it doesn't depend on t, what means either

- $LH(X_v) = 0$ for every value of t (except for $t = 0$, when $LH(X_v) = 1$ by definition). This possibility occurs, when the nominator equals to 0, but it doesn't correspond to the physical case.
- $LH(X_v) \neq 0$ for any value of t, when the nominator is different from 0.

It means that $F(t) = 0$ only if

$$1 - X(t)^2 = 0 \tag{5.24}$$

and from the definition of $X(t)$ (5.23)

- if $t = t_0$, then $X(t) = 0$.
- if $t \neq t_{0,}$ (5.23) can be simplified to

$$X(t) = i\frac{\sqrt{t_{in} - t_0} - \sqrt{t_{in} - t}}{\sqrt{t - t_0}}. \tag{5.25}$$

Now we can solve (5.24)

$$\begin{aligned} 1 - X(t)^2 &= 0 \\ X(t)^2 &= 1 \\ -\frac{(t_{in} - t_0) + (t_{in} - t) - 2\sqrt{t_{in} - t_0}\sqrt{t_{in} - t}}{t - t_0} &= 1 \\ -2t_{in} + t_0 + t + 2\sqrt{t_{in} - t_0}\sqrt{t_{in} - t} &= t - t_0 \\ \sqrt{t_{in} - t_0}\sqrt{t_{in} - t} &= t_{in} - t_0 \\ t_{in} - t &= t_{in} - t_0 \\ t &= t_0, \end{aligned}$$

which can not be the solution, because Eq. (5.25) is not defined at $t = t_0$ and moreover $X(t_0) = 0$, what doesn't fulfill condition (5.24). Therefore in special case, when $(n = m)$, $F(t)$ can not equal 0 for any value of t.

So in the case of existence of a node one need at least $m + 1$ vector mesons and to use general U&A parametrization of the FF (5.21) to parametrize such electromagnetic FF

$$F_h(t) = \left(\frac{1 - W(t)^2}{1 - W_N^2}\right)^{2m} \left[\left(F_0 - \sum_{k=m+1}^{n} a_k\right) \prod_{v=1}^{m} LH(W_v) + \sum_{k=m+1}^{n} \mathcal{LH}(W_k) a_k\right], \tag{5.26}$$

where

$$\mathcal{LH}(W_k) = LH(W_k) \left[\sum_{i=1}^{m} \prod_{v=1, v\neq i}^{m} \left\{LH(W_v)\frac{C(W_v) - C(W_k)}{C(W_v) - C(W_i)}\right\}\right]. \tag{5.27}$$

As it has been already proved neither $LH(W_i)$ nor $1-W(t)^2$ can equal zero. Therefore the only possibility for $F_h(t)$ to cross the x-axis is to fulfill following condition for the a_k's

$$\left(F_0 - \sum_{k=m+1}^{n} a_k\right) \prod_{v=1}^{m} LH(W_v(t_{node})) + \sum_{k=m+1}^{n} LH(W_k(t_{node}))\mathcal{LH}(W_k(t_{node}))a_k = 0, \tag{5.28}$$

which leads to the following condition for the ratio a_{m+1}

$$a_{m+1} = \frac{\left(F_0 - \sum_{k=m+2}^{n} a_k\right) \prod_{v=1}^{m} LH(W_v(t_{node})) + \sum_{k=m+2}^{n} \mathcal{LH}(W_k(t_{node}))a_k}{\prod_{v=1}^{m} LH(W_v(t_{node})) - \mathcal{LH}(W_{m+1}(t_{node}))}. \tag{5.29}$$

In the minimal case, when $n = m + 1$, this condition can be simplified to

$$a_{m+1} = \frac{F_0 \prod_{v=1}^{m} LH(W_v(t_{node}))}{\prod_{v=1}^{m} LH(W_v(t_{node})) - \mathcal{LH}(W_{m+1}(t_{node}))}. \tag{5.30}$$

6. THE PROTON ELECTRIC FORM FACTOR SPACE-LIKE BEHAVIOR PUZZLE

6.1 Introduction

The electromagnetic structure of the proton and neutron can be described by four independent form factors, which are functions of the square momentum transfer $t = -Q^2$ of the virtual photon. There are several ways to define these form factors, e.g. as the Dirac and Pauli form factors (F_1^p, F_1^n and F_2^p, F_2^n), isoscalar and isovector Dirac and Pauli form factors (F_1^s, F_1^v and F_2^s, F_2^v), or Sachs form factors (G_E^p, G_E^n and G_M^p, G_M^n).

The Dirac and Pauli form factors, standard form factors for particles with spin=1/2 in view of the definition in Chapter 1, are used to parametrize the nucleon matrix element

$$\left\langle N \left| J_\mu^{e.m.} \right| N \right\rangle = e\overline{u}(p') \left\{ \gamma_\mu F_1^N(t) + \frac{i}{2m_N} \sigma_{\mu\nu}(p'-p)_\nu F_2^N(t) \right\} u(p),$$

where m_N is the nucleon mass. And the relation between these three sets of nucleon form factors is

$$\begin{aligned}
G_{Ep}(t) &= F_1^p(t) + \frac{t}{4m_p^2} F_2^p(t) = \left[F_1^s(t) + F_1^v(t)\right] + \frac{t}{4m_p^2} \left[F_2^s(t) + F_2^v(t)\right], \\
G_{Mp}(t) &= F_1^p(t) + F_2^p(t) = \left[F_1^s(t) + F_1^v(t)\right] + \left[F_2^s(t) + F_2^v(t)\right], \\
G_{En}(t) &= F_1^n(t) + \frac{t}{4m_p^2} F_2^n(t) = \left[F_1^s(t) - F_1^v(t)\right] + \frac{t}{4m_p^2} \left[F_2^s(t) - F_2^v(t)\right], \\
G_{Mn}(t) &= F_1^n(t) + F_2^n(t) = \left[F_1^s(t) - F_1^v(t)\right] + \left[F_2^s(t) - F_2^v(t)\right]. \qquad (6.1)
\end{aligned}$$

In this chapter we will use the Sachs form factors to derive charge distribution in the proton as well as the isoscalar and isovector Dirac and Pauli form factors, which are suitable for a construction of various phenomenological models of the nucleon electromagnetic structure e.g. the vector meson dominance model [4, 5].

6.2 Two contradicting proton electric form factor behaviors in the space-like region

The electron-proton elastic scattering used to be the most common way of the proton electromagnetic structure study from the half of 50's of the last century [1] and more than 400 data points on proton electric $G_{Ep}(t)$ and magnetic $G_{Mp}(t)$ FFs in the space-like region $-Q^2 = q^2 = t < 0$ appeared (for references see paper [13]). They have been obtained from the measured differential cross-section of the elastic scattering of unpolarized electrons on unpolarized protons in laboratory system

$$\begin{aligned}\frac{d\sigma^{lab}(e^-p \to e^-p)}{d\Omega} &= \frac{\alpha^2}{4E^2}\frac{\cos^2(\theta/2)}{\sin^4(\theta/2)}\frac{1}{1+(\frac{2E}{m_p})\sin^2(\theta/2)} \\ &\times \left[A(t) + B(t)\tan^2(\theta/2)\right],\end{aligned}$$

where $\alpha = 1/137$, E is the incident electron energy and

$$A(t) = \frac{G_{Ep}^2(t) - \frac{t}{4m_p^2}G_{Mp}^2(t)}{1-\frac{t}{4m_p^2}}, \quad B(t) = -2\frac{t}{4m_p^2}G_{Mp}^2(t) \tag{6.2}$$

by the Rosenbluth technique. Their ratio $\mu_p G_{Ep}(t)/G_{Mp}(t)$ is in error bars roughly one, showing the electric and magnetic distributions in the proton to be equal.

Recently in JLab [14, 15, 16], measuring transverse

$$P_t = \frac{h}{I_0}(-2)\sqrt{\tau(1+\tau)}G_{Mp}G_{Ep}\tan(\theta/2) \tag{6.3}$$

and longitudinal

$$P_l = \frac{h(E+E')}{I_0 m_p}\sqrt{\tau(1+\tau)}G_{Mp}^2\tan^2(\theta/2) \tag{6.4}$$

components of the recoil proton's polarization (as suggested in Refs. [17]) in the electron scattering plane of the polarization transfer process $\vec{e}^{\,-}p \to e^-\vec{p})$, h is the electron beam helicity, I_0 is the unpolarized cross-section excluding σ_{Mott} and $\tau = Q^2/4m_p^2)$ simultaneously, the very precise and surprising data on the ratio $\mu_p G_{Ep}(t)/G_{Mp}(t)$ have been obtained, showing the electric and magnetic distributions in the proton to be different, contrary to what was followed from Rosenbluth data.

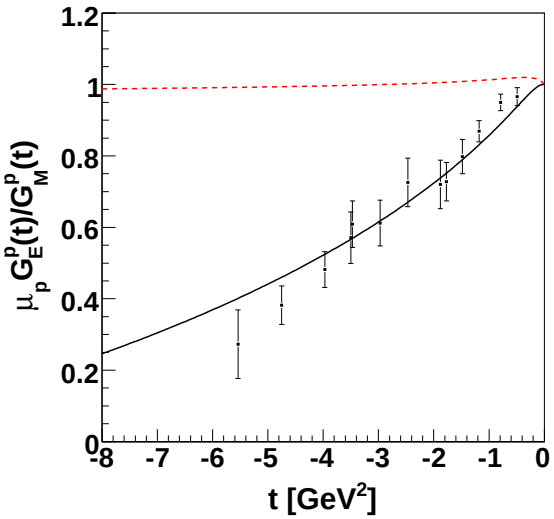

Fig. 6.1: Predicted behavior of $\mu_p G_E^p(t)/G_M^p(t)$ by the Unitary and Analytic ten-resonance model of the nucleon (full line – fit of JLab data, dashed line – fit of Rosenbluth data) and the Jefferson laboratory data obtained from polarization transfer measurements [14, 15, 16].

This contradiction is now well known as the JLab proton polarization data puzzle and a natural question is arisen "Which data are correct"? The difference between Rosenbluth and JLab data is shown in Fig. 6.1.

A lot of effort has been devoted to an explanation of the problem [18, 19, 20, 21, 22, 23, 24] but still it suffers from a definite solution.

However there are indications already in the form of the differential cross-section (6.2), where the proton magnetic FF is multiplied by factor $-t/(4m_p^2)$. As $-t$ increases, the measured cross-section (6.2) becomes dominated by $G_{Mp}^2(t)$ part contribution, making the extraction of $G_{Ep}^2(t)$ more and more difficult. As a result, one can have confidence only in the proton magnetic FF data obtained by the Rosenbluth technique in higher values of momentum transfer squared.

In this chapter we assume that inaccurate Rosenbluth data on the proton electric form factor in space like region are responsible for the mentioned contradiction and we exclude them from our analysis. We test consistency of JLab polarization data with the rest of the data on EM FFs of nucleon and we construct a ten-resonance U&A model

of the nucleon EM FFs. The result is compared with the same model, which fits old Rosenbluth data on proton electric FF.

6.3 Ten-resonance Unitary and Analytic model of nucleon electromagnetic structure

In order to construct Unitary and Analytic model of the nucleon EM structure [13], we will use technique shown in chapters 4 and 5 for parametrization of isoscalar and isovector Dirac and Pauli form factors, where isoscalar form factors F_1^s, F_2^s are saturated with isoscalar vector mesons $\omega, \phi, \omega', \omega'', \phi'$ and isovector form factors F_1^v, F_2^v are saturated with isovector vector mesons $\rho, \rho', \rho'', \rho''', \rho''''$.

The asymptotic behavior of the Sachs form factors G_E^p, G_E^n and G_M^p, G_M^n is

$$G_{E,M}^N(t)_{|t|\to\infty} \sim t^{-2},$$

because there are 3 constituent quarks in nucleons $(u, u, d$ or $u, d, d)$ [2, 3]. Now from the relation between different sets of form factors of nucleon (6.1) we can deduce that asymptotic behavior of the isoscalar and isovector Dirac and Pauli form factors is at least

$$\begin{aligned} F_1^{s,v}(t)_{|t|\to\infty} &\sim t^{-2} \\ F_2^{s,v}(t)_{|t|\to\infty} &\sim t^{-3} \end{aligned} \tag{6.5}$$

and we know enough to construct an U&A model as it is shown in Chapter 5.

$$\begin{aligned} F_1^s[V(t)] &= \left(\frac{1-V^2}{1-V_N^2}\right)^4 \left\{\frac{1}{2}H_{\omega''}(V)\cdot L_{\omega'}(V) + \left[H_{\omega''}(V)\cdot L_{\omega}(V)\cdot\frac{C_{\omega''}^{1s}-C_{\omega}^{1s}}{C_{\omega''}^{1s}-C_{\omega'}^{1s}} - \right.\right. \\ &- \left.L_{\omega'}(V)\cdot L_{\omega}(V)\frac{C_{\omega'}^{1s}-C_{\omega}^{1s}}{C_{\omega''}^{1s}-C_{\omega'}^{1s}} - H_{\omega''}(V)\cdot L_{\omega'}(V)\right](f_{\omega NN}^{(1)}/f_{\omega}) + \\ &+ \left[H_{\omega''}(V)\cdot L_{\phi}(V)\frac{C_{\omega''}^{1s}-C_{\phi}^{1s}}{C_{\omega''}^{1s}-C_{\omega'}^{1s}} - L_{\omega'}(V)\cdot L_{\phi}(V)\frac{C_{\omega'}^{1s}-C_{\phi}^{1s}}{C_{\omega''}^{1s}-C_{\omega'}^{1s}} - \right. \\ &- \left.H_{\omega''}(V)\cdot L_{\omega'}(V)\right](f_{\phi NN}^{(1)}/f_{\phi}) - \left[H_{\phi'}(V)\cdot H_{\omega''}(V)\frac{C_{\phi'}^{1s}-C_{\omega''}^{1s}}{C_{\omega''}^{1s}-C_{\omega'}^{1s}} - \right. \\ &- \left.\left.H_{\phi'}(V)\cdot L_{\omega'}(V)\frac{C_{\phi'}^{1s}-C_{\omega'}^{1s}}{C_{\omega''}^{1s}-C_{\omega'}^{1s}} + H_{\omega''}(V)\cdot L_{\omega'}(V)\right](f_{\phi' NN}^{(1)}/f_{\phi'})\right\} \end{aligned} \tag{6.6}$$

$$
\begin{aligned}
F_1^v[W(t)] &= \left(\frac{1-W^2}{1-W_N^2}\right)^4 \left\{\frac{1}{2}L_{\rho''}(W)\cdot L_{\rho'}(W) + \left[L_{\rho''}(W)\cdot L_{\rho}(W)\frac{C^{1v}_{\varrho''}-C^{1v}_{\varrho}}{C^{1v}_{\varrho''}-C^{1v}_{\varrho'}} - \right.\right. \\
&- \left.\left. L_{\rho'}(W)\cdot L_{\rho}(W)\frac{C^{1v}_{\varrho'}-C^{1v}_{\varrho}}{C^{1v}_{\varrho''}-C^{1v}_{\varrho'}} - L_{\rho''}(W)\cdot L_{\rho'}(W)\right](f^{(1)}_{\varrho NN}/f_{\varrho}) + \right. \\
&+ \left[H_{\rho'''}(W)\cdot L_{\rho'}(W)\frac{C^{1v}_{\varrho'''}-C^{1v}_{\varrho'}}{C^{1v}_{\varrho''}-C^{1v}_{\varrho'}} - H_{\rho'''}(W)\cdot L_{\rho''}(W)\frac{C^{1v}_{\varrho'''}-C^{1v}_{\varrho''}}{C^{1v}_{\varrho''}-C^{1v}_{\varrho'}} - \right. \qquad (6.7) \\
&- \left. L_{\rho''}(W)\cdot L_{\rho'}(W)\right](f^{(1)}_{\varrho''' NN}/f_{\varrho'''}) - \left[H_{\rho''''}(W)\cdot L_{\rho''}(W)\frac{C^{1v}_{\varrho''''}-C^{1v}_{\varrho''}}{C^{1v}_{\varrho''}-C^{1v}_{\varrho'}}\right. \\
&\left. -H_{\rho''''}(W)\cdot L_{\rho'}(W)\frac{C^{1v}_{\varrho''''}-C^{1v}_{\varrho'}}{C^{1v}_{\varrho''}-C^{1v}_{\varrho'}} + L_{\rho''}(W)\cdot L_{\rho'}(W)\right](f^{(1)}_{\varrho'''' NN}/f_{\varrho''''})\Bigg\}
\end{aligned}
$$

$$
\begin{aligned}
F_2^s[U(t)] &= \left(\frac{1-U^2}{1-U_N^2}\right)^6 \left\{\frac{1}{2}(\mu_p+\mu_n)H_{\omega''}(U)\cdot L_{\omega'}(U)\cdot L_{\omega}(U) + \right. \\
&+ \left[H_{\omega''}(U)\cdot L_{\phi}(U)\cdot L_{\omega}(U)\frac{C^{2s}_{\omega''}-C^{2s}_{\phi}}{C^{2s}_{\omega''}-C^{2s}_{\omega'}}\cdot\frac{C^{2s}_{\phi}-C^{2s}_{\omega}}{C^{2s}_{\omega'}-C^{2s}_{\omega}} + \right. \\
&+ H_{\omega''}(U)\cdot L_{\omega'}(U)\cdot L_{\phi}(U)\frac{C^{2s}_{\omega''}-C^{2s}_{\phi}}{C^{2s}_{\omega''}-C^{2s}_{\omega}}\cdot\frac{C^{2s}_{\omega'}-C^{2s}_{\phi}}{C^{2s}_{\omega'}-C^{2s}_{\omega}} - \\
&- L_{\omega'}(U)\cdot L_{\phi}(U)\cdot L_{\omega}(U)\frac{C^{2s}_{\omega'}-C^{2s}_{\phi}}{C^{2s}_{\omega''}-C^{2s}_{\omega'}}\cdot\frac{C^{2s}_{\phi}-C^{2s}_{\omega}}{C^{2s}_{\omega''}-C^{2s}_{\omega}} - \\
&- \left. H_{\omega''}(U)\cdot L_{\omega'}(U)\cdot L_{\omega}(U)\right](f^{(2)}_{\phi NN}/f_{\phi}) + \qquad (6.8) \\
&+ \left[H_{\phi'}(U)\cdot H_{\omega''}(U)\cdot L_{\omega'}(U)\frac{C^{2s}_{\phi'}-C^{2s}_{\omega''}}{C^{2s}_{\omega''}-C^{2s}_{\omega}}\cdot\frac{C^{2s}_{\phi'}-C^{2s}_{\omega'}}{C^{2s}_{\omega'}-C^{2s}_{\omega}} - \right. \\
&- H_{\phi'}(U)\cdot H_{\omega''}(U)\cdot L_{\omega}(U)\frac{C^{2s}_{\phi'}-C^{2s}_{\omega''}}{C^{2s}_{\omega''}-C^{2s}_{\omega'}}\cdot\frac{C^{2s}_{\phi'}-C^{2s}_{\omega}}{C^{2s}_{\omega'}-C^{2s}_{\omega}} + \\
&+ H_{\phi'}(U)\cdot L_{\omega'}(U)\cdot L_{\omega}(U)\frac{C^{2s}_{\phi'}-C^{2s}_{\omega'}}{C^{2s}_{\omega''}-C^{2s}_{\omega'}}\cdot\frac{C^{2s}_{\phi'}-C^{2s}_{\omega}}{C^{2s}_{\omega''}-C^{2s}_{\omega}} - \\
&- \left. H_{\omega''}(U)\cdot L_{\omega'}(U)\cdot L_{\omega}(U)\right](f^{(2)}_{\phi' NN}/f_{\phi'})\Bigg\}
\end{aligned}
$$

$$
\begin{aligned}
F_2^v[X(t)] &= \left(\frac{1-X^2}{1-X_N^2}\right)^6 \left\{\frac{1}{2}(\mu_p-\mu_n)L_{\rho''}(X)\cdot L_{\rho'}(X)\cdot L_{\rho}(X) + \right. \\
&+ \left[H_{\rho'''}(X)\cdot L_{\rho'}(X)\cdot L_{\rho}(X)\frac{C^{2v}_{\varrho'''}-C^{2v}_{\varrho'}}{C^{2v}_{\varrho''}-C^{2v}_{\varrho'}}\cdot\frac{C^{2v}_{\varrho'''}-C^{2v}_{\varrho}}{C^{2v}_{\varrho''}-C^{2v}_{\varrho}} - \right. \\
&- H_{\rho'''}(X)\cdot L_{\rho''}(X)\cdot L_{\rho}(X)\frac{C^{2v}_{\varrho'''}-C^{2v}_{\varrho''}}{C^{2v}_{\varrho''}-C^{2v}_{\varrho'}}\cdot\frac{C^{2v}_{\varrho'''}-C^{2v}_{\varrho}}{C^{2v}_{\varrho'}-C^{2v}_{\varrho}} + \\
&+ H_{\rho'''}(X)\cdot L_{\rho''}(X)\cdot L_{\rho'}(X)\frac{C^{2v}_{\varrho'''}-C^{2v}_{\varrho''}}{C^{2v}_{\varrho''}-C^{2v}_{\varrho}}\cdot\frac{C^{2v}_{\varrho'''}-C^{2v}_{\varrho'}}{C^{2v}_{\varrho'}-C^{2v}_{\varrho}} - \\
&- \left. L_{\rho''}(X)\cdot L_{\rho'}(X)\cdot L_{\rho}(X)\right](f^{(2)}_{\varrho'''\,NN}/f_{\varrho'''}) + \\
&+ \left[H_{\rho''''}(X)\cdot L_{\rho'}(X)\cdot L_{\rho}(X)\frac{C^{2v}_{\varrho''''}-C^{2v}_{\varrho'}}{C^{2v}_{\varrho''}-C^{2v}_{\varrho'}}\cdot\frac{C^{2v}_{\varrho''''}-C^{2v}_{\varrho}}{C^{2v}_{\varrho''}-C^{2v}_{\varrho}} - \right. \\
&- H_{\rho''''}(X)\cdot L_{\rho''}(X)\cdot L_{\rho}(X)\frac{C^{2v}_{\varrho''''}-C^{2v}_{\varrho''}}{C^{2v}_{\varrho''}-C^{2v}_{\varrho'}}\cdot\frac{C^{2v}_{\varrho''''}-C^{2v}_{\varrho}}{C^{2v}_{\varrho'}-C^{2v}_{\varrho}} + \\
&+ H_{\rho''''}(X)\cdot L_{\rho''}(X)\cdot L_{\rho'}(X)\frac{C^{2v}_{\varrho''''}-C^{2v}_{\varrho''}}{C^{2v}_{\varrho''}-C^{2v}_{\varrho}}\cdot\frac{C^{2v}_{\varrho''''}-C^{2v}_{\varrho'}}{C^{2v}_{\varrho'}-C^{2v}_{\varrho}} - \\
&- \left. \left. L_{\rho''}(X)\cdot L_{\rho'}(X)\cdot L_{\rho}(X)\right](f^{(2)}_{\varrho''''\,NN}/f_{\varrho''''})\right\},
\end{aligned}
\tag{6.9}
$$

where

$$L_r(V) = \frac{(V_N - V_r)(V_N - V_r^*)(V_N - 1/V_r)(V_N - 1/V_r^*)}{(V - V_r)(V - V_r^*)(V - 1/V_r)(V - 1/V_r^*)}; \tag{6.10}$$

$$C_r^{1s} = \frac{(V_N - V_r)(V_N - V_r^*)(V_N - 1/V_r)(V_N - 1/V_r^*)}{-(V_r - 1/V_r)(V_r^* - 1/V_r^*)}; \qquad r = \omega, \phi, \omega^{'},$$

$$H_l(V) = \frac{(V_N - V_l)(V_N - V_l^*)(V_N + V_l)(V_N + V_l^*)}{(V - V_l)(V - V_l^*)(V + V_l)(V + V_l^*)}; \tag{6.11}$$

$$C_l^{1s} = \frac{(V_N - V_l)(V_N - V_l^*)(V_N + V_l)(V_N + V_l^*)}{-(V_l - 1/V_l)(V_l^* - 1/V_l^*)}; \qquad l = \omega^{''}, \phi^{'}$$

$$L_k(W) = \frac{(W_N - W_k)(W_N - W_k^*)(W_N - 1/W_k)(W_N - 1/W_k^*)}{(W - W_k)(W - W_k^*)(W - 1/W_k)(W - 1/W_k^*)}; \tag{6.12}$$

$$C_k^{1v} = \frac{(W_N - W_k)(W_N - W_k^*)(W_N - 1/W_k)(W_N - 1/W_k^*)}{-(W_k - 1/W_k)(W_k^* - 1/W_k^*)}; \qquad k = \rho, \rho^{'}, \rho^{''},$$

$$H_n(W) = \frac{(W_N - W_n)(W_N - W_n^*)(W_N + W_n)(W_N + W_n^*)}{(W - W_n)(W - W_n^*)(W + W_n)(W + W_n^*)}; \tag{6.13}$$

$$C_n^{1v} = \frac{(W_N - W_n)(W_N - W_n^*)(W_N + W_n)(W_N + W_n^*)}{-(W_n - 1/W_n)(W_n^* - 1/W_n^*)}; \qquad n = \rho^{'''}, \rho^{''''}$$

$$L_r(U) = \frac{(U_N - U_r)(U_N - U_r^*)(U_N - 1/U_r)(U_N - 1/U_r^*)}{(U - U_r)(U - U_r^*)(U - 1/U_r)(U - 1/U_r^*)}; \tag{6.14}$$

$$C_r^{2s} = \frac{(U_N - U_r)(U_N - U_r^*)(U_N - 1/U_r)(U_N - 1/U_r^*)}{-(U - 1/U_r)(U - 1/U_r^*)}; \qquad r = \omega, \phi, \omega^{'},$$

$$L_k(X) = \frac{(X_N - X_k)(X_N - X_k^*)(X_N - 1/X_k)(X_N - 1/X_k^*)}{(X - X_k)(X - X_k^*)(X - 1/X_k)(X - 1/X_k^*)}; \tag{6.15}$$

$$C_k^{2v} = \frac{(X_N - X_k)(X_N - X_k^*)(X_N - 1/X_k)(X_N - 1/X_k^*)}{-(X_k - 1/X_k)(X_k^* - 1/X_k^*)}; \qquad k = \rho, \rho^{'}, \rho^{''},$$

$$H_n(X) = \frac{(X_N - X_n)(X_N - X_n^*)(X_N + X_n)(X_N + X_n^*)}{(X - X_n)(X - X_n^*)(X + X_n)(X + X_n^*)}; \tag{6.16}$$

$$C_n^{2v} = \frac{(X_N - X_n)(X_N - X_n^*)(X_N + X_n)(X_N + X_n^*)}{-(X_n - 1/X_n)(X_n^* - 1/X_n^*)}; \qquad n = \rho^{'''}, \rho^{''''}$$

$$H_l(U) = \frac{(U_N - U_l)(U_N - U_l^*)(U_N + U_l)(U_N + U_l^*)}{(U - U_l)(U - U_l^*)(U + U_l)(U + U_l^*)}; \tag{6.17}$$

$$C_l^{2s} = \frac{(U_N - U_l)(U_N - U_l^*)(U_N + U_l)(U_N + U_l^*)}{-(U_l - 1/U_l)(U_l^* - 1/U_l^*)}; \qquad l = \omega^{''}, \phi^{'}$$

and $V(t)$ (similarly $W(t), U(t)$ and $X(t)$) takes the form

$$V(t) = i\frac{\sqrt{\left(\frac{t_{in}^{1s}-t_0^s}{t_0^s}\right)^{1/2}+\left(\frac{t-t_0^s}{t_0^s}\right)^{1/2}}-\sqrt{\left(\frac{t_{in}^{1s}-t_0^s}{t_0^s}\right)^{1/2}-\left(\frac{t-t_0^s}{t_0^s}\right)^{1/2}}}{\sqrt{\left(\frac{t_{in}^{1s}-t_0^s}{t_0^s}\right)^{1/2}+\left(\frac{t-t_0^s}{t_0^s}\right)^{1/2}}+\sqrt{\left(\frac{t_{in}^{1s}-t_0^s}{t_0^s}\right)^{1/2}-\left(\frac{t-t_0^s}{t_0^s}\right)^{1/2}}} \tag{6.18}$$

where the lowest square-root branch point for isoscalar form factors F_1^s, F_2^s is $t_0^s = 9m_\pi^2$ and the lowest square-root branch point for isovector form factors F_1^v, F_2^v is $t_0^v = 4m_\pi^2$. Average branch square-root points for the isovector form factors F_1^v, F_2^v are $t_{in}^{1v} = t_{in}^{2v} = 4m_N^2$ and ones for isoscalar form factors are t_{in}^{1v}, t_{in}^{2s}, which however can not be fixed at two-nucleon threshold as in the isoscalar case and they have to be obtained from fitting experimental data.

In this way we have constructed the ten-resonance U&A model of the nucleon EM structure.

6.4 Achievements of ten-resonance Unitary and Analytic model of the nucleon electromagnetic structure

Ten-resonance U&A model of the nucleon EM structure includes all known properties of EM form factors of the nucleon: correct asymptotic behavior, unitarity and reality condition, analytic properties and normalization. It has been successfully applied to the description of all existing experimental data on the nucleon Sachs form factors. In [13] this model was applied to describe experimental data on $G_E^p(t)$ for $t < 0$ obtained by Rosenbluth technique, on $|G_E^p(t)|$ for $t > 0$ and on $G_M^p(t), G_E^n(t), G_M^n(t)$ for $t < 0, t > 0$ (see dashed line in Fig. 6.2).

But, as it was said at the beginning of this chapter, experimental data obtained by Rosenbluth technique are in strong disagreement with JLab polarization data, so only one of them can be valid. Besides this, Rosenbluth data on $G_E^p(t)$ are not very accurate for higher values of $t(= -Q^2)$. On the other hand JLab polarization data are very accurate even for higher values of t. So we rely on JLab polarization data, contrary to the previous paper [13] and in the space-like region of $G_E^p(t)$ we used only JLab polarization data. In this way we obtained behavior of nucleon Sachs form factors [25] shown in the Fig. 6.2 by full line.

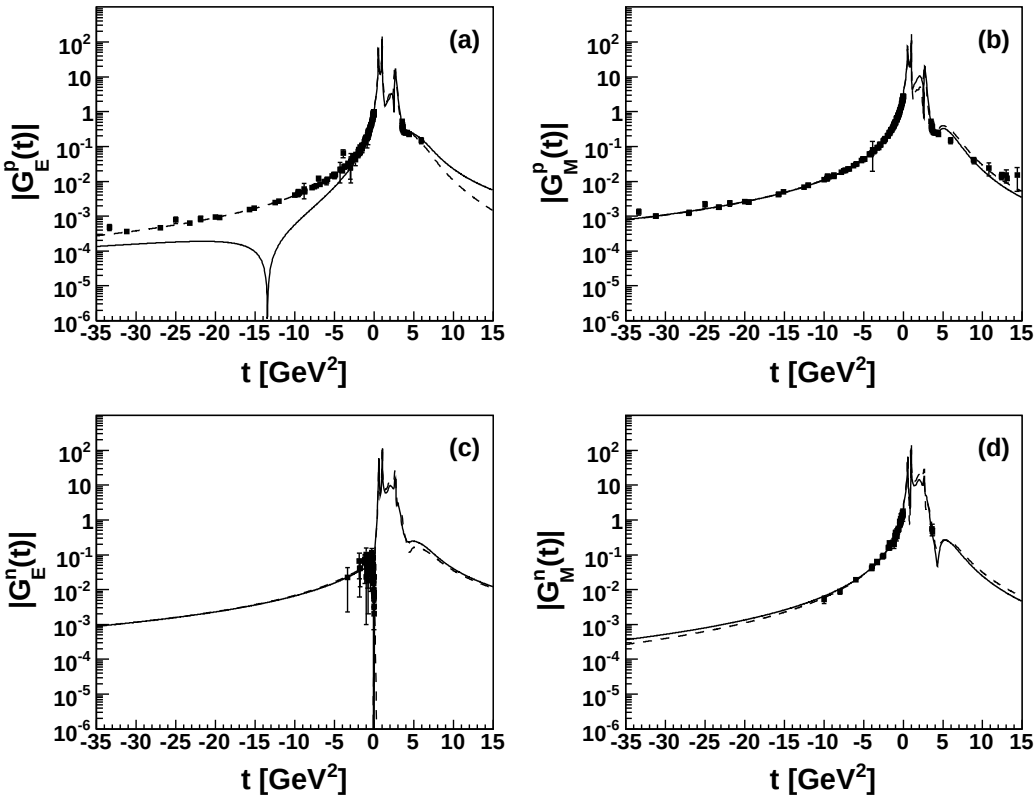

Fig. 6.2: A simultaneous optimal fit of all existing data on nucleon form factors. The dashed line represents old fit, which used Rosenbluth technique for extraction of $G_E^p(t)$ in the space-like region and the full line represents new fit, which used JLab polarization data on $G_E^p(t)$ in the space-like region.

As we can see in the Fig. 6.2, behavior of the nucleon Sachs form factors $G_{Mp}(t)$, $G_{En}(t)$, $G_{Mn}(t)$ remain almost unchanged and only the space-like part of $G_{Ep}(t)$ changed significantly.

6.5 Consequences of new G_E^p behavior on the proton charge distribution

While the proton charge distribution is defined as inverse Fourier transformation of the electric form factor of the proton $G_{Ep}(t)$, we can easily derive, that for the spherically

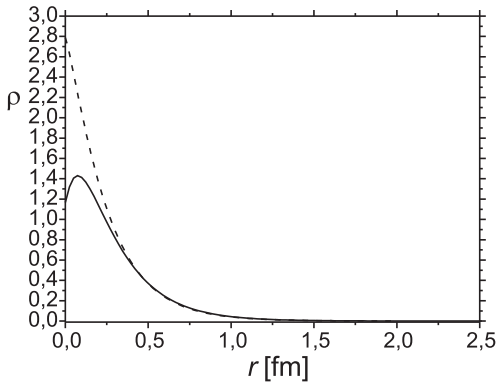

Fig. 6.3: Proton charge distribution. The dashed line represents the old distribution predicted from Rosenbluth data and the full line represents the new distribution predicted from JLab data.

symmetrical charge distribution we will obtain following relation

$$\rho_{Ep}(r) = (2\pi)^{-2} \int_0^\infty \frac{2Q}{r} \sin(Q.r) G_{Ep}(|Q|) dQ, \tag{6.19}$$

where $t = -Q^2$.

Now by using a numeric integration with sufficient precision we obtained different proton charge distribution for each case [25]. Fig. 6.3 shows the classic proton charge distribution obtained by fitting Rosenbluth data and new proton charge distribution obtained from new JLab polarization data.

Also proton charge radius will change. While for old behavior (using Rosenbluth data) it is

$$\left\langle r_p^2 \right\rangle_{Rosenbluth} = 0.684367 \text{ fm}^2,$$

for new behavior (using JLab data) it is

$$\left\langle r_p^2 \right\rangle_{JLab} = 0.719201 \text{ fm}^2$$

7. NONRELATIVISTIC IMPULSE APPROXIMATION OF DEUTERON FORM FACTORS

7.1 Introduction

A study of the deuteron electromagnetic structure is very interesting as the deuteron is the most simple bound state system of nucleons, which provides an excellent opportunity to study nucleon-nucleon (NN) interaction as well as its dependence on electromagnetic structure of underlying nucleons. Up to now several (phenomenological) models and fits of the deuteron electromagnetic structure have been published. The purely phenomenological fits [6] give small χ^2 but they come without any physical background. The vector meson dominance models (and their generalization by incorporating correct deuteron form factor analytic properties) [26, 27, 28] describe deuteron EM structure through exchange of isoscalar vector mesons ω, ϕ (and their excitations) and they don't assume NN interaction effects explicitly. Another class of models, non-relativistic (NIA) and relativistic (RIA) impulse approximations, reviewed in [29], assume NN interaction based on deuteron wave functions and describe the deuteron EM FFs through the nucleon EM FFs. Just such models seem to be able to bring some light [30] into existence of two contradicting space-like behaviors of the electric nucleon FF, obtained in elastic scattering of unpolarized electrons on unpolarized protons by Rosenbluth method and in polarization transfer process $\vec{e}^{-}p \rightarrow e^{-}\vec{p}$ measuring transversal and longitudinal components of the recoil proton's polarization simultaneously.

As the impulse approximation models of the deuteron depend on nucleon EM FFs, they give us possibility to make an independent test of two contradicting behaviors of

the proton electric FF in the space-like region described in the previous chapter by using data on the deuteron structure functions $A(t)$ and $B(t)$. In this chapter we will use NIA together with commonly used Paris potential for the deuteron form factors.

7.2 Non-relativistic impulse approximation for deuteron EM structure

In the one-photon exchange approximation the deuteron EM structure can be described by three scalar functions - EM FFs [31], which are connected to the matrix element of the deuteron EM current in the most general form as it is given in Chapter 1 in Eqs. (1.5,1.6).

The calculation of the deuteron EM FFs within impulse approximation requires a knowledge of the deuteron wave function and nucleon EM FFs. As deuteron can be found in S- ($\approx 96\%$) and D-state ($\approx 4\%$), then NN non-relativistic full wave function of the deuteron can be written in terms of two scalar wave functions

$$\begin{aligned}\Psi_{abm} &= \sum_l \sum_{m_s} \frac{z_l(r)}{r} Y_{l,m-m_s}(\widehat{\mathbf{r}}) \chi_{ab}^{1m_s} \langle l,1,m-m_s,m_s|1,m\rangle \\ &= \frac{u(r)}{r} Y_{0,0}(\widehat{\mathbf{r}}) \chi_{ab}^{1m} + \frac{w(r)}{r} \sum_{m_s} Y_{2,m-m_s} \chi_{ab}^{1m_s} \langle 2,1,m-m_s,m_s|1,m\rangle \,, \quad (7.1)\end{aligned}$$

where $\langle l,1,m-m_s,m_s|1,m\rangle$ are Clebsh-Gordan coefficients, Y_{l,m_l} are spherical harmonics normalized to unity on the unit sphere and $z_0 = u$, $z_2 = w$ are reduced $S-$ and D-state wave functions, respectively.

The normalization condition

$$\int d^3r \Psi^\dagger_{abm'} \Psi_{abm} = \delta_{m'm}$$

implies normalization

$$\int_0^\infty dr \left[u^2(r) + w^2(r)\right] = 1, \quad (7.2)$$

which could be understood as probability of finding deuteron in $S-$ or D-state. The D-state probability

$$P_D = \int_0^\infty dr w^2(r)$$

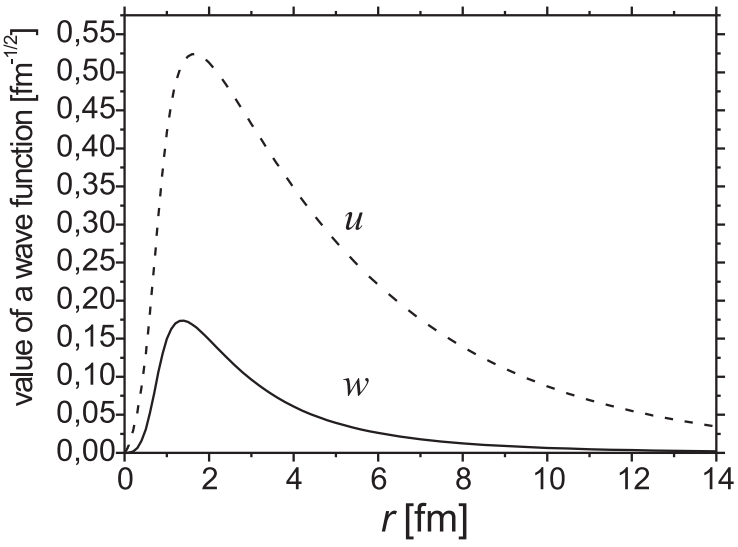

Fig. 7.1: The $S-$ and $D-$state wave functions behaviors for Paris potential.

is an interesting measurement of the strength of the tensor component of the NN force.

The best non-relativistic wave functions are calculated from the Schrödinger equation using a potential adjusted to fit NN scattering data for lab energies from 0 to 350 MeV. In this paper we will use one of the most common potentials called *Paris potential* [32], which was among the first potentials to be determined from such realistic fit. The $S-$ and $D-$state wave functions determined from this model are presented in Fig. 7.1.

The deuteron is an isoscalar target, therefore within non-relativistic impulse approximation, its FFs depend only on the isoscalar nucleon form factors G_E^{Ns} and G_M^{Ns}

$$\begin{aligned} G_E^{Ns} &= G_E^p + G_E^n \\ G_M^{Ns} &= G_M^p + G_M^n \end{aligned} \tag{7.3}$$

in the following way

$$\begin{aligned} G_C &= G_E^{Ns} D_C \\ G_M &= \frac{m_d}{2m_p} \left[G_M^{Ns} D_M + G_E^{Ns} D_E \right] \\ G_Q &= G_E^{Ns} D_Q \end{aligned} \tag{7.4}$$

where the body form factors D_C, D_M, D_E and D_Q are functions of the momentum transfer squared t. The non-relativistic formulas for the body form factors D involve

overlaps of the wave functions $u(r), w(r)$, weighted by spherical Bessel functions

$$\begin{aligned} D_C(q^2) &= \int_0^\infty dr \left[u^2(r) + w^2(r)\right] j_0(\kappa) \\ D_M(q^2) &= \int_0^\infty dr \left[2u^2(r) - w^2(r)\right] j_0(\kappa) + \left[\sqrt{2}u(r)w(r) + w^2(r)\right] j_2(\kappa) \\ D_E(q^2) &= \frac{3}{2}\int_0^\infty dr w^2(r) \left[j_0(\kappa) + j_2(\kappa)\right] \\ D_Q(q^2) &= \frac{3}{\sqrt{2}\eta}\int_0^\infty dr w(r) \left[u(r) - \frac{w(r)}{\sqrt{8}}\right] j_2(\kappa) \end{aligned} \tag{7.5}$$

where $\kappa = qr/2$. At $q^2 = 0$, the body form factors become

$$\begin{aligned} D_C(0) &= \int_0^\infty dr \left[u^2(r) + w^2(r)\right] = 1 \\ D_M(0) &= \int_0^\infty dr \left[2u^2(r) - w^2(r)\right] = 2 - 3P_D \\ D_E(0) &= \frac{3}{2}\int_0^\infty dr w^2(r) = \frac{3}{2}P_D \\ D_Q(0) &= \frac{m_d^2}{\sqrt{50}}\int_0^\infty dr w(r) \left[u(r) - \frac{w(r)}{\sqrt{8}}\right] \end{aligned} \tag{7.6}$$

giving the non-relativistic predictions

$$\begin{aligned} Q_d &= D_Q(0) \\ \mu_d &= \mu_N^s D_M(0) + D_E(0) = \mu_N^s(2 - 3P_D) + 1.5P_D, \end{aligned} \tag{7.7}$$

where Q_d is the quadrupole moment of the deuteron, μ_d is the magnetic moment of the deuteron and $\mu_N^s = \frac{1}{2}(\mu_p + \mu_n - 1)$ is the isoscalar nucleon magnetic moment. The experimental value of the deuteron magnetic moment $\mu_d = 1.7139$, leads to probability of D-state $P_D = 4.0\%$. But this is only approximate value, because the magnetic moment is very sensitive to relativistic corrections.

Experimentally the EM structure of the deuteron is measured in the elastic scattering of electrons on deuterons, described by the differential cross-section (6.2) with

$$A(t) = G_C^2(t) + \frac{2}{3}\eta(1+\eta)G_M^2(t) + \frac{8}{9}\eta^2 G_Q^2(t), \quad B(t) = \frac{4}{3}\eta(1+\eta)^2 G_M^2(t), \tag{7.8}$$

and applying the Rosenbluth technique. As a result the data on structure functions $A(t)$, $B(t)$ are obtained, which are found to be compiled in the paper [29].

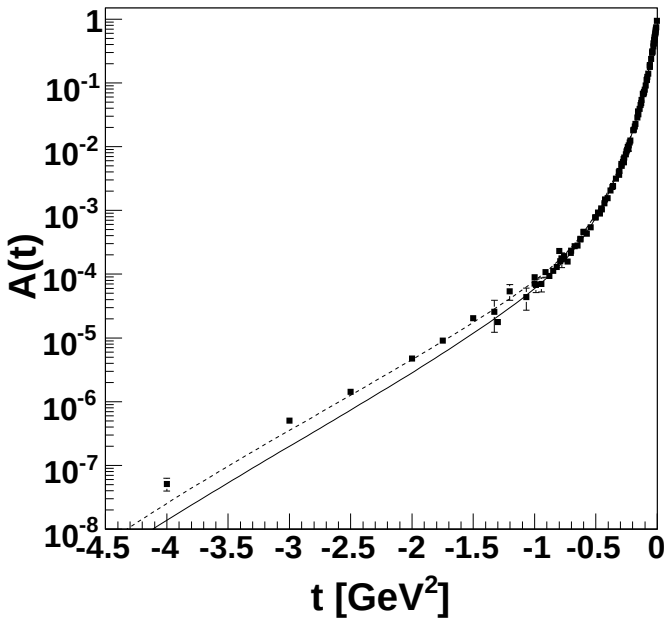

Fig. 7.2: Deuteron structure function $A(t)$ behavior.

7.3 Results

In order to test the two contradicting behaviors of $G_E^p(t)$, as shown in Fig.6.2(a), in comparison with the deuteron structure functions $A(t)$, $B(t)$ data, we use expressions for deuteron EM FFs (7.4) to be expressed through nucleon EM FFs. First, the fits of Rosenbluth data were made within Unitary and Analytic model of nucleon EM FFs [13], then the fits of JLab proton polarization data with all other existing nucleon EM FFs data. From both behaviors the isoscalar nucleon FFs were determined, by means of which the deuteron FFs have been found and as a result the two different behaviors of deuteron structure functions $A(t)$, $B(t)$ were calculated.

The comparison of these two behaviors (see Figs. 7.2 and 7.3) with existing experimental data on deuteron structure functions, leads to corresponding χ^2s, which are presented in Table 7.1. One can see immediately that the behaviors of $A(t)$, $B(t)$, obtained by means of the $G_E^p(t)$ with the zero around $t = -13$ GeV^2 are unambiguously preferred.

	χ^2_A	χ^2_B
JLab	926	476
Rosenbluth	2080	574

Tab. 7.1: The χ^2 of deuteron structure functions $A(t), B(t)$ for two different scenarios.

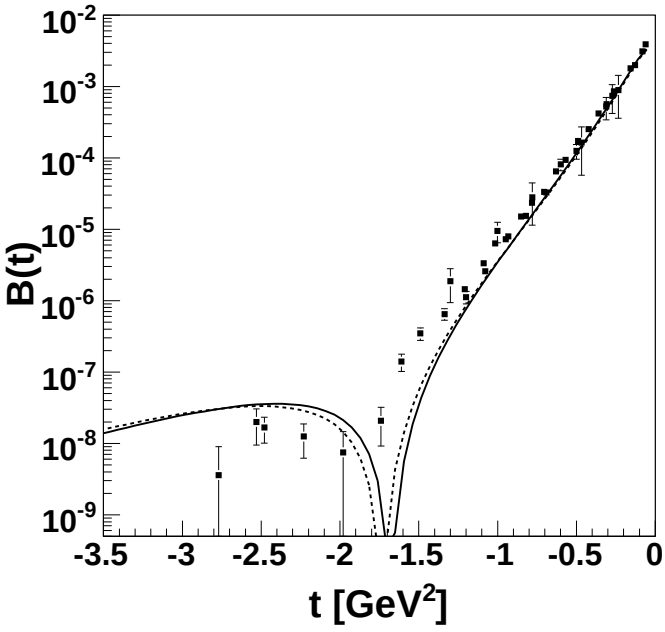

Fig. 7.3: Deuteron structure function $B(t)$ behavior.

For completeness we present (see Figs. 7.4,7.5 and 7.6) also the obtained behaviors of deuteron EM FFs $G_C(t)$, $G_M(t)$ and $G_Q(t)$ with the data [29] obtained in recent polarization experiments.

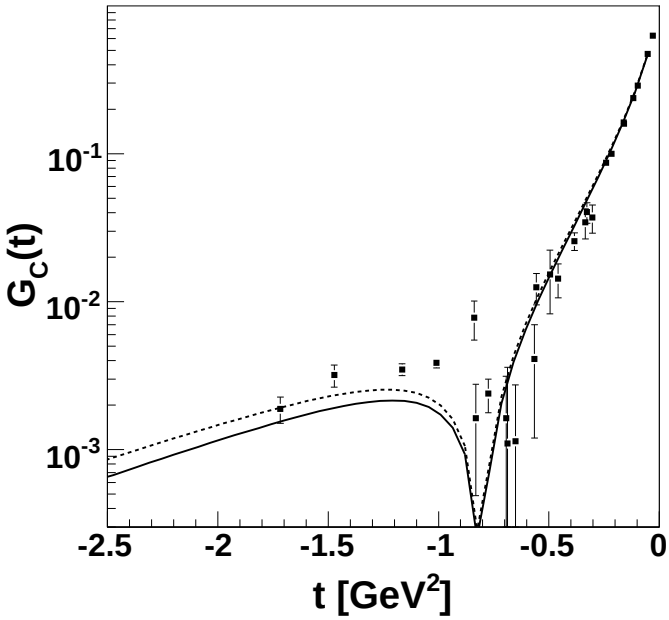

Fig. 7.4: Charge deuteron FF $G_C(t)$ behavior.

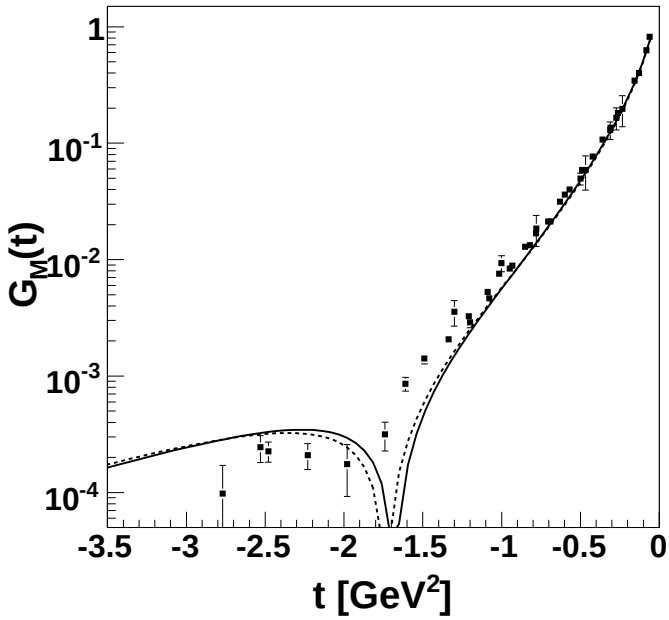

Fig. 7.5: Magnetic deuteron FF $G_M(t)$ behavior.

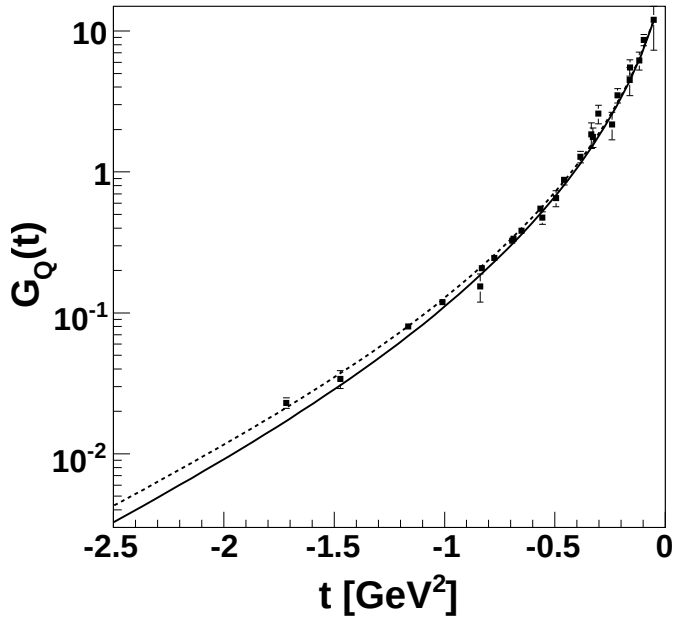

Fig. 7.6: Quadrupole deuteron FF $G_Q(t)$ behavior.

8. TWO COMPONENT MODEL OF THE DEUTERON ELECTROMAGNETIC STRUCTURE

In this chapter we will introduce another, more simple model of the deuteron electromagnetic structure with transparent physical background and very low number of free parameters. The idea of this model comes from Iachello, Jackson, Land (IJL) model of the nucleon [33].

8.1 Iachello, Jackson, Land model of the nucleon

The IJL model describes the nucleon as a hard core with a surrounding meson cloud (Fig.8.1), where the structure of the meson cloud can be described within vector meson dominance model and hard core has the well known dipole structure. Therefore Dirac and Pauli isoscalar and isovector nucleon form factors can be written as a product of dipole term

$$g(t) = \frac{1}{(1-\gamma t)^2} \tag{8.1}$$

and VMD term, where isoscalar vector mesons ω, ϕ saturate isoscalar FFs and isovector vector meson ρ saturates isovector FFs

$$\begin{aligned} F_1^S(t) &= \frac{e}{2}\frac{1}{(1-\gamma t)^2}\left[(1-\beta_\omega-\beta_\phi)+\beta_\omega\frac{m_\omega^2}{m_\omega^2-t}+\beta_\phi\frac{m_\phi^2}{m_\phi^2-t}\right] \\ F_1^V(t) &= \frac{e}{2}\frac{1}{(1-\gamma t)^2}\left[(1-\beta_\rho)+\beta_\rho\frac{m_\rho^2}{m_\rho^2-t}\right] \end{aligned}$$

$$F_2^S(t) = \frac{e}{2}\frac{1}{(1-\gamma t)^2}\left[(-0.12-\alpha_\phi)\frac{m_\omega^2}{m_\omega^2-t}+\alpha_\phi\frac{m_\phi^2}{m_\phi^2-t}\right]$$
$$F_2^V(t) = \frac{e}{2}\frac{1}{(1-\gamma t)^2}\left[(3.706\frac{m_\rho^2}{m_\rho^2-t}\right]. \quad (8.2)$$

As one can see, Dirac FFs F_1^S, F_1^V contain non-VMD terms in VMD part $((1-\beta_\omega-\beta_\phi),\ (1-\beta_\rho))$, which correspond to direct coupling of the photon to hard core of the nucleon.

IJL model of the nucleon provides very good description of the nucleon FFs in space-like region and after some modification also in time-like region.

8.2 Two component model of the deuteron

The idea similar to IJL model of nucleon was used in constructing two component model of the deuteron [28]. Contrary to impulse approximation models, we assumed that the deuteron is composed from one hard core and a surrounding meson cloud (Fig.8.2). Similar to IJL model all 3 deuteron FFs can be written as product of normalization N_i,hardcore part $g_i(t)$ and VMD part $F_i(t)$

$$G_i(t) = N_i g_i(t) F_i(t),\ ii = C, M, Q. \quad (8.3)$$

While the deuteron is an isoscalar particle, the VMD part $F_i(t)$ is saturated only by isoscalar vector mesons ω and ϕ

$$F_i(t) = 1-\alpha_i-\beta_i+\alpha_i\frac{m_\omega^2}{m_\omega^2-t}+\beta_i\frac{m_\phi^2}{m_\phi^2-t}, \quad (8.4)$$

where m_ω (m_ϕ) is the mass of the ω (ϕ)-meson. Note that the t dependence of $F_i(t)$ is parametrized in such form that $F_i(0) = 1$, for any values of the free parameters α_i and β_i, which are real numbers.

The hard core part $g_i(t)$ was chosen in a form similar to IJL case (8.1), with unknown asymptotic behavior, as function of two parameters, also real, γ_i and δ_i, generally different for each FF

$$g_i(t) = 1/\left[1+i\gamma_i t\right]^{\delta_i}. \quad (8.5)$$

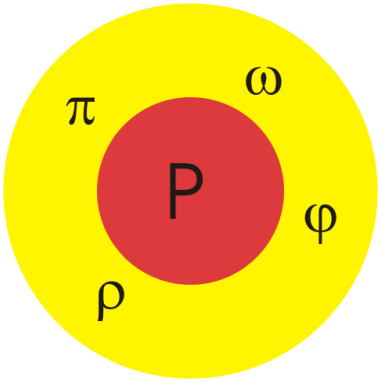

Fig. 8.1: A schematic picture of IJL model of the nucleon.

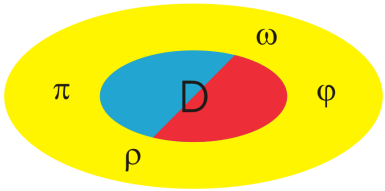

Fig. 8.2: A schematic picture of two component model of the deuteron.

8.3 Results and discussion

In general this parametrization uses 12 free parameters - 4 free parameters for every deuteron form factor $(\alpha_i, \beta_i, \gamma_i, \delta_i)$. However one can use constrains given by nodes in G_C and G_M behavior (8.6), which reduce the number of free parameters by 2 or assume common structure of hard core for every deuteron form factor ($\gamma_C = \gamma_M = \gamma_Q = \gamma$, $\delta_C = \delta_M = \delta_Q = \delta$) , which reduces the number of parameters by 4.

As it was mentioned, the experimental data on G_C and G_M show the existence of a zero, for $t_{0C} \simeq -0.7$ GeV^2 and $t_{0M} \simeq -2$ GeV^2. The requirement of a node gives the following relation between the parameters α_i and β_i, $i = C$ and M:

$$\alpha_i = -\frac{m_\omega^2 - t_{0i}}{t_{0i}} - \beta_i \frac{m_\omega^2 - t_{0i}}{m_\phi^2 - t_{0i}}. \tag{8.6}$$

In the fitting procedure this relation allows to obtain a better description of the data and a faster convergence, giving physical constraints to the problem.

The data basis of the present study consists of the data from [6] and completed by more recent measurements from Ref. [34].

As a result of the procedure for the extraction of the values of $G_C(t)$ and $G_Q(t)$ from $A(t)$, $B(t)$ and $t_{20}(t)$, some experimental points show a large asymmetry of the errors, which can not be neglected in this analysis. While there is still no general guide how to treat asymmetric errors, we used two different ways to handle them. At first no asymmetry was assumed and the average of the upper (σ_+) and lower (σ_-) errors was taken. Then, an approach recently proposed in Ref. [35] was applied: linear dependencies are assumed and the contribution to a modified χ^2 is defined as

$$\chi^2 = \sum_i \frac{\epsilon_i^2}{\sigma_{-i}^2}, \quad \text{for} \;\; \epsilon_i > 0, \;\; \chi^2 = \sum_i \frac{\epsilon_i^2}{\sigma_{+i}^2}, \quad \text{for} \;\; \epsilon_i < 0, \tag{8.7}$$

where ϵ_i is the discrepancy between the i-th experimental point and the value of the corresponding function. In Ref. [35] another model, based on a quadratic approximation, was preferred by the author, but it is not always suitable for our analysis, because, in some cases it doesn't give real solutions for the contribution to χ^2.

In any case, the analysis which takes into account the asymmetry of errors (8.7) gives significant reduction of χ^2 in all cases, but it didn't influence significantly the resulting parameters of the fit, except for $G_Q(t)$, where the errors on the parameters were significantly reduced.

The results were firstly obtained with a three parameter fit β, γ, δ, and the constraint (8.6) for G_C and G_M and a four parameter fit α, β, γ, δ, according to Eq. (8.3), for G_Q and are given in Table 8.1. Two solutions for FFs G_C and G_Q are consequence of quadratic dependence on $A(t), B(t), t_{20}(t)$ (1.11).

The parameters γ and δ, which characterize the global structure of the deuteron (8.5) are similar for all deuteron FFs, especially G_C and G_M, with good accuracy (Table 8.1) and the fit is quite sensitive to the choice of initial parameters, in particular for G_Q. In case of G_Q, which is not constrained by a node, a good fit can be obtained with a large cancellation of the terms driven by α and β. This means that FFs would be mostly sensitive to the meson cloud (with common hard core for all deuteron FFs). In order to test this hypothesis, a global fit was performed, keeping the γ and δ the same for the three FFs, which reduces the number of free parameters to 6. In such fit, two solutions appear also for G_M, related to the choice of the other two FFs. Results are given in Table 8.2.

	α	β	γ [GeV]$^{-2}$	δ	$\chi 2/ndf$
G_C (I)	5.9 ± 0.1	-5.2 ± 0.2	13.9 ± 1.4	0.96 ± 0.07	0.8
G_C (II)	5.0 ± 0.2	-4.5 ± 0.3	11.5 ± 1.2	1.11 ± 0.09	1.2
G_Q(I)	3.1 ± 1.1	-2.1 ± 1.2	7.2 ± 2.8	1.6 ± 0.5	0.5
G_Q(II)	1.4 ± 2.0	-0.1 ± 2.4	7.7 ± 1.6	1.7 ± 0.4	0.8
G_M	3.78 ± 0.04	-2.87 ± 0.04	11.4 ± 0.5	1.07 ± 0.03	1.5

Tab. 8.1: Parameters for the three deuteron electromagnetic FFs. In case of G_C and G_M, α is derived from Eq. (8.6).

	α	β	$\chi 2/ndf$
G_C (I)	5.75 ± 0.07	-5.11 ± 0.09	0.9
G_C (II)	5.50 ± 0.06	-4.78 ± 0.08	1.3
G_Q(I)	4.21 ± 0.05	-3.41 ± 0.07	0.9
G_Q(II)	4.08 ± 0.07	-3.25 ± 0.09	1.6
$G_M(I)$	3.77 ± 0.04	-2.86 ± 0.05	1.6
$G_M(II)$	3.74 ± 0.04	-2.83 ± 0.05	1.7

Tab. 8.2: Parameters α and β for the three deuteron electromagnetic FFs, from the global fit. Parameters δ and γ are common to all form factors and, in case of G_C and G_M, α is derived from Eq. (8.6).

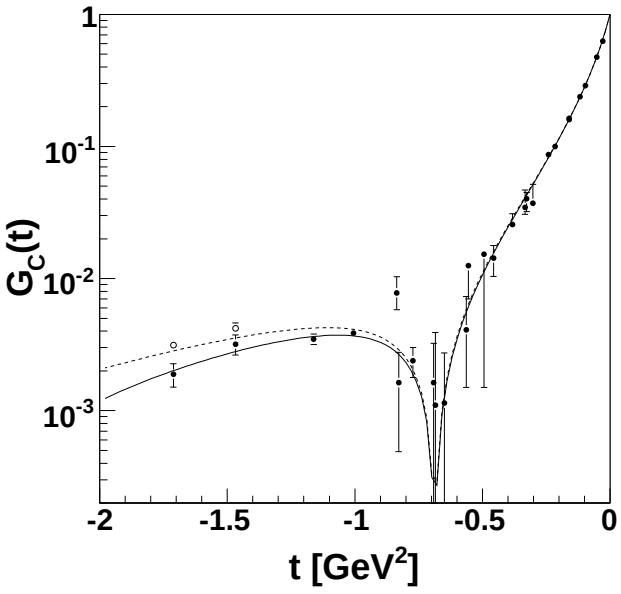

Fig. 8.3: Fit to deuteron charge form factor data. The solid and dashed lines correspond to the fits for the two different solutions for the data (solid and empty circles).

In Figs. 8.3, 8.4 and 8.5, the data points are shown, together with the result of the second fit where solid (dashed) lines correspond respectively to the first (second) solution. Open symbols in Figs. 8.3 and 8.5 correspond to the second solution for G_C and G_Q. The values of the best fit parameters are reported in Table 8.2. The common parameters are $\delta = 1.04 \pm 0.03$, $\gamma = 12.1 \pm 0.5$, for the first solution, corresponding to $\chi 2/ndf = 1.1$, whereas, for the second one, $\delta = 1.05 \pm 0.03$, $\gamma = 12.1 \pm 0.5$ and $\chi 2/ndf = 1.5$. The individual $\chi 2/ndf$ are reported in last column of Table 8.2. They are slightly larger than in Table 8.1, as expected.

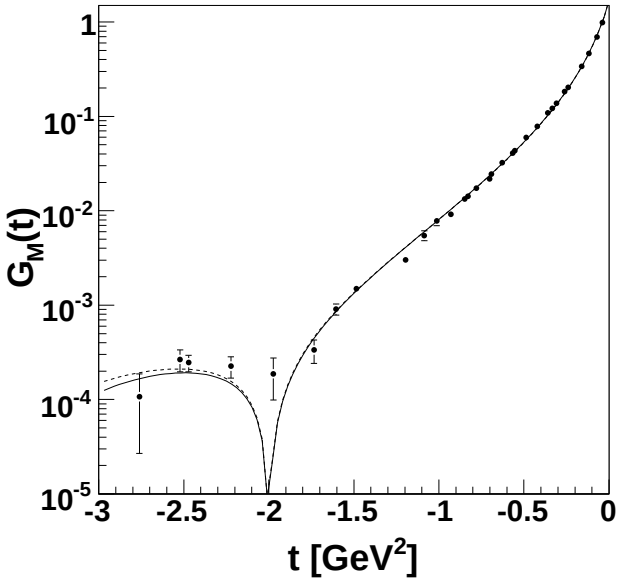

Fig. 8.4: Fit to deuteron magnetic form factor data.

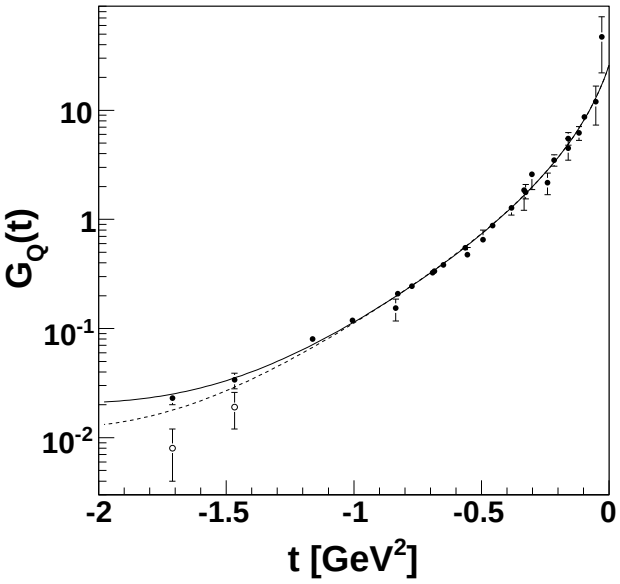

Fig. 8.5: Fit to deuteron quadrupole form factor data. Notations as in Fig. 8.3.

9. UNITARY AND ANALYTIC MODEL OF THE DEUTERON ELECTROMAGNETIC STRUCTURE

9.1 Properties of electromagnetic form factors of the deuteron

Besides the impulse approximations of the deuteron form factors and Iachello-like two component model of the deuteron, it is possible to construct also an unitary and analytic model of the deuteron EM structure. Within such model one considers deuteron as a single hadron containing 6 constituent quarks. This assumption is well suited for energies significantly higher than coupling energy of the proton-neutron pair in the deuteron - 2.2 MeV. As it was said in chapter 1, the electromagnetic structure of deuteron, can be described by 3 form factors, e.g. $G_C(t)$, $G_M(t)$, $G_Q(t)$, which experimental values can be extracted from measurements of deuteron structure functions $A(t)$ and $B(t)$ and polarization observable t_{20} (1.11). Moreover, as deuteron is a spin 1 particle, the ratios [36] of the deuteron FFs at large space-like and time-like momentum transfered squared is given by

$$G_C(t) : G_M t : G_Q(t) = (1 - \tfrac{2}{3}\eta) : 2 : -1, \tag{9.1}$$

which together with the perturbative QCD [37, 38] predictions for the asymptotic behavior of the deuteron electromagnetic structure function $A(t)$

$$[A(t)]^{1/2} \sim t^{-5}_{|t|\to-\infty}, \tag{9.2}$$

imply the asymptotics of all deuteron EM FFs in both space-like and time-like to be

$$\begin{aligned} G_C(t) &\sim t^{-5}_{|t|\to-\infty} \\ G_M(t) &\sim t^{-6}_{|t|\to-\infty} \\ G_Q(t) &\sim t^{-6}_{|t|\to-\infty}. \end{aligned} \tag{9.3}$$

According to Chapter 4 one generally need at least m vector mesons to construct unitary and analytic model of a hadron form factor with asymptotic behavior

$$F(t) \sim t^{-m}_{|t|\to-\infty}.$$

Therefore in the case of the deuteron at least 6 vector mesons are needed to describe its EM structure and due to the isoscalar nature of the deuteron nucleus, they should be also isoscalar vector mesons. However, experimentally revealed nodes in the space-like region of the deuteron FFs G_C and G_M (see Figs. 8.3 8.4) require the modified U&A parametrization, developed in section 5.1, to reproduce such behavior. The modified U&A parametrization (5.26, 5.29) of $G_M(t)$ requires an additional isoscalar vector meson increasing the number of required mesons to 7. Here we will describe [39] the deuteron EM structure by the minimal unitary and analytic model of deuteron EM structure with 7 isoscalar vector mesons.

9.2 Constructing of unitary and analytic model of deuteron form factors

In Chapter 5 it has been already shown how to construct unitary and analytic model of any hadron form factor. We only need to know an asymptotic behavior of a hadron form factor, whether or not there are some nodes in a FF behavior, t_0 – the square-root branch point corresponding to the lowest threshold and t_{in} – an effective square-root branch point simulating contributions of all other relevant thresholds, ratios of corresponding coupling constants, normalization of a form factor at $t = 0$ and we also need to know masses and widths of all vector mesons included to the model. Naturally, some of them are unknown and they have to be obtained from fitting experimental data.

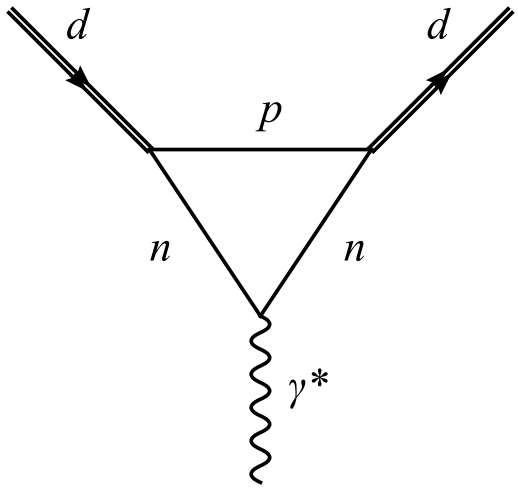

Fig. 9.1: The Feynman diagram of the deuteron electromagnetic vertex generating the lowest anomalous threshold in deuteron electromagnetic form factors.

In our case we know asymptotic behavior of all three deuteron form factors (9.3), approximate position of the nodes in the space-like behavior of G_C and G_M ($t_{0C} \simeq -0.7$ GeV^2 and $t_{0M} \simeq -2.0$ GeV^2), the lowest threshold

$$t_0 = 4m_p^2 - \frac{(m_d^2 - m_p^2 - m_n^2)^2}{m_n^2} = 1.7298 m_\pi^2, \tag{9.4}$$

which is generated [40, 41] by the diagram shown in Fig. 9.1 and practically calculated from the dual diagram presented in Fig. 9.2, normalization of all three deuteron form factors

$$G_C(0) = 1; \qquad G_M(0) = \frac{m_d}{m_p}\mu_d; \qquad G_C(0) = m_d^2 Q, \tag{9.5}$$

where $\mu_d = 0.8574061$ is the magnetic moment and $Q = 0.286015$ fm^2 is the quadrupole moment of the deuteron and we also know masses and widths of five light isoscalar vector mesons – $\omega, \omega', \omega'', \phi, \phi'$. As another isoscalar vector meson we will use somewhat heavier J/ψ.

A mass and a width of an additional isoscalar vector meson x, an effective thresholds for G_C, G_M, G_Q – t_{inC}, t_{inM}, t_{inQ} and an unknown ratios of coupling constants need to be obtained from fitting experimental data.

Now we can use general (5.21) unitary and analytic parametrization for deuteron FFs together with additional conditions (5.29, 5.30) for coupling constant ratios for G_C

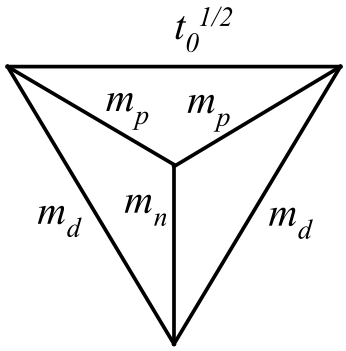

Fig. 9.2: The dual diagram from which by means of methods of elementary geometry the position of the lowest anomalous threshold is calculated.

and G_M given by the node positions.

$$\begin{aligned}
G_C(t) &= \left(\frac{1-W(t)^2}{1-W_N^2}\right)^{10}\left[(1-a_{C:J/\Psi}-a_{C:x})\prod_{v=\omega,\omega',\omega'',\phi,\phi'} LH(W_v)\right. \\
&+ \left.\mathcal{LH}(W_{J/\Psi})a_{C:J/\Psi}+\mathcal{LH}(W_x)a_{C:x}\right] \qquad (9.6)\\
G_M(t) &= \left(\frac{1-V(t)^2}{1-V_N^2}\right)^{12}\left[\left(\frac{m_d}{m_p}\mu_d - a_{M:x}\right)\prod_{v=\omega,\omega',\omega'',\phi,\phi',J/\Psi} LH(V_v)+\mathcal{LH}'(V_x)a_{M:x}\right]\\
G_Q(t) &= \left(\frac{1-U(t)^2}{1-U_N^2}\right)^{12}\left[\left(m_d^2 Q - a_{Q:x}\right)\prod_{v=\omega,\omega',\omega'',\phi,\phi',J/\Psi} LH(U_v)+\mathcal{LH}'(U_x)a_{Q:x}\right],
\end{aligned}$$

where

$$\begin{aligned}
a_{C:J/\Psi} &= \frac{(1-a_{C:x})\prod_{v=\omega,\omega',\omega'',\phi,\phi'} LH(W_v(t_{0C}))+\mathcal{LH}(W_x(t_{0C}))a_{C:x}}{\prod_{v=\omega,\omega',\omega'',\phi,\phi'} LH(W_v(t_{0C}))-\mathcal{LH}(W_{J/\Psi}(t_{0C}))}\\
a_{M:x} &= \frac{\frac{m_d}{m_p}\mu_d\prod_{v=\omega,\omega',\omega'',\phi,\phi',J/\Psi} LH(V_v(t_{0M}))}{\prod^m_{v=\omega,\omega',\omega'',\phi,\phi',J/\Psi} LH(V_v(t_{0M}))-\mathcal{LH}(V_x(t_{0M}))} \qquad (9.7)\\
\mathcal{LH}(X_w) &= LH(X_w)\sum_{i=\omega,\omega',\omega'',\phi,\phi'}\prod_{v=\omega,\omega',\omega'',\phi,\phi',v\neq i}\left\{LH(X_v)\frac{C(X_v)-C(X_w)}{C(X_v)-C(X_i)}\right\}\\
\mathcal{LH}'(X_w) &= LH(X_w)\sum_{i=\omega,\omega',\omega'',\phi,\phi',J/\Psi}\prod_{v=\omega,\omega',\omega'',\phi,\phi',J/\Psi,v\neq i}\left\{LH(X_v)\frac{C(X_v)-C(X_w)}{C(X_v)-C(X_i)}\right\}
\end{aligned}$$

and

$$
\begin{aligned}
LH(X_w) &= \frac{(X_N - X_w)(X_N - X_w^*)(X_N - 1/X_w)(X_N - 1/X_w^*)}{(X - X_w)(X - X_w^*)(X - 1/X_w)(X - 1/X_w^*)}; \quad \text{if } m_w^2 - \tfrac{\Gamma_w^2}{4} < t_{inX} \\
LH(X_w) &= \frac{(X_N - X_w)(X_N - X_w^*)(X_N + X_w)(X_N + X_w^*)}{(X - X_w)(X - X_w^*)(X + X_w)(X + X_w^*)}; \qquad \text{if } m_w^2 - \tfrac{\Gamma_w^2}{4} > t_{inX} \\
C(X_w) &= \frac{(X_N - X_w)(X_N - X_w^*)(X_N - 1/X_w)(X_N - 1/X_w^*)}{-(X_w - 1/X_w)(X_w - 1/X_w^*)}; \quad \text{if } m_w^2 - \tfrac{\Gamma_w^2}{4} < t_{inX} \\
C(X_w) &= \frac{(X_N - X_w)(X_N - X_w^*)(X_N + X_w)(X_N + X_w^*)}{-(X_w - 1/X_w)(X_w - 1/X_w^*)}; \qquad \text{if } m_w^2 - \tfrac{\Gamma_w^2}{4} > t_{inX}
\end{aligned}
$$

and X takes different form for each deuteron form factor – W for G_C, V for G_M and U for G_Q

$$
\begin{aligned}
W(t) &= i\frac{\sqrt{\left(\frac{t_{inC}-t_0}{t_0}\right)^{1/2} + \left(\frac{t-t_0}{t_0}\right)^{1/2}} - \sqrt{\left(\frac{t_{inC}-t_0}{t_0}\right)^{1/2} - \left(\frac{t-t_0}{t_0}\right)^{1/2}}}{\sqrt{\left(\frac{t_{inC}-t_0}{t_0}\right)^{1/2} + \left(\frac{t-t_0}{t_0}\right)^{1/2}} + \sqrt{\left(\frac{t_{inC}-t_0}{t_0}\right)^{1/2} - \left(\frac{t-t_0}{t_0}\right)^{1/2}}} \\
V(t) &= i\frac{\sqrt{\left(\frac{t_{inM}-t_0}{t_0}\right)^{1/2} + \left(\frac{t-t_0}{t_0}\right)^{1/2}} - \sqrt{\left(\frac{t_{inM}-t_0}{t_0}\right)^{1/2} - \left(\frac{t-t_0}{t_0}\right)^{1/2}}}{\sqrt{\left(\frac{t_{inM}-t_0}{t_0}\right)^{1/2} + \left(\frac{t-t_0}{t_0}\right)^{1/2}} + \sqrt{\left(\frac{t_{inM}-t_0}{t_0}\right)^{1/2} - \left(\frac{t-t_0}{t_0}\right)^{1/2}}} \\
U(t) &= i\frac{\sqrt{\left(\frac{t_{inQ}-t_0}{t_0}\right)^{1/2} + \left(\frac{t-t_0}{t_0}\right)^{1/2}} - \sqrt{\left(\frac{t_{inQ}-t_0}{t_0}\right)^{1/2} - \left(\frac{t-t_0}{t_0}\right)^{1/2}}}{\sqrt{\left(\frac{t_{inQ}-t_0}{t_0}\right)^{1/2} + \left(\frac{t-t_0}{t_0}\right)^{1/2}} + \sqrt{\left(\frac{t_{inQ}-t_0}{t_0}\right)^{1/2} - \left(\frac{t-t_0}{t_0}\right)^{1/2}}}
\end{aligned}
$$

If no parameter is given for U, V, W or X, it should be evaluated at the same t where FF is evaluated or at t_{node} for calculation of the ratios (9.7).

9.3 Analysis of the data on deuteron structure functions and polarization observables

In the previous Section we constructed the U&A model of deuteron electromagnetic structure, which uses 7 vector mesons. The constructed model depends on physical parameters like m_v, Γ_v for $v = \omega, \omega', \omega'', \phi, \phi', J/\Psi, x$, on the effective thresholds $t_{inC}, t_{inM}, t_{inQ}$ and on unknown ratios $a_{C:x}$ and $a_{Q:x}$. Naturally, we can fix masses m_v

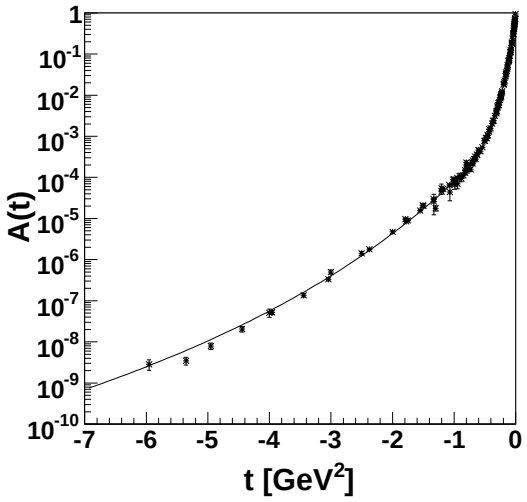

Fig. 9.3: Behavior of the deuteron structure function $A(t)$ predicted by the U&A model of the deuteron electromagnetic structure and its comparison to the experimental data.

and widths Γ_v of all known vector mesons $(\omega, \omega', \omega'', \phi, \phi', J/\Psi)$, what means, that there will remain 7 free parameters, which can be numerically evaluated in the optimal description of all available experimental data on the deuteron structure functions $A(t)$, $B(t)$ and the polarization observable $\tilde{t}_{20}(t)$. The results were obtained by using CERN program ROOT [42] and corresponding behaviors are shown on Figs. 9.3, 9.4, 9.5 together with data. The values of free parameters are given in Table 9.1.

$\frac{m_x}{\text{MeV}}$	$\frac{\Gamma_x}{\text{MeV}}$	$\frac{t_{inC}}{\text{GeV}^2}$	$\frac{t_{inM}}{\text{GeV}^2}$	$\frac{t_{inQ}}{\text{GeV}^2}$	$a_{C:x}$	$a_{Q:x}$
504.9 ± 0.1	677.6 ± 0.2	18.2 ± 0.1	20.2 ± 0.2	7.8 ± 0.1	3.43 ± 0.01	28.14 ± 0.03

Tab. 9.1: Fitted parameters of the U&A model of the deuteron EM structure.

As one can see, we obtained a good description of the deuteron structure functions $A(t)$, $B(t)$ and polarization observable $\tilde{t}_{20}(t)$ with $\chi^2/n.d.f. = 4.61$. Moreover the constructed model with the same values of free parameters can be used for the description of experimental data on other deuteron EM FFs $G_C(t)$ and $G_Q(t)$ (see Figs. 9.6, 9.7) as well as for estimation of all deuteron EM FFs time-like behavior (see Fig. 9.8), which allows us to estimate measurable quantity - the total cross section of the annihilation process $e^-e^+ \to d\bar{d}$

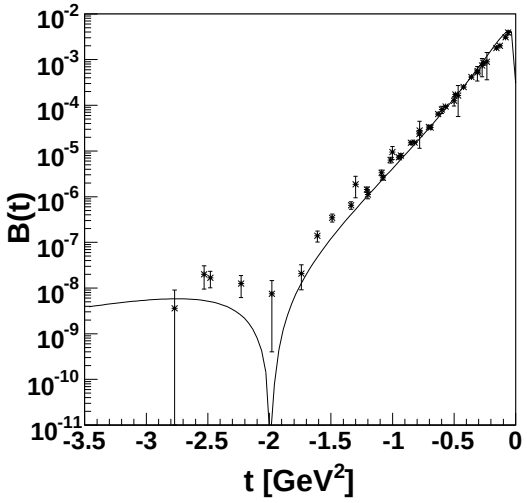

Fig. 9.4: Behavior of the deuteron structure function $B(t)$ predicted by the U&A model of the deuteron electromagnetic structure and its comparison to the experimental data

$$\sigma_{tot}(e^-e^+ \to d\bar{d}) = \frac{\pi\alpha^2\beta^3}{3t}\left[3|G_C(t)|^2 + 4\tau\left(|G_M(t)|^2 + \tfrac{2}{3}\tau|G_Q(t)|^2\right)\right], \qquad (9.8)$$

which is planned to be measured during years 2007-2010 in Peking (BES3). The estimated behavior of σ_{tot} is given in Fig. 9.9.

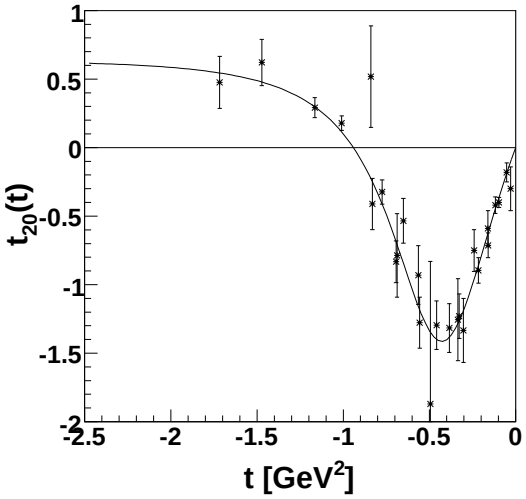

Fig. 9.5: Behavior of the deuteron polarization observable $\tilde{t}_{20}(t)$ predicted by the U&A model of the deuteron electromagnetic structure and its comparison to the experimental data

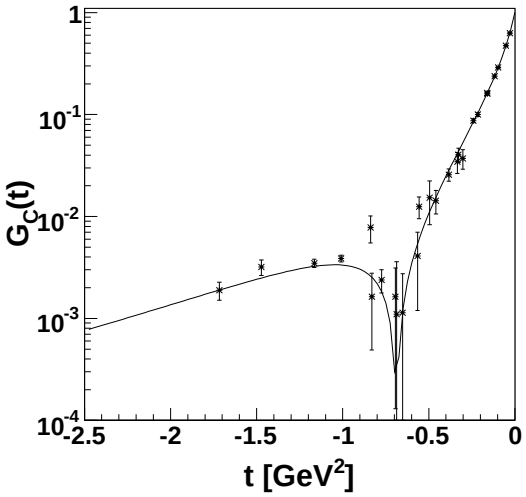

Fig. 9.6: The behavior of the deuteron charge form factor $G_C(t)$ predicted by the U&A model of the deuteron electromagnetic structure and its comparison to the experimental data.

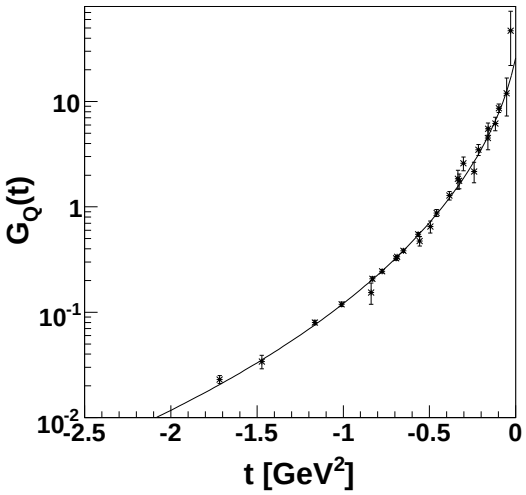

Fig. 9.7: The behavior of the deuteron quadrupole form factor $G_Q(t)$ predicted by the U&A model of the deuteron electromagnetic structure and its comparison to the experimental data

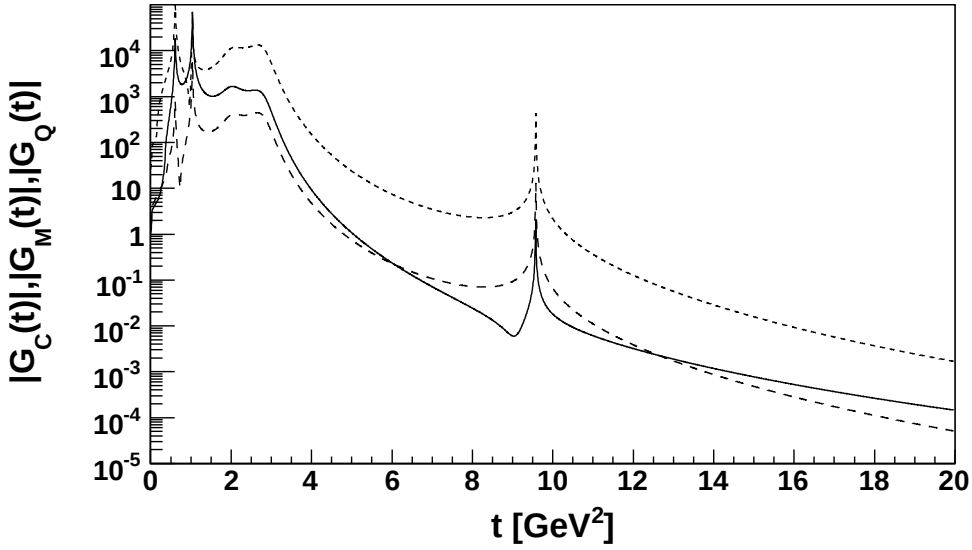

Fig. 9.8: The behavior of the deuteron EM form factors $G_C(t), G_M(t), G_Q(t)$ in the time-like region estimated by the U&A model of the deuteron electromagnetic structure. Full line corresponds to charge FF $G_C(t)$, dashed line corresponds to magnetic FF $G_M(t)$ and dotted line corresponds to quadrupole FF $G_Q(t)$.

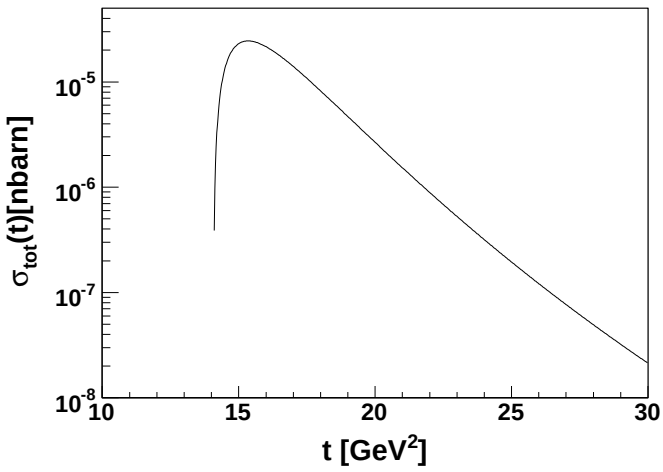

Fig. 9.9: The total cross section of the annihilation process $e^-e^+ \to d\bar{d}$ behavior estimated by the U&A model of the deuteron electromagnetic structure.

10. AXIAL FORM FACTOR OF THE NUCLEON

10.1 Introduction

The axial form factor of the nucleon, introduced in the Chapter 1, describes weak structure of the nucleon. Usually the dipole parametrization is assumed in the space-like region

$$g_A(q^2) = g_A(0)(1 - q^2/m_A^2)^{-2} \tag{10.1}$$

where $m_A = 1.06$ GeV stands for mass of the axial meson and $g_A(0) = 1.2673 \pm 0.0035$ is the normalization of the nucleon axial form factor. However similarly to the dipole form factor of the nucleon EM form factors this parametrization is rather inaccurate and it has poor physical background, while there is no real axial meson with mass 1.06 GeV. Moreover, up to now there is no model of the nucleon axial form factor to describe its behavior in the time-like region, which will be needed in the next Chapter to estimate pion production in nucleon-antinucleon annihilations.

Therefore we suggest [43] a simple phenomenological parametrization of the axial nucleon form factor and we make a fit on the available experimental data. The present description of the nucleon structure is based on IJL model of nucleon [33] with a compact core surrounded by a meson cloud. Its advantage is a possibility of a reasonable extension to the time-like region where no experimental data are available.

Up to now, the axial form factor of the nucleon has been measured directly in neutrino scattering experiments and in pion electroproduction experiments. In our analysis we consider data from the pion electroproduction only, as in the neutrino scattering experiments the dipole approximation is assumed a priori and only an axial meson mass is extracted from the data. On the other hand in the pion electroproduction experiments

the axial form factor is related to the slope of differential cross section as a function of ε near threshold. Low energy theorems calculate electric dipole amplitude at threshold in case of soft pions. In order to compare with real data model dependent corrections must be introduced to take into account finite pion mass. The data and their corrections will be discussed below.

10.2 Formalism

In the framework of the IJL model [33], it is possible to parametrize the axial form factor of the nucleon as

$$g_A(t) = g(t)\left[1 - \alpha + \alpha\frac{m_A^2}{m_A^2 - t}\right] g_A(0) \tag{10.2}$$

where α is a fitting parameter, $m_A = 1.17$ GeV is the mass of the lightest axial meson h_1 and

$$g(t) = (1 - \gamma t)^{-2} \tag{10.3}$$

is the function describing the internal core of the nucleon and according to IJL model of the nucleon $\gamma \simeq 0.25$ GeV^{-2} is a fixed parameter.

The asymptotic behavior of this parametrization is driven by

$$g_A(t) = \frac{(1-\alpha)g_A(0)}{(\gamma t)^2}$$

with a negative value for $\alpha > 1$.

A possible generalization can include the contribution of two or more axial mesons, with different masses.

10.3 Analysis of data

The considered set of data includes all points measured in pion electroproduction on nucleon experiments. A compilation can be found in Ref. [44].

The t-dependence of the nucleon axial form factor $g_A(t)$, was measured in several pion electroproduction experiments at the threshold since a few decades. The slope

of the total unpolarized differential cross section at threshold, contains information on $g_A(t)$. The numerical value of this FF is model dependent.

In general, four different approaches were used to extract values on the axial form factor of the nucleon. Soft pion approximation (SP) [45], partially conserved axial current approximation (PCAC) [46], enhanced soft pion approximation – Fulran approximation (FPV) [47] and Dombey and Read approximation (DR) [48].

As a consequence of these competing approaches, up to four experimental values may be extracted from a single measurement (at fixed t). Alltogether 67 experimental points are available, corresponding to only 32 measurements. Data from Ref. [49] were considered separately, as they correspond to Δ excitation in final state. In order to evaluate the systematic error, the data were therefore separated in 5 groups according to used approach (measured processes). The data from [50] were not considered in the final fit, following Ref. [44] as they are systematically higher as well as data from [45].

The data are plotted in Fig. 10.1(a). Different symbols correspond to different models used for the extraction of the data but may correspond to the same experiment.

A global one parameter fit was performed, as well as individual fits to the 5 data sets, according to Eq. 10.2. The results are shown in Table 10.1 and in Fig. 10.1. The final global fit gives $\alpha = 1.46 \pm 0.04$, with $\chi^2/n.d.f. = 81.47/48 = 1.70$.

Model	DR	FPV	SP	PCAC	Δ	all
α	1.29 ± 0.08	1.74 ± 0.13	1.08 ± 0.06	1.66 ± 0.05	1.13 ± 0.07	1.46 ± 0.04
$\chi^2/n.d.f.$	1.38	0.80	3.75	0.76	0.45	1.70

Tab. 10.1: Fitted α parameter for various approaches of extracting data on axial FF.

10.4 Extension to time-like region

An extension to the TL region of the presented model can be made in the similar way as in the original IJL model of nucleon EM FFs. It can be summarized in following steps

- An complex phase δ, the same as for IJL model, is introduced in the internal core term (10.3).

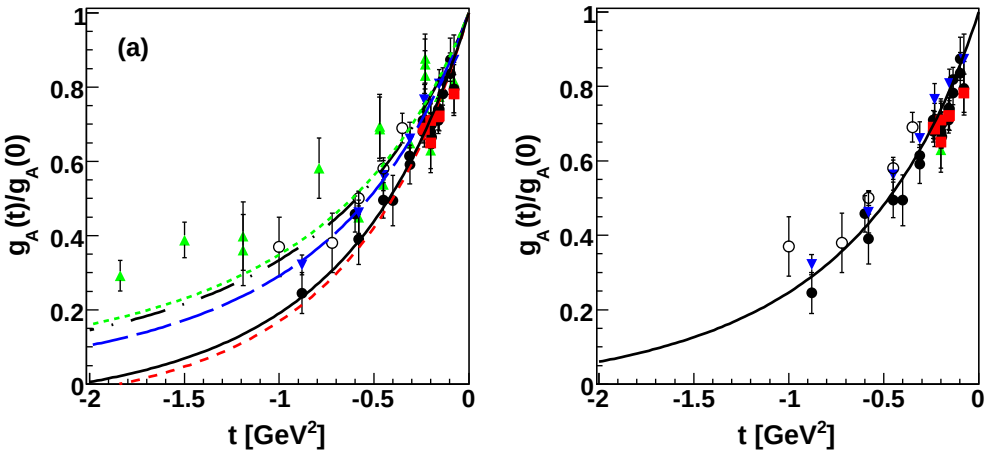

Fig. 10.1: *(a)*: Fits of the nucleon axial form factor made separately for different approaches, where triangle points and dotted line corresponds to SP [45], square points and dashed line – FPV [47], reversed triangle points and long dashed line – DR [48], full circle points and full line – PCAC [46], empty circle points and dashed-dotted line – Δ excitation [49]. *(b)*: The final global fit of the nucleon axial FF.

- VMD term corresponding to exchange of axial meson should be substituted by Breit-Wigner formula due to considerable width of assumed axial meson.

These modifications leads to following parametrization of axial FF in TL region

$$g_A(t) = g(t)\left[1-\alpha+\alpha\frac{m_A^2\left(m_A^2-t+im_A\Gamma_A\right)}{\left(m_A^2-t\right)^2+\left(m_A\Gamma_A\right)^2}\right]g_A(0) \tag{10.4}$$

where

$$g(t) = \left(1-e^{i\delta}\gamma t\right)^{-2}. \tag{10.5}$$

The TL behavior of the nucleon axial FF is given in Fig.10.2 and the value of axial FF is significantly higher than in the SL region. The position and shape of the presented peak is given by values of γ and δ in the internal core term (10.5). However appropriateness of such TL behavior can not be verified due to no available data on the nucleon axial FF in TL region.

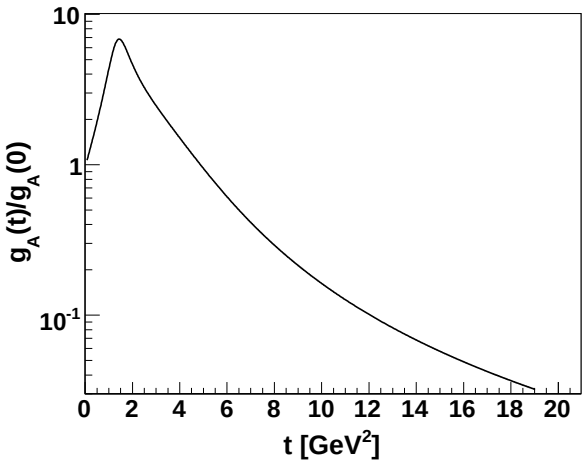

Fig. 10.2: Predicted nucleon axial form factor behavior in the TL region.

10.5 Dipole limit for IJL formula

There is also an alternative way to obtain reasonable description of available data on the nucleon axial form factor with presented model by satisfying compatibility with old dipole fit. The idea of this method is to force same small q^2 behavior of both models. In the first order of Taylor series

$$\begin{aligned} \lim_{t\to\infty} g_A(t) &= g_A(0)(1+\frac{2}{M_A^2}t) \\ \lim_{t\to\infty} g_A(t) &= g_A(0)(1+(2\gamma+\frac{\alpha}{m_A^2})t), \end{aligned} \tag{10.6}$$

where M_A is mass of axial meson fitted in dipole approximation and m_A is mass of real(lightest) axial meson. By assuming the same behavior one gets

$$\alpha = 2m_A^2(\frac{1}{M_A^2}-\gamma) = 1.71 \tag{10.7}$$

As we can see in the Fig. 10.3 such method also provides reasonable description of the available data.

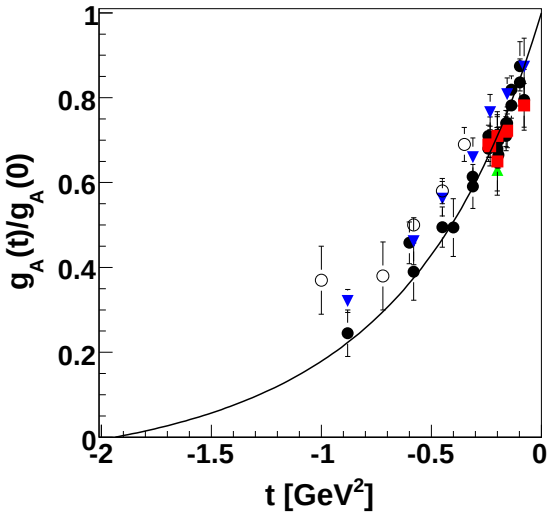

Fig. 10.3: The nucleon axial form factor in the dipole limit as a function of t

11. MEASUREMENT OF THE NUCLEON EM AND AXIAL FFS

11.1 Motivation

Up to now it has not been possible to measure nucleon electromagnetic form factors in the time-like region under threshold of the annihilation – so called unphysical region, because this region is kinematically forbidden for the annihilation reaction $\bar{p} + p \to e^+ + e^-$ usually used for measurement of nucleon time-like EM form factors. Also there are no experimental data on axial form factor of the nucleon in the time-like region.

In this Chapter we will study [51] the annihilation reactions

$$\begin{aligned} &\bar{p}(p_1) + n(p_2) \to \pi^-(q_\pi) + \ell^-(p_-) + \ell^+(p_+) \\ &\bar{p}(p_1) + p(p_2) \to \pi^0(q_\pi) + \ell^-(p_-) + \ell^+(p_+)\ ,\ \ell = e, \mu \end{aligned} \tag{11.1}$$

which are the crossed processes of pion electroproduction on a nucleon $e^- + N \to e^- + N + \pi$. They contain the same information on the nucleon form factors in the different kinematical region. These processes are also related to the pion scattering process $\pi + N \to N + \ell^- + \ell^+$ which was studied in [52]. In that paper it was pointed out, that annihilation processes (11.1) give possibility of determination of the nucleon electromagnetic form factors in the unphysical region, which is otherwise unreachable by the annihilation reaction $\bar{p} + p \to e^+ + e^-$. In another paper [53] a general expression for the cross section was derived and numerical estimations were given in the kinematical region near threshold. Now we will take into account a larger set of diagrams contributing to the processes and we will give special emphasis to the possibility of extraction of the axial nucleon form factor in the time-like region. The aim of this Chapter is to estimate differential cross section for experimental conditions achievable at the future

FAIR facility [54] by using existing models of nucleon structure extended to time-like region.

11.2 Formalism

Our approach is based on Compton-like annihilation Feynman amplitudes and aims to establish the matrix elements of the processes (11.1). The main uncertainty in this description in terms of Green functions of mesons and nucleons is related to the model dependent description of hadron FFs. Possible tree level Feynman diagrams of the considered processes (11.1) are shown in Figs. 11.1, 11.2 and they differ in a particle emitting lepton-antilepton pair. In the case of the first process there are only two possible tree level diagrams, while spinless neutral particle π^0 can not emit the $\ell\bar{\ell}$ pair.

As it has been already discussed in [53] vertices of pion and nucleons, $\gamma^* NN^*$ and $\gamma^*\pi\pi^*$, contain virtual hadrons, and rigorously speaking, electromagnetic form factors should be modified taking into account off mass shell effects. However we will use standard on mass shell form factors as errors of such approximation are at the level of 3% [55].

Therefore the expression for nucleon electromagnetic current can be written as

$$\left\langle N(p')\left|\Gamma^N_\mu(q)\right|N(p)\right\rangle = \bar{u}(p')\left[F_1^N(q^2)\gamma_\mu + \frac{F_2^N(q^2)}{4M}(\hat{q}\gamma_\mu - \gamma_\mu\hat{q})\right]u(p)\ ,\ N = n,p, \tag{11.2}$$

where M is the nucleon mass, q is the four-momentum of the virtual photon and F_1^N, F_2^N are Dirac and Pauli form factors of the proton and neutron.

The pion (π^-) electromagnetic form factor $F_\pi(q^2)$ is also introduced in the standard way through corresponding EM current as

$$J^\pi_\mu = (q_1+q_2)_\mu F_\pi(q^2_\pi), \tag{11.3}$$

where q_1, q_2 are momenta of incoming and outgoing charged pion and $q_\pi = q_1 - q_2$. Special attention must be devoted to the pion nucleon interaction in the vertices πNN, which are parametrized as

$$\bar{v}(p_1)\gamma_5 u(p_2) g_{\pi NN}(s), \quad \text{and} \quad \bar{v}(p_1-q)\gamma_5 u(p_2) g_{\pi NN}(m^2_\pi) \tag{11.4}$$

with $s = (p_1 + p_2)^2$.

The vertex of πNN interaction can be related to the general axial vector current matrix element

$$\left\langle N(p') \left| A_j^\mu(0) \right| N(p) \right\rangle = \bar{u}(p') \left[G_A(q^2)\gamma_\mu + \frac{q^\mu}{2M} G_P^2(q^2) + i\frac{\sigma^{\mu\nu}}{2M} G_T(q^2) \right] \gamma_5 \frac{\tau_j}{2} u(p), \tag{11.5}$$

where $q_\mu = p'_\mu - p_\mu$, $G_A(q^2)$ is the axial nucleon FF, $G_P(q^2)$ the induced pseudoscalar FF and $G_T(q^2)$ the induced pseudotensor FF. In the chiral limit, the requirement of conservation of the axial current leads to the relation:

$$4MG_A(q^2) + q^2 G_P(q^2) = 0, \tag{11.6}$$

which shows that $G_P(q^2)$ has a pole at small q^2. Indeed, assuming that the axial current interacts with the nucleon through the conversion to pion interaction, one obtains

$$G_P(q^2) = -\frac{4Mf_\pi g_{\pi NN}(q^2)}{q^2} \tag{11.7}$$

By comparing Eqs. (11.6) and (11.7) one obtains the Golberger-Treiman relation

$$\frac{G_A}{f_\pi} = \frac{g_{\pi NN}}{M}. \tag{11.8}$$

Assuming a generalization of this relation in the form

$$g(s) = g_{\pi\bar{N}N}(s) = \frac{MG_A(s)}{f_\pi},\ G_A(0) = 1.2673 \pm 0.0035, \tag{11.9}$$

where $g(s)$, $g(m_\pi^2)$ are the pion-nucleon coupling constants for pion off and on mass shell. This assumption can be justified by the fact that f_π is weakly depending on q^2 and it is in agreement with the ChPT expansion at small q^2 [56]. Therefore measuring the $g_{\pi\bar{N}N}(s)$ coupling constant gives information on the axial and induced pseudoscalar FFs of the nucleon in the chiral limit (neglecting the pion mass).

The matrix element can be expressed in terms of the hadronic H and leptonic J currents

$$M^i = \frac{4\pi\alpha}{q^2} H_\mu^i J^\mu(q),\ H_\mu^i = \bar{v}(p_1) O_\mu^i u(p_2),\ J^\mu(q) = \bar{v}(p_+)\gamma_\mu u(p_-), \tag{11.10}$$

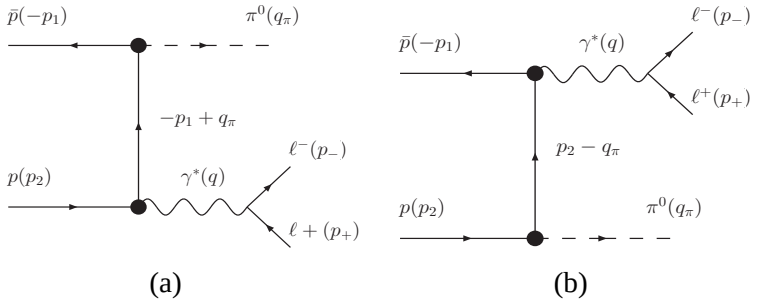

Fig. 11.1: Feynman diagrams for the reaction $\bar{p}+p \to \pi^0+\ell^+ +\ell^-$.

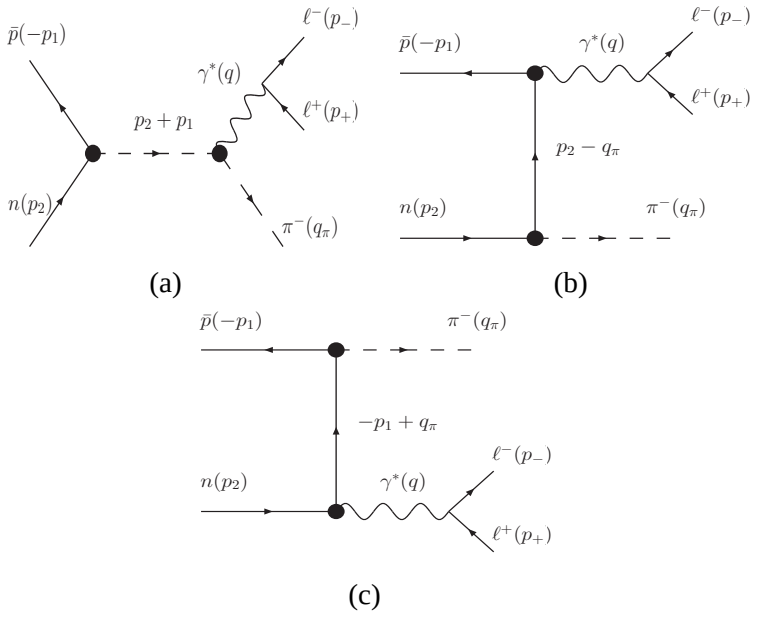

Fig. 11.2: Feynman diagrams for the reaction $\bar{p}+n \to \pi^- +\ell^+ +\ell^-$.

where the index $i = 0, -$ refers to π^0 and π^- respectively. The cross section for the case of unpolarized particles has a standard form (we imply that the nucleon target is at rest in the Laboratory frame)

$$d\sigma^i = \frac{1}{16PM} \sum |M^i|^2 d\Gamma, \;\; P^2 = E^2 - M^2, \tag{11.11}$$

where E is the energy, P is the modulus of the momentum and $d\Gamma$ is the phase space volume

$$d\Gamma = \frac{1}{(2\pi)^5} \frac{d^3p_+}{2\epsilon_+} \frac{d^3p_-}{2\epsilon_-} \frac{d^3q_\pi}{2E_\pi} \delta^4(p_1 + p_2 - p_+ - p_- - q_\pi). \tag{11.12}$$

The phase space volume can be written as

$$d\Gamma = \frac{d^3q_\pi}{2E_\pi} d\Gamma_q \frac{d^4q}{(2\pi)^5} \delta^4(p_1 + p_2 - q - q_\pi),$$

with

$$d\Gamma_q = \frac{d^3p_+}{2\epsilon_+} \frac{d^3p_-}{2\epsilon_-} \delta^4(q - p_+ - p_-).$$

Considering an experimental set-up with the fully measured pion four-momentum, we can perform the integration on the phase space volume of the lepton pair

$$\int d\Gamma_q \sum J_\mu(q) J^*_\nu(q) = -\frac{2\pi}{3}(q^2 + 2\mu^2)\beta\Theta(q^2 - 4\mu^2) \left(g_{\mu\nu} - \frac{q_\mu q_\nu}{q^2} \right), \tag{11.13}$$

where Θ is the usual step function, μ is the lepton mass and $\beta = \sqrt{1 - (4\mu^2/q^2)}$.

The cross section can be expressed in the form

$$d\sigma^i = \frac{\alpha^2}{6s\pi r} \frac{\beta(q^2 + 2\mu^2)}{(q^2)^2} \mathcal{D}^i \frac{d^3q_\pi}{2\pi E_\pi}, \tag{11.14}$$

with

$$s = (q_\pi + q)^2 = 2M(M + E), \;\; r = \sqrt{1 - (4M^2/s)} \tag{11.15}$$

and

$$\mathcal{D}^i = \left(g_{\mu\nu} - \frac{q_\mu q_\nu}{q^2} \right) \frac{1}{4} Tr(\hat{p}_1 - M) O^i_\mu (\hat{p}_2 + M) (O^i_\nu)^*, \;\; i = 0, -. \tag{11.16}$$

Using Feynman rules we can write (see Figs. 11.1, 11.2)

$$\begin{aligned} O^-_\mu &= \Gamma^p_\mu(q) \frac{\hat{p}_1 - \hat{q} - M}{(p_1 - q)^2 - M^2} \gamma_5 g(m^2_\pi) - \\ &\quad \gamma_5 \frac{\hat{p}_2 - \hat{q} + M}{(p_2 - q)^2 - M^2} \Gamma^n_\mu(q) g(m^2_\pi) + \frac{(2q_\pi + q)_\mu}{s - m^2_\pi} g(s) F_\pi(q^2) \gamma_5 \end{aligned} \tag{11.17}$$

$$O^0_\mu = \Gamma^p_\mu(q) \frac{\hat{p}_1 - \hat{q} - M}{(p_1 - q)^2 - M^2} \gamma_5 g(m^2_\pi) - \gamma_5 \frac{\hat{p}_2 - \hat{q} + M}{(p_2 - q)^2 - M^2} \Gamma^p_\mu(q) g(m^2_\pi). \tag{11.18}$$

Note that the hadronic current $\mathcal{J}^0_\mu = \bar{v}(p_1)O^0_\mu u(p_2)$ is conserved $J^0_\mu q^\mu = 0$, but $J^-_\mu = \bar{v}(p_1)O^-_\mu u(p_2)$ is not conserved

$$q_\mu \mathcal{J}^-_\mu = \left[(-F_1^p(q^2) + F_1^n(q^2))g(m_\pi^2) + g(s)F_\pi(q^2)\right]\bar{v}(p_1)\gamma_5 u(p_2) = \mathcal{C}\bar{v}(p_1)\gamma_5 u(p_2). \tag{11.19}$$

Therefore, to provide gauge invariance, it is necessary to add to O^-_μ a contact term with the appropriate structure (11.19).

The explicit expression for $\mathcal{D}^0$ (corresponds to the process $p + \bar{p} \to \ell^+ + \ell^- + \pi^0$) can be written as

$$\mathcal{D}^0 = |f_{2p}|^2 \left[\frac{E-M}{M} - \frac{1}{2}\left(1 - \frac{q^2}{4M^2}\right)\frac{(1-X)^2}{X}\right] + |f_{1p} - f_{2p}|^2 \frac{(X+1)^2}{X}. \tag{11.20}$$

and the expression for $\mathcal{D}^-$, which corresponds to the process $n + \bar{p} \to \ell^+ + \ell^- + \pi^-$ is

$$\mathcal{D}^- = \frac{1}{4}\left[\sum_i C_{i,i}|f_i|^2 + 2\sum_{j,k;j<k} C_{j,k} Re(f_j f_k^*) + \frac{2|\mathcal{C}|^2 s}{q^2}\right], \quad i,j,k = 1p, 2p, 1n, 2n, a, \tag{11.21}$$

where q^2-dependent terms, which contain FFs are

$$f_a(s) = F_\pi(q^2)G_{\pi N\bar{N}}(s),\ f_{iN}(q^2) = g(m_\pi^2)F_i^N(q^2),\ i = 1,2,\ N = n,p,$$

$$\mathcal{C}(s) = f_a(s) - f_{1p}(q^2) + f_{1n}(q^2),$$

quantity X is defined as

$$X = \frac{p_1 q_\pi}{p_2 q_\pi} = (s - q^2)/(2ME_\pi) - 1 \tag{11.22}$$

and coefficients used in (11.21) have the following form

$$\begin{aligned}
C_{1p,1p} &= 4X,\ C_{2p,2p} = \frac{s}{M^2}\left(1 + \frac{q^2}{2s}X\right),\ C_{1p,2p} = -3\,(1+X)\,,\ C_{a,a} = \frac{2q^2}{s} - 4,\\
C_{1n,1n} &= 4\frac{1}{X},\ C_{2n,2n} = \frac{s}{M^2}\left(1 + \frac{q^2}{2sX}\right),\ C_{1n,2n} = -3\left(1 + \frac{1}{X}\right),\\
C_{a,1p} &= 2,\ C_{a,2p} = \left(1 - \frac{q^2}{s}\right)(1+X)\,,\ C_{1p,1n} = 4,\ C_{1p,2n} = \left(\frac{1}{X} - 2X - 1\right),\\
C_{2p,2n} &= \left(2 + \frac{2}{X} - \frac{q^2}{2M^2} + X\right),\ C_{2p,1n} = \left(X - \frac{2}{X} - 1\right),\\
C_{a,1n} &= -2,\ C_{a,2n} = -\left(1 - \frac{q^2}{s}\right)\left(1 + \frac{1}{X}\right).
\end{aligned} \tag{11.23}$$

Selecting the coefficients which depend on pion energy in $\mathcal{D}_i$, Eq. (11.16), one can perform an analytical integration on the pion energy can be performed. In the limit of small lepton pair invariant mass, q^2, after integration on pion energy, the differential cross section with respect to q^2 becomes

$$(q^2)^2 \left.\frac{d\sigma}{dq^2}\right|_{q^2 \ll M^2} \simeq \frac{\alpha^2[g(s) - g(m_\pi^2)]^2}{24\pi r}. \tag{11.24}$$

Eq. (11.24) shows that the measurement of the cross section at small q^2 allows to determine experimentally the off mass shell pion nucleon coupling constant.

Writing the differential cross section in the form

$$\frac{d\sigma}{dq^2} = \frac{(q^2 + 2\mu^2)\beta}{(q^2)^2}\left[\frac{c}{q^2} + R(q^2)\right], \tag{11.25}$$

where c and $R(0)$ are finite functions of s. After integration of lepton invariant mass, we find

$$\sigma_{tot} = \int_{4\mu^2}^{s} \frac{d\sigma}{dq^2} dq^2 = \frac{c(s)}{5\mu^2} + R(0,s)\left(\log\frac{s}{\mu^2} - \frac{5}{3}\right) + \int_0^s \frac{dq^2}{q^2}[R(q^2,s) - R(0,s)]. \tag{11.26}$$

The first term in the right hand side of Eq. (11.26) is divergent for massless leptons, and induces a rise of the cross section (especially in the case of electron positron pair). However it is very hard to achieve experimentally such kinematics, $q^2 \to 4\mu^2$. The total cross section can be integrated within the experimental limits of detection of the particles. Such (partial) total cross section will be calculated below.

11.3 Kinematics

In the Laboratory system, useful relations can be derived between the kinematical variables, which characterize the reaction. The allowed kinematical region, at a fixed incident total energy s can be illustrated as a function of different useful variables.

One can find the following relation between q^2, the invariant mass of the lepton pair and the pion energy

$$q^2 = (p_1 + p_2 - q_\pi)^2 = 2M^2 + m_\pi^2 + 2M(E - E_\pi) - 2p_1 q_\pi = s + m_\pi^2 - 2E_\pi M - 2p_1 q_\pi, \tag{11.27}$$

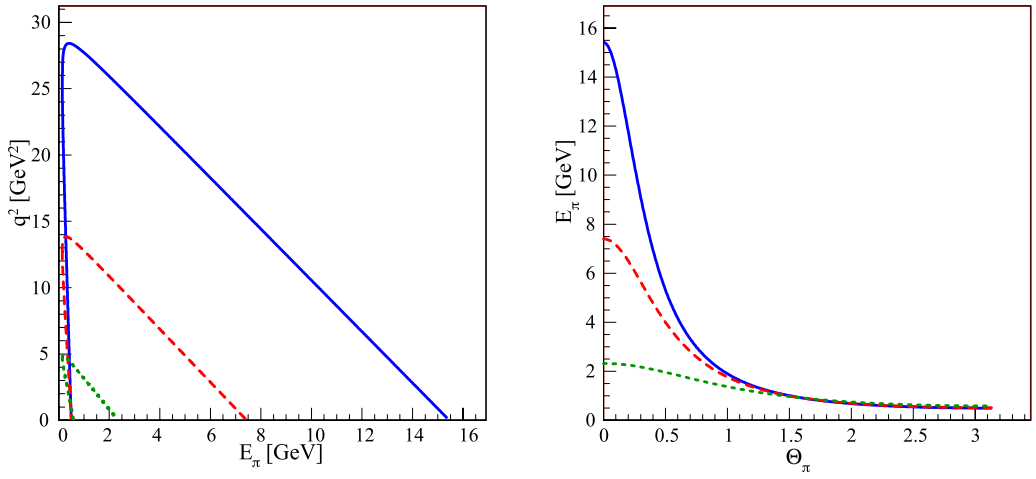

Fig. 11.3: *Left:* The kinematical limit for q^2 is shown for $\cos\theta_\pi = -1$ and for $\cos\theta_\pi = 1$ in the Lab system as function of the pion energy for different values of the beam energy: E=2 GeV^2 (dotted line), E=7 GeV^2 (dashed line), E=15 GeV^2 (solid line). The allowed kinematical region lies below the curves. *Right:* Kinematical limit for the pion energy E_π as a function of the pion angle (Lab system), for E=2 GeV^2 (dotted line), E = 7GeV^2 (dashed line), E = 15GeV^2 (solid line), for the minimum value of $q^2 \simeq m_\pi^2$.

with

$$2p_1q_\pi = 2E_\pi E - 2\sqrt{E_\pi^2 - m_\pi^2}P\cos\theta_\pi, \tag{11.28}$$

where $\theta_\pi = \widehat{\vec{p}_1\vec{q}_\pi}$ is the angle between the antiproton and the pion momenta (in the Laboratory frame).

The limit $-1 \leq \cos\theta_\pi \leq 1$ translates into a maximal and a minimal value for the pion energy. The allowed kinematical region is shown in Fig. 11.3 left, for three values of the beam energy: E = 2, 7, 15 GeV. To this constraint, one should add the minimal thresholds $q^2 \geq 4m_\ell^2$ and $E_\pi \geq m_\pi$. For the minimal value of $q^2 \simeq m_\pi^2$, one can plot the dependence of the pion energy on θ_π (Fig. 11.3, right), for different values of the beam energy. As the energy increases the kinematically allowed region becomes wider. At backward angles the maximum pion energy becomes larger at small s values. For larger values of q^2, E_π is smaller.

For fixed values of the lepton pair invariant mass, the pion energy can take values in the region

$$\frac{E_\pi^{min}}{M} = \frac{s-q^2}{s(1+r)} \leq \frac{E_\pi}{M} \leq \frac{s-q^2}{s(1-r)} = \frac{E_\pi^{max}}{M}, \tag{11.29}$$

neglecting the pion mass.

The phase space volume of the produced pion can be written (neglecting terms $\simeq m_\pi^2/m_N^2$) in three (equivalent) forms

$$\begin{aligned}
\frac{d^3q_i}{2\pi E_\pi} &= dq^2\delta[q^2 - 2E_\pi(E+M-P\cos\theta_\pi)]E_\pi dE_\pi d\cos\theta_\pi \\
&= E_\pi dE_\pi d\cos\theta_\pi && \text{(11.30a)} \\
&= M\frac{dq^2}{sr}dE_\pi && \text{(11.30b)} \\
&= \frac{q^2M^2dq^2d\cos\theta_\pi}{s^2(1-r\cos\theta_\pi)^2} && \text{(11.30c)}
\end{aligned}$$

11.4 Axial and EM form factors

In order to estimate cross sections of the considered processes we will use existing models of nucleon and pion structure. The nucleon EM form factors in the time-like region can be described by the simple pQCD inspired model with smooth behavior, which does not show any discontinuities and can be considered an 'average' expectation

$$|G_E^N| = |G_M^N| = \frac{A(N)}{q^4\left(\ln^2\frac{q^2}{\Lambda^2} + \pi^2\right)},\ q^2 > \Lambda^2, \tag{11.31}$$

where $\Lambda = 0.3$ GeV is the QCD scale parameter and A is fitted to the data. This parametrization is taken to be the same for proton and neutron. The best fit is obtained with a parameter $A(p)$= 98 GeV^4 for the proton and $A(n)$= 134 GeV^4 for the neutron, which reflects the fact that in the TL region, neutron FFs are systematically larger than for the proton. In principle, this parametrization holds only for very large q^2 values, but, in practice, it reproduces the existing data quite well in the whole physical region. Evidently it is meaningless at small q^2, ($q^2 < \Lambda^2$), and it has not the good normalization properties for $q^2 \to 0$.

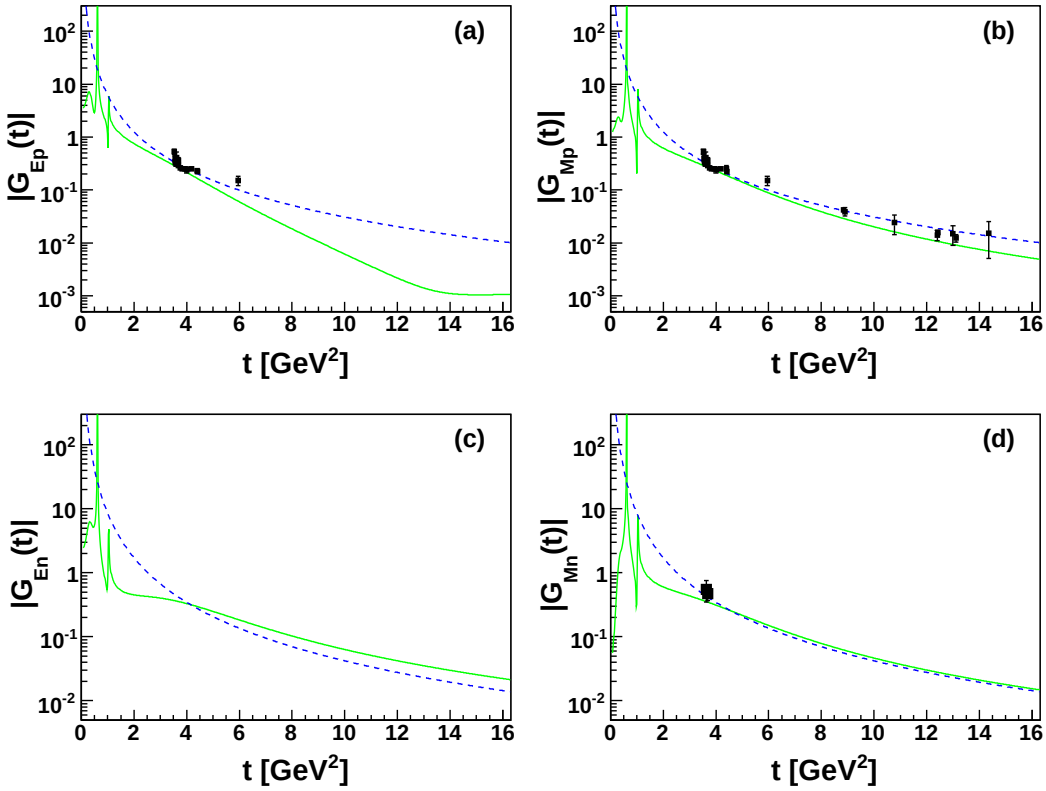

Fig. 11.4: Nucleon electromagnetic FFs in time-like region: proton electric FF (a), proton magnetic FF (b), neutron electric FF (c), neutron magnetic FF (d). Data are from [59] and predictions from model [33] (solid line), and from pQCD (dashed line).

For a comparison we will use VMD-based model [33, 57] of the nucleon EM form factors, with characteristic resonance behavior in the unphysical region. Both models have been well discussed in the [58] and the behavior of these FFs is shown in Fig. 11.4.

Data on the nucleon axial FFs in TL region do not exist, and they suffer in SL region from a model dependent derivation. In SL region, the nucleon axial FF, $G_A(q^2)$, for the transition $W^* + p \to n$ (W^* is the virtual W-boson), can be described by the following simple formula [44]

$$G_A(q^2) = G_A(0)(1 - q^2/m_A^2)^{-n} \tag{11.32}$$

with $m_A = 1.06$ GeV, if $n = 2$. A simple analytical continuation of this prescription to the TL region, presents a pole in the unphysical region. Therefore we used a 'mirror'

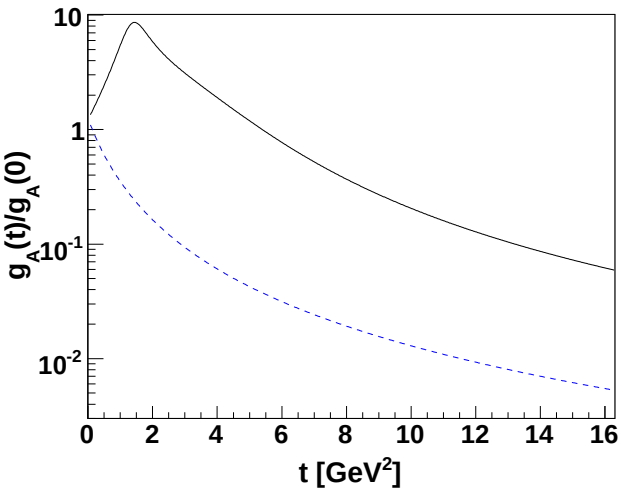

Fig. 11.5: Proton axial FF from VMD inspired model (solid line) and from a dipole extrapolation (dashed line).

parametrization from SL region

$$FF^{(TL)}(|q^2|) = FF^{(SL)}(|q^2|).$$

Such a prescription is, in principle, valid only at very large q^2, since it obeys to asymptotic analytical properties of FFs [60].

Again for a comparison we will use the VMD-inspired model of the nucleon axial form factor discussed in Chapter 10 extended to time-like region (10.4,10.5). The behavior of both models is shown in Fig. 11.5

Concerning the pion FF, a reasonable description exists in the kinematical region of interest here, for a recent discussion see Ref. [61]. For the sake of simplicity, we use here a ρ meson saturated monopole-like parametrization, which takes a Breit Wigner form in TL region

$$F_\pi(q^2) = \frac{m_\rho^2}{m_\rho^2 - q^2 - im_\rho\Gamma_\rho}. \tag{11.33}$$

11.5 Results

The differential and integrated cross sections were calculated for several values of the antiproton energy and different choices of FFs described above.

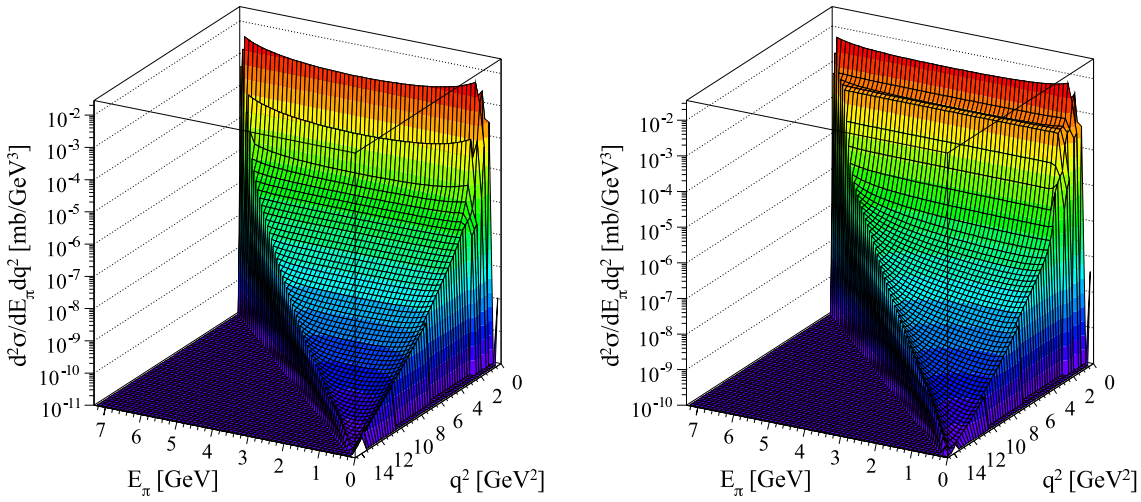

Fig. 11.6: *Left:* Double differential cross section for the reaction $\bar{p} + p \to \pi^0 + \ell^+ + \ell^-$ as a function of q^2 and E_π, using FFs from [33] for nucleon and (10.4) for axial FF. *Right:* Same quantity as in the left plot for the reaction $\bar{p} + n \to \pi^- + \ell^+ + \ell^-$. The kinematical constraints in the (E_π, q^2)-plane shown in Fig. 11.3 are visible here.

The differential cross sections, Eq. (11.14), as a function of E_π and q^2, Eq. (11.30a), are shown in Figs. 11.6 and 11.7 for the reactions $\bar{p} + p \to \pi^0 + \ell^+ + \ell^-$ and $\bar{p} + n \to \pi^- + \ell^+ + \ell^-$ and at E= 7 GeV^2. As one can see from the figures, the differential cross sections are large and measurable in a wide range of the considered variables. It is reasonable to assume that the region up to $q^2 = 7$ GeV^2, at least, will be accessible by the experiments at FAIR.

The discontinuities in the small q^2 regions are smoothed out by the steps chosen to histogram the variables. However, depending on the resolution and the reconstruction efficiency, it will be experimentally possible to identify the meson and nucleon resonances.

In order to illustrate the kinematical region in the plane E_π - θ_π, the double differential cross section for the process $\bar{p} + n \to \pi^0 + \ell^+ + \ell^-$ is shown in Fig. 11.8, for $s = 7$ GeV^2.

The differential cross section as a function of q^2 can be obtained after integrating on

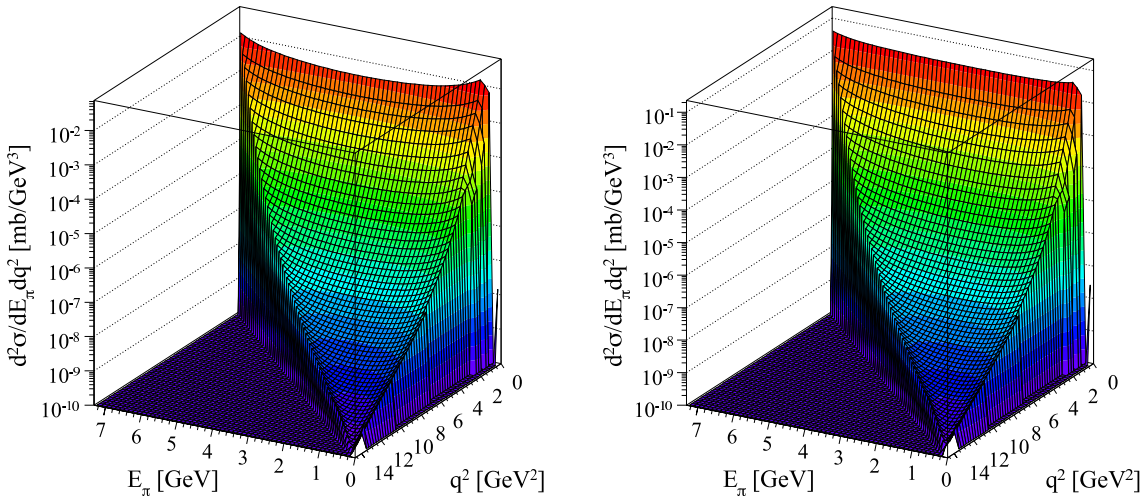

Fig. 11.7: *Left:* Double differential cross section for the reaction $\bar{p} + p \to \pi^0 + \ell^+ + \ell^-$ as a function of q^2 and E_π, using pQCD inspired nucleon FFs and dipole axial FFs. *Right:* Same quantity as in the left plot for the reaction $\bar{p} + n \to \pi^- + \ell^+ + \ell^-$.

the pion energy, Eq. (11.14), with the help of Eq. (11.30b)

$$\frac{d\sigma^i}{dq^2} = \frac{\alpha^2}{6s\pi r}\frac{\beta(q^2+2\mu^2)}{(q^2)^2}\frac{M}{sr}\int_{E_\pi^{min}}^{E_\pi^{max}} \mathcal{D}^i dE_\pi, \tag{11.34}$$

where the integration of the hadronic terms (11.20, 11.21) can be done analytically by using following integrals

$$\int_{E_\pi^{min}}^{E_\pi^{max}} \frac{dE_\pi}{M} = \frac{r(s-q^2)}{2M^2} = rb\ ,\ b = \frac{s-q^2}{2M^2} \tag{11.35}$$

$$\int_{E_\pi^{min}}^{E_\pi^{max}} \frac{dE_\pi}{M} X = \int_{E_\pi^{min}}^{E_\pi^{max}} \frac{dE_\pi}{M}\frac{1}{X} = \frac{s-q^2}{2M^2}\left[\ln\frac{1+r}{1-r} - r\right] = b(\ell - r), \tag{11.36}$$

where r is given in (11.15) and $\ell = \ln[(1+r)/(1-r)]$. The result of the integration on the pion energy is

- for the process $p + \bar{p} \to \ell^+ + \ell^- + \pi^0$

$$\int_{E_\pi^{min}}^{E_\pi^{max}} \mathcal{D}^0\ \frac{dE_\pi}{M} = b\left\{2|f_{1p} - f_{2p}|^2\ell + |f_{2p}|^2\left[\frac{E-M}{M}r + \left(1 - \frac{q^2}{4M^2}\right)(2r-\ell)\right]\right\} \tag{11.37}$$

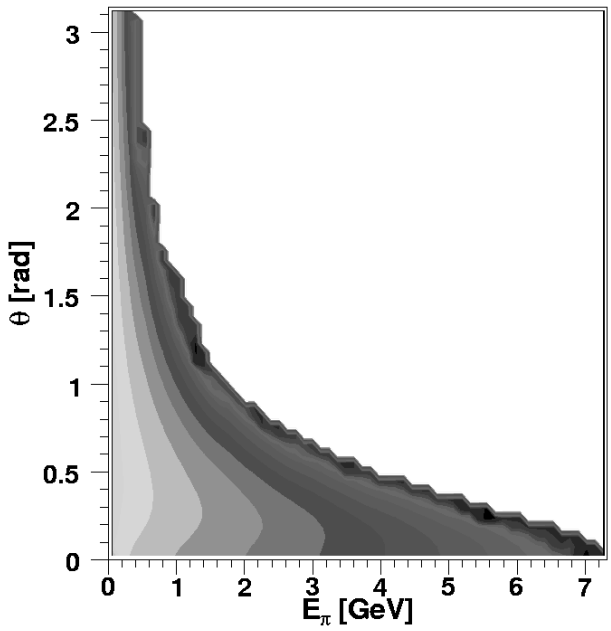

Fig. 11.8: Double differential cross section for the process $\bar{p} + n \to \pi^0 + \ell^+ + \ell^-$ as a function E_π and $\cos\theta_\pi$ using FFs from [33] for nucleon and (10.4) for axial FF (darker gray correspond to larger values).

- for the process $p + \bar{p} \to \ell^+ + \ell^- + \pi^0$

$$\int_{E_\pi^{min}}^{E_\pi^{max}} \mathcal{D}^- \frac{dE_\pi}{M} = \frac{b}{4}\left[\sum_i K_{i,i}|f_i|^2 + 2\sum_{j,k;j<k} K_{j,k} Re(f_j f_k^*) + |\mathcal{C}|^2 \frac{2rs}{q^2}\right], \qquad (11.38)$$

where

$$\begin{aligned}
K_{1p,1p} &= 4(\ell - r),\ K_{2p,2p} = \frac{s}{M^2}\left(r + \frac{q^2}{2s}(\ell - r)\right),\\
K_{1p,2p} &= -3\ell,\ K_{a,a} = \left(\frac{2q^2}{s} - 4\right) r,\\
K_{1n,1n} &= 4(\ell - r),\ K_{2n,2n} = \frac{s}{M^2}\left(r + \frac{q^2}{2s}(\ell - r)\right),\ K_{1n,2n} = -3\ell,\\
K_{a,1p} &= 2r,\ K_{a,2p} = \left(1 - \frac{q^2}{s}\right)\ell,\ K_{1p,1n} = 4r,\ K_{1p,2n} = -\ell,\\
K_{2p,2n} &= \left[3\ell - \left(1 + \frac{q^2}{2M^2}\right) r\right],\ K_{2p,1n} = -\ell,\\
K_{a,1n} &= -2r,\ K_{a,2n} = -\left(1 - \frac{q^2}{s}\right)\ell, \qquad (11.39)
\end{aligned}$$

The result of the calculation is shown in Fig. 11.9. For charged pion production, the presence of the axial FF is the reason of a larger cross section as compared to the neutral pion case. For both reactions, again, the present calculation gives an integrated cross section of the order of several μb in the unphysical region, for both choices of FFs.

The q^2 dependence is driven by the choice of FFs. In case of pQCD-like FFs, the behavior is smooth and similar for proton and neutron. In case of FFs from [33], the resonant behavior due to ρ, ω and ϕ poles appears in the figures.

It is also important to mention that a similar experimental setup allows to study a multipion production. In such case the quantity $s_1 = (p_1 + p_2 q)^2 m_\pi^2$ becomes positive and by varying of s_1 at xed beam energy, by changing q^2 and θ_π, it is in principle possible to identify and study other mechanisms, as the excitation of heavy pion resonances, π' , or the possible presence of a $N\bar{N}$ quasi-deuteron state under the kinematical threshold for $p\bar{p}$ annihilation in two leptons. The study of multipion production will be the subject of a forthcoming publication [62].

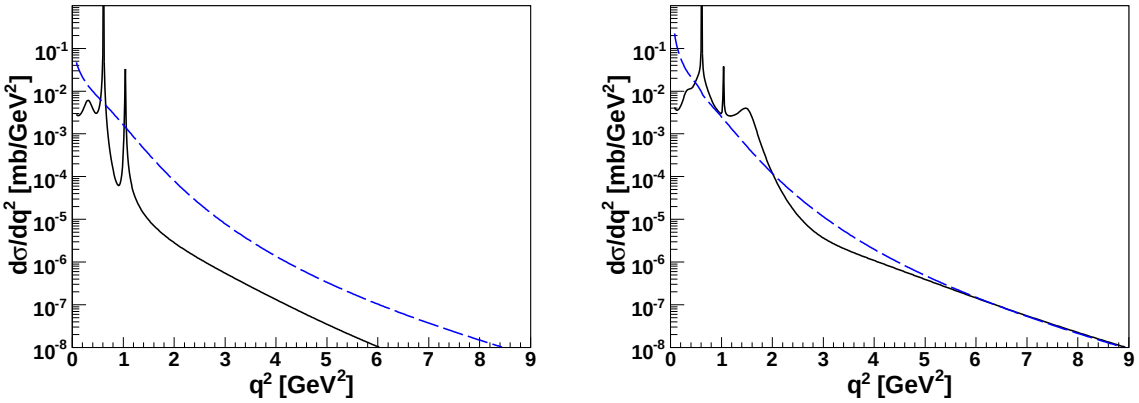

Fig. 11.9: *Left:* Differential cross section for the process $\bar{p} + p \to \pi^0 + \ell^+ + \ell^-$ as a function of q^2, with FFs from [33] for nucleon and (10.4) for axial FF (solid line) and with FFs from pQCD inspired nucleon FFs and dipole axial FFs (dashed line). *Right:* Same quantity as left, for the reaction $\bar{p} + n \to \pi^- + \ell^+ + \ell^-$.

12. POLARIZATION OBSERVABLES OF THE DEUTERON IN THE TIME-LIKE REGION

12.1 Motivation

The elastic electron-deuteron scattering has been investigated in many experiments and cross section data covers a large range of momentum transfers. However the measurement of the differential cross section of unpolarized elastic scattering allows to determine only the structure functions $A(t), B(t)$ and we don't have enough experimental information to extract all 3 deuteron form factors. Fortunately during last years, it has become possible to measure not only unpolarized cross section, but also polarization observables, due to the development of polarized electron beams, polarized deuteron targets and polarimeters. Recent polarization data for electron-deuteron elastic scattering, especially polarization observable t_{20}, allowed determination of deuteron charge quadrupole form factors up to a value of momentum transfered squared $t = -1.8\text{GeV}^2$.

The situation in the annihilation channel $e^-e^+ \to d\bar{d}$ is even more complicated. Even though the unpolarized cross section still has not been measured, it is already clear, that 2 real structure function extracted from Rosenbluth separation wouldn't be sufficient for extraction of 3 deuteron form factors, which are complex functions in time-like region (equivalent to 6 real functions). Therefore the measurement of polarization observables is even more essential in annihilation channel. In this Chapter we will derive [63] general expressions of polarization observables as functions of deuteron form factors for the case of longitudinally polarized electron beam and arbitrary polarized produced deuteron and we will give numerical estimation of these observables based on models of deuteron

form factors developed in previous Chapters.

12.2 Polarization Observables

In the one photon approximation the differential cross section of the annihilation reaction

$$e^-(k_1) + e^+(k_2) \to d(p_1) + \bar{d}(p_2) \tag{12.1}$$

can be written in terms of the leptonic $L_{\mu\nu}$ and the hadronic $W_{\mu\nu}$ tensors as

$$\frac{d\sigma}{d\Omega} = \frac{\alpha^2\beta}{4q^2}\frac{L_{\mu\nu}W_{\mu\nu}}{q^4}. \tag{12.2}$$

For the case of longitudinally polarized electron beam the leptonic tensor (3.46) is

$$L_{\mu\nu} = -q^2 g_{\mu\nu} + 2(k_{1\mu}k_{2\nu} + k_{1\nu}k_{2\mu}) + 2i\lambda_e \langle \mu\nu k_1 q\rangle \,, \tag{12.3}$$

where λ is the degree of the beam polarization and further we will assume a completely polarized beam with $\lambda = 1$.

The hadronic tensor can expressed in terms of deuteron electromagnetic current J_μ as

$$W_{\mu\nu} = J_\mu J^*_\nu, \tag{12.4}$$

where deuteron electromagnetic current describes transition $\gamma^* \to \bar{d}d$, which can be written similarly to (1.5) as [64]

$$\begin{aligned} J_\mu &= (p_1 - p_2)_\mu \left[-G_1(q^2) U_1^* \cdot U_2^* + \frac{G_3(q^2)}{M^2}(U_1^* \cdot q U_2^* \cdot q - \frac{q^2}{2} U_1^* \cdot U_2^*) \right] \\ &\quad + G_2(q^2)(U^*_{1\mu} U_2^* \cdot q - U^*_{2\mu} U_1^* \cdot q), \end{aligned} \tag{12.5}$$

where $U_{1\mu}, U_{2\mu}$ are the polarization four-vectors describing the spin 1 deuteron and antideuteron, and $G_i(q^2)$ $(i = 1, 2, 3)$ are the deuteron electromagnetic FFs. The FFs $G_i(q^2)$ are complex functions of the variable $q^2 = t$ in the region of the TL momentum transfer. They are related to standard deuteron FFs as

$$G_M = G_2,\ G_Q = G_1 - G_2 + 2G_3,\ \ G_C = \frac{2}{3}\tau(G_2 + G_3) + (1 - \frac{2}{3}\tau)G_1,\ \ \tau = \frac{q^2}{4M^2}\ . \tag{12.6}$$

In the case when polarization of the deuteron is measured and the polarization of the antideuteron is not measured, the spin-density matrices of the deuteron and antideuteron can be written as

$$\begin{aligned} U_{1\mu}U^*_{1\nu} &= -\left(g_{\mu\nu} - \frac{p_{1\mu}p_{1\nu}}{M^2}\right) + \frac{3i}{2M}\langle\mu\nu sp_1\rangle + 3Q_{\mu\nu} \\ U_{2\mu}U^*_{2\nu} &= -\left(g_{\mu\nu} - \frac{p_{2\mu}p_{2\nu}}{M^2}\right), \end{aligned} \tag{12.7}$$

where s_μ and $Q_{\mu\nu}$ are deuteron polarization four-vector and quadrupole-polarization tensor and they satisfy following conditions

$$s^2 = -1,\ sp_1 = 0,\ Q_{\mu\nu} = Q_{\nu\mu},\ \ Q_{\mu\mu} = 0,\ p_{1\mu}Q_{\mu\nu} = 0\ .$$

Taking into account Eqs. (12.4), (12.5) and (12.7), the hadronic tensor in the general case can be written as the sum of three terms

$$W_{\mu\nu} = W_{\mu\nu}(0) + W_{\mu\nu}(V) + W_{\mu\nu}(T), \tag{12.8}$$

where $W_{\mu\nu}(0)$ corresponds to the case of unpolarized deuteron and $W_{\mu\nu}(V)(W_{\mu\nu}(T))$ corresponds to the case of the vector (tensor) polarized deuteron. The explicit form of these terms is

- the unpolarized term $W_{\mu\nu}(0)$:

$$\begin{aligned} W_{\mu\nu}(0) &= W_1(q^2)\tilde{g}_{\mu\nu} + \frac{W_2(q^2)}{M^2}\tilde{p}_{1\mu}\tilde{p}_{1\nu} \\ \tilde{g}_{\mu\nu} &= g_{\mu\nu} - \frac{q_\mu q_\nu}{q^2}\ ,\ \ \tilde{p}_{1\mu} = p_{1\mu} - \frac{p_1 q}{q^2}q_\mu \\ W_1(q^2) &= 8M^2\tau(1-\tau)|G_M|^2, \\ W_2(q^2) &= 12M^2(|G_C|^2 - \frac{2}{3}\tau|G_M|^2 + \frac{8}{9}\tau^2|G_Q|^2). \end{aligned} \tag{12.9}$$

- the term for vector polarization $W_{\mu\nu}(V)$:

$$\begin{aligned} W_{\mu\nu}(V) &= \frac{i}{M}S_1(q^2)\langle\mu\nu sq\rangle + \frac{i}{M^3}S_2(q^2)[\tilde{p}_{1\mu}\langle\nu sqp_1\rangle - \tilde{p}_{1\nu}\langle\mu sqp_1\rangle] \\ &\quad + \frac{1}{M^3}S_3(q^2)[\tilde{p}_{1\mu}\langle\nu sqp_1\rangle + \tilde{p}_{1\nu}\langle\mu sqp_1\rangle] \\ S_1(q^2) &= -3M^2(\tau-1)|G_M|^2 \\ S_2(q^2) &= 3M^2[|G_M|^2 - 2\mathrm{Re}(G_C - \frac{\tau}{3}G_Q)G_M^*] \\ S_3(q^2) &= 6M^2\mathrm{Im}(G_C - \frac{\tau}{3}G_Q)G_M^*. \end{aligned} \tag{12.10}$$

- the term for tensor polarization $W_{\mu\nu}(T)$:

$$\begin{aligned} W_{\mu\nu}(T) &= V_1(q^2)\bar{Q}\tilde{g}_{\mu\nu} + V_2(q^2)\frac{\bar{Q}}{M^2}\tilde{p}_{1\mu}\tilde{p}_{1\nu} + V_3(q^2)(\tilde{p}_{1\mu}\widetilde{Q}_\nu + \tilde{p}_{1\nu}\widetilde{Q}_\mu) \\ &\quad + V_4(q^2)\widetilde{Q}_{\mu\nu} + iV_5(q^2)(\tilde{p}_{1\mu}\widetilde{Q}_\nu - \tilde{p}_{1\nu}\widetilde{Q}_\mu), \end{aligned} \tag{12.11}$$

where

$$\begin{aligned} \widetilde{Q}_\mu &= Q_{\mu\nu}q_\nu - \frac{q_\mu}{q^2}\bar{Q}\ , \quad \widetilde{Q}_\mu q_\mu = 0 \\ \widetilde{Q}_{\mu\nu} &= Q_{\mu\nu} + \frac{q_\mu q_\nu}{q^4}\bar{Q} - \frac{q_\nu q_\alpha}{q^2}Q_{\mu\alpha} - \frac{q_\mu q_\alpha}{q^2}Q_{\nu\alpha}\ ,\ \widetilde{Q}_{\mu\nu}q_\nu = 0,\ \bar{Q} = Q_{\alpha\beta}q_\alpha q_\beta. \end{aligned} \tag{12.12}$$

The tensor structure functions $V_i(q^2)$ are combinations of deuteron FFs as follows

$$\begin{aligned} V_1(q^2) &= -3|G_M|^2 \\ V_2(q^2) &= 3\left[|G_M|^2 + \frac{4}{1-\tau}]\mathrm{Re}(G_C - \frac{\tau}{3}G_Q - \tau G_M)G_Q^*\right] \\ V_3(q^2) &= -6\tau\left[|G_M|^2 + 2ReG_Q G_M^*\right] \\ V_4(q^2) &= -12M^2\tau(1-\tau)|G_M|^2 \\ V_5(q^2) &= -12\tau\mathrm{Im}(G_Q G_M^*). \end{aligned} \tag{12.13}$$

Using the definitions of the cross–section (12.2), leptonic (12.3) and hadronic (12.8) tensors, one can easily derive the expression for the unpolarized differential cross section in terms of the structure functions $W_{1,2}$ (after averaging over the spins of the initial particles)

$$\frac{d\sigma^{un}}{d\Omega} = \frac{\alpha^2\beta}{4q^4}\left\{-W_1(q^2) + \frac{1}{2}W_2(q^2)\left[\tau - 1 - \frac{(u-t)^2}{4M^2q^2}\right]\right\}\ , \tag{12.14}$$

where $t = (k_1 - p_1)^2$, $u = (k_1 - p_2)^2$.

In the reaction CMS this expression can be written as

$$\frac{d\sigma^{un}}{d\Omega} = \frac{\alpha^2\beta^3}{4q^2}D,\ D = \tau(1+\cos^2\theta)|G_M|^2 + \frac{3}{2}\sin^2\theta\left(|G_C|^2 + \frac{8}{9}\tau^2|G_Q|^2\right), \tag{12.15}$$

where θ is the angle between the momenta of the outgoing deuteron ($\vec{p}_1$) and the incoming electron beam ($\vec{k}_1$). Integrating the expression (eq:eq16) with respect to the

deuteron angular variables one obtains the following formula for the total cross section of the reaction (8.3)

$$\sigma_{tot}(e^+e^- \to \bar{d}d) = \frac{\pi\alpha^2\beta^3}{3q^2}\left[3|G_C|^2 + 4\tau(|G_M|^2 + \frac{2}{3}\tau|G_Q|^2)\right]. \tag{12.16}$$

One can define also an angular asymmetry, R, with respect to the differential cross section measured at $\theta = \pi/2, \sigma_0$

$$\frac{d\sigma^{un}}{d\Omega} = \sigma_0(1 + R\cos^2\theta), \tag{12.17}$$

where R can be expressed as a function of the deuteron FFs

$$R = \frac{2\tau(|G_M|^2 - \frac{4}{3}\tau|G_Q|^2) - 3|G_C|^2}{2\tau(|G_M|^2 + \frac{4}{3}\tau|G_Q|^2) + 3|G_C|^2}. \tag{12.18}$$

This observable should be sensitive to the different underlying assumptions on deuteron FFs. Therefore, a precise measurement of this quantity, which does not require polarized particles, would be very interesting.

One can see that, as in the space-like (SL) region, the measurement of the angular distribution of the outgoing deuteron determines the modulus of the magnetic form factor, but the separation of the charge and quadrupole form factors requires the measurement of polarization observables [65]. The outgoing–deuteron polarization can be measured in a secondary analyzing scattering.

The cross section can be written, in the general case, as the sum of unpolarized and polarized terms, corresponding to the different polarization states and polarization directions of the incident and scattered particles:

$$\frac{d\sigma}{d\Omega} = \frac{d\sigma^{un}}{d\Omega}\left[1 + P_y + \lambda P_x + \lambda P_z + P_{zz}R_{zz} + P_{xz}R_{xz} + P_{xx}(R_{xx} - R_{yy}) + \lambda P_{yz}R_{yz}\right], \tag{12.19}$$

where P_i (P_{ij}), $i, j = x, y, z$ are the components of the polarization vector (tensor) of the outgoing deuteron, R_{ij}, $i, j = x, y, z$ the components of the quadrupole polarization tensor of the outgoing deuteron $Q_{\mu\nu}$, in its rest system and $\frac{d\sigma^{un}}{d\Omega}$ is the differential cross section for the unpolarized case.

The degree of longitudinal polarization of the electron beam λ is explicitly indicated in order to stress the origin of the specific polarization observables.

Let us consider the different polarization observables and give their expression in terms of the deuteron FFs.

(i) The vector polarization of the outgoing deuteron, P_y, which does not require polarization in the initial state is

$$P_y = -\frac{3}{2D}\sqrt{\tau}\sin(2\theta)\mathrm{Im}\left[\left(G_C - \frac{\tau}{3}G_Q\right)G_M^*\right]. \tag{12.20}$$

(ii) The part of the differential cross section that depends on the tensor polarization can be written as follows

$$\begin{aligned}
\frac{d\sigma_T}{d\Omega} &= \frac{d\sigma_{zz}}{d\Omega}R_{zz} + \frac{d\sigma_{xz}}{d\Omega}R_{xz} + \frac{d\sigma_{xx}}{d\Omega}(R_{xx} - R_{yy}), &(12.21)\\
\frac{d\sigma_{zz}}{d\Omega} &= \frac{\alpha^2\beta^3}{4q^2}\frac{3\tau}{4}\Big[(1+\cos^2\theta)|G_M|^2 \\
&\quad +8\sin^2\theta\left(\frac{\tau}{3}|G_Q|^2 - \mathrm{Re}(G_C G_Q^*)\right)\Big], &(12.22)\\
\frac{d\sigma_{xz}}{d\Omega} &= -\frac{\alpha^2\beta^3}{4q^2}3\tau^{3/2}\sin(2\theta)\mathrm{Re}(G_Q G_M^*), &(12.23)\\
\frac{d\sigma_{xx}}{d\Omega} &= -\frac{\alpha^2\beta^3}{4q^2}\frac{3\tau}{4}\sin^2\theta|G_M|^2, &(12.24)
\end{aligned}$$

(iii) Let us consider now the case of a longitudinally polarized electron beam. The other two components of the deuteron vector polarization (P_x, P_z) require the initial particle polarization and are

$$\begin{aligned}
P_x &= -3\frac{\sqrt{\tau}}{D}\sin\theta\mathrm{Re}\left(G_C - \frac{\tau}{3}G_Q\right)G_M^* &(12.25)\\
P_z &= \frac{3\tau}{2D}\cos\theta|G_M|^2. &(12.26)
\end{aligned}$$

From angular momentum and helicity conservations it follows that the sign of the deuteron polarization component P_z in the forward direction ($\theta = 0$) must coincide with the sign of the electron beam polarization. This requirement is satisfied by Eq. (12.26).

A possible nonzero phase difference between the deuteron FFs leads to another T–odd polarization observable proportional to the R_{yz} component of the tensor polarization of the deuteron. The part of the differential cross section that depends on the correlation

between the longitudinal polarization of the electron beam and the deuteron tensor polarization can be written as follows

$$\frac{d\sigma_{\lambda T}}{d\Omega} = \frac{\alpha^2\beta^3}{4q^2} 6\tau^{3/2} \sin\theta \mathrm{Im}(G_M G_Q^*) R_{yz}. \tag{12.27}$$

The deuteron FFs in the TL region are complex functions. In the case of unpolarized initial and final particles, the differential cross section depends only on the squared modulus $|G_M|^2$ and on the combination $G = |G_C|^2 + \frac{8}{9}\tau^2|G_Q|^2$. So, the measurement of the angular distribution allows one to determine $|G_M|$ and the quantity G, as in the elastic electron–deuteron scattering.

Let us discuss which information can be obtained by measuring the polarization observables derived above. Three relative phases exist for three FFs, which we note as follows: $\alpha_1 = \alpha_M - \alpha_Q$, $\alpha_2 = \alpha_M - \alpha_C$, and $\alpha_3 = \alpha_Q - \alpha_C$, where $\alpha_M = \arg G_M$, $\alpha_C = \arg G_C$, and $\alpha_Q = \arg G_Q$. These phases are important characteristics of FFs in the TL region since they result from the strong interaction between final particles.

Let us consider the ratio of the polarizations P_{yz} (let us remind that it requires a longitudinally polarized electron beam) and P_{xz} (when the electron beam is unpolarized). One finds

$$R_1 = \frac{P_{xz}}{P_{yz}} = -\cos\theta \cot\alpha_1. \tag{12.28}$$

So, the measurement of this ratio gives us information about the relative phase α_1. The measurement of another ratio of polarizations, $R_2 = P_{xz}/P_{xx}$ gives us information about the quantity $|G_Q|$

$$R_2 = \frac{P_{xz}}{P_{xx}} = 8\sqrt{\tau}\cot\theta\cos\alpha_1 \frac{|G_Q|}{|G_M|}. \tag{12.29}$$

This allows one to obtain the modulus of the charge FF, $|G_C|$, from the quantity G, known from the measurement of the differential cross section. The measurement of a third ratio

$$R_3 = \frac{P_y}{P_x} = -\cos\theta \frac{\sin\alpha_2 - r\sin\alpha_1}{\cos\alpha_2 - r\cos\alpha_1}, \quad r = \frac{\tau}{3}\frac{|G_Q|}{|G_C|} \tag{12.30}$$

allows to determine the phase difference α_2. And at last, if we measure the ratio of the polarizations P_{zz} and P_{xx}

$$R_4 = \frac{P_{zz}}{P_{xx}} = -\frac{1}{\sin^2\theta}\left[1 + \cos^2\theta + 8\sin^2\theta \frac{|G_C||G_Q|}{|G_M|^2}(r - \cos\alpha_3)\right] \tag{12.31}$$

we can obtain information about the third phase difference α_3. Moreover, one can verify the relation

$$\alpha_3 = \alpha_2 - \alpha_1.$$

Thus, the measurement of these polarization observables allows to fully determine the deuteron FFs in TL region.

Note that using the ratio of two polarization components that are simultaneously measured, greatly reduces systematic uncertainties. It is not necessary to know neither the beam polarization or the polarimeter analyzing power, since both of these quantities cancel in the ratio.

12.3 Numerical estimations

In the previous section, the expressions for cross section and polarization observables have been given, in terms of the deuteron FFs. Numerical estimations require the knowledge of such FFs, in TL region. Due to the hermiticity of the electromagnetic current, FFs are real in the SL region, and complex in the TL region. Two phenomenological models of the deuteron structure presented in Chapters 8 and 9 belong to the few existing models of the deuteron structure with complex FFs in TL extension. Therefore they will be used for the following numerical estimations.

The q^2 dependence of moduli of these models is illustrated in Fig. 12.1. One can see that two models coincide in the SL region, where they are constrained by the experimental data (shaded area), but outside this kinematical region, they show different behavior. Two poles coincide in TL region, as they correspond to the ω and ϕ contributions. More resonances are built, by construction, in the U&A model and occur in the unphysical region. These two models show a similar trend, near the threshold, for the moduli of FFs, however the sign, which is reflected in the relevant polarization observables, may differ. Threshold, which corresponds to $q^2 \simeq 14\text{GeV}^2$, is indicated by a vertical line.

The predictions for the different observables are shown in Fig. 12.2, for E=1.9 GeV, not far above threshold. Two parametrizations, as expected, give different results, especially concerning the predictions for the observables P_y and P_{yz}, which vanish for two component parametrization due to technique of obtaining complex parts of FFs in

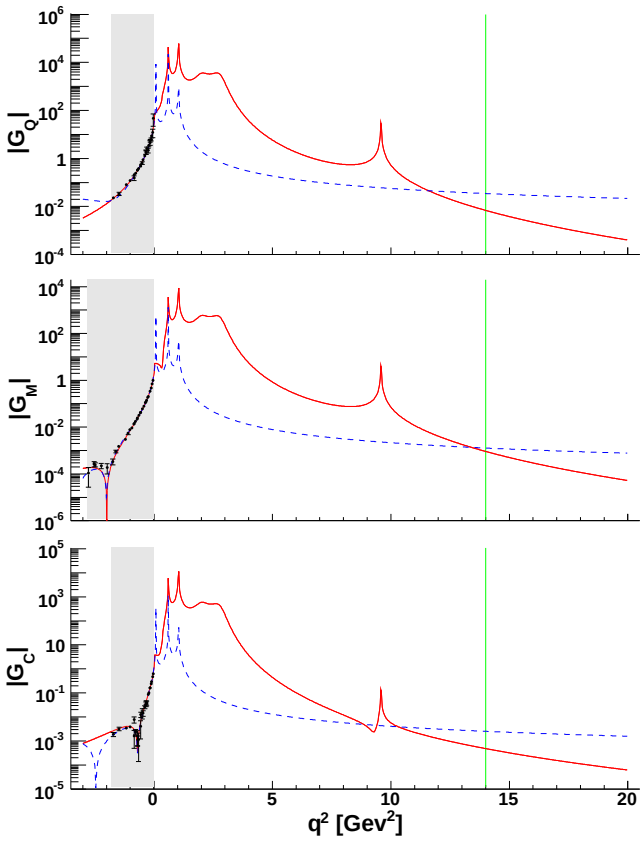

Fig. 12.1: q^2-dependence of the G_Q, G_M, G_C from top to bottom (moduli): U&A model of the deuteron from Chapter 9 (solid line), two component model of the deuteron from Chapter 8 (dashed line).

this model. In spite of this, the angular distributions are very similar, as it appears from Fig. 12.2b, as it is driven by the underlying assumption of the one-photon exchange mechanism.

It should be noted that the CMS threshold energy of the reaction $e^-e^+ \to d\bar{d}$ is quite large, $E_T = 2M \simeq 3.75$ GeV, which corresponds to $q^2 \simeq 14$ GeV^2. There are no data in this momentum range in SL region, which could better constrain models and parametrizations. Although the cross section of this process is expected to be very small, the search for the corresponding events it is not excluded in future at high luminosity e^+e^- rings.

The formalism developed here is model independent and based on symmetry prop-

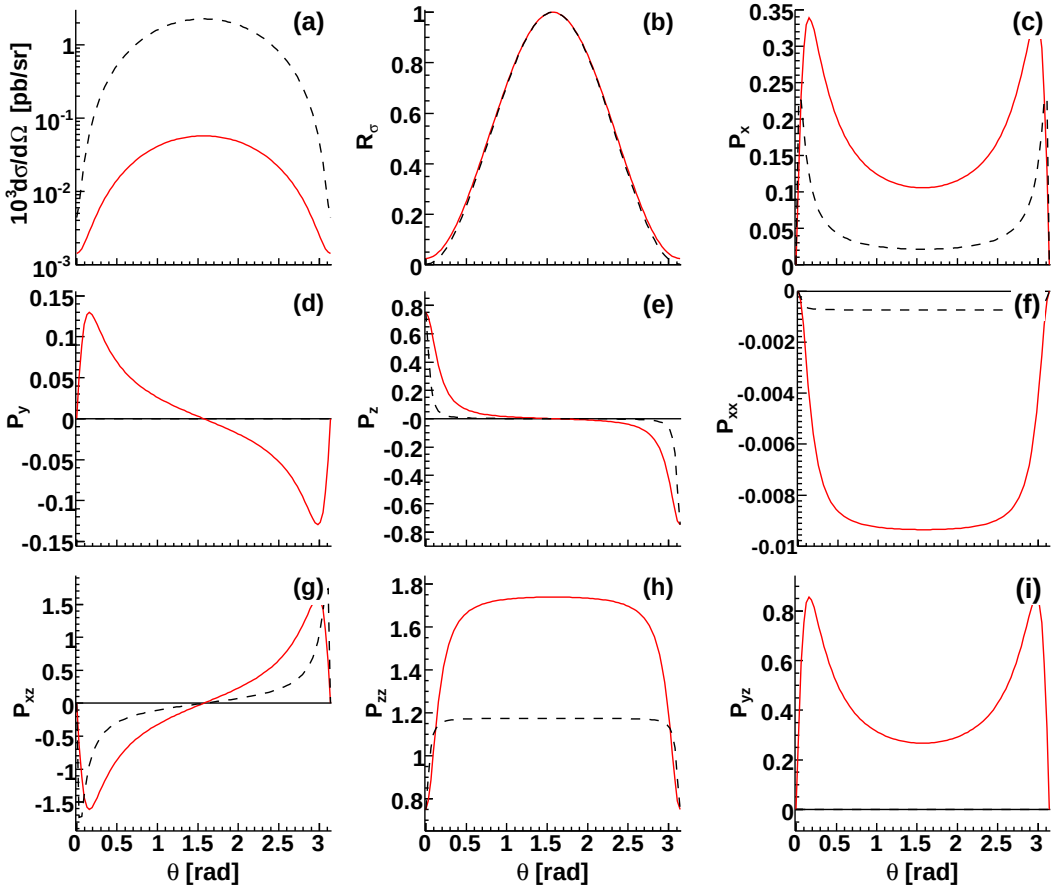

Fig. 12.2: Predictions of the different observables, for the considered parametrizations of deuteron FFs, extrapolated to the TL region. Notations same as in Fig. 12.1.

erties of electromagnetic and strong interactions. It allows to establish properties of observables that should be satisfied by any model calculation. Moreover, it applies as well to the annihilation reactions involving the production of other spin one particles in the final state, such as $e^+ + e^- \to \rho^+ + \rho^-$ [66].

CONCLUSIONS

In the presented Dissertation Thesis applications of the universal approach of a description of the electromagnetic structure of hadrons to a solution of specific problems concerning nucleons and deuteron were demonstrated.

The first three Chapters are serving as an introduction, where general concepts of electromagnetic, weak and strange form factors are reviewed, polarization observables are introduced and the four-component polarization formalism is elaborated in detail.

The first original contribution is contained in the Chapter devoted to VMD model, where the old problem of VMD model with the asymptotics is solved generally and expressions for normalized form factors and the required asymptotics for arbitrary finite number of vector mesons are presented.

The Unitary and Analytic model, which reflects all known form factors properties, is in universal form given in the next Chapter. Its application to the Rosenbluth and Jefferson Lab proton polarization data has led to two contradicting behaviors of the proton electric form factors in the space-like region, what is well known as the JLab proton polarization data puzzle. In order to prefer one of them to be more reliable, they are brought into a comparison with other independent data on deuteron structure functions by means of the non-relativistic impulse approximation of deuteron EM structure. From the values of χ^2 it has been unambiguously demonstrated that the $G_E^p(t)$ from the JLab proton polarization data analysis with the zero around $t = -13\ GeV^2$ are more consistent with the deuteron structure functions $A(t), B(t)$ data than the older Rosenbluth behavior.

In the eighth Chapter a simple parametrization of the three deuteron electromagnetic FFs, with a minimal number of parameters, based on a transparent physical picture was suggested. It can be used in the comparison of different theoretical models with experi-

ments involving deuteron, and for a precise analytical interpolation of the experimental points in the region $Q^2 < 2$ GeV^2.

An application of the Unitary and Analytic model to a description of the deuteron electromagnetic structure is made in the ninth Chapter. Due to its unitary and analytic properties and possibility of a transparent extension to the time-like region we obtained not only fit of the experimental data on the deuteron structure function an polarization observables in the space-like region, but also the prediction of the differential cross section of the annihilation process $e^-e^+ \to d\bar{d}$, which is going to be measured in the near future.

In the tenth Chapter a simple model of the nucleon axial form factor has been developed. The aim of this model is to provide a reasonable estimation of the nucleon axial form factor in the time-like region for the measurement proposal described in the next Chapter, where we studied nucleon antinucleon annihilation processes with the pion, nucleon and lepton-antilepton pair in the final state. The latter allows measurement of the nucleon electromagnetic form factors in the unphysical region and measurement of the nucleon axial form factor in the time-like region. We also provided an estimation of the differential cross section of such processes based on existing models of nucleon electromagnetic and axial form factors.

In the last Chapter polarization effects in the electron-positron annihilation into the deuteron-antideuteron pair for the case of longitudinally polarized electron beam and arbitrary polarization of the produced deuteron, with the aim on a determination of the time-like complex deuteron electromagnetic form factors has been investigated for the first time. We derived general expressions for polarization observables as a functions of deuteron form factors and we made their numerical estimations by means of various models of deuteron electromagnetic form factors, for kinematical conditions near threshold.

The obtained original results are published in 10 papers given in the bibliography and they were also presented at various international conferences and seminars in some well known centers abroad.

BIBLIOGRAPHY

[1] R. Hofstadter, F. Burniller and M. R. Yearan, *Rev. Mod. Phys.* **, 30** (1958) 482.

[2] G. P. Lepage and S. J. Brodsky, *Phys. Lett.* **B87** (1979) 359.

[3] A. V. Efremov and A. V. Radyushkin, *Phys. Lett.* **B94** (1980) 245.

[4] J. J. Sakurai, *Annals Phys.* **11** (1960) 1.

[5] M. Gell-Mann and F. Zachariasen, *Phys. Rev.* **124** (1961) 953.

[6] D. Abbott et al., *Eur. Phys. J.* **A7** (2000) 421.

[7] G. G. Ohlsen, *Rep. Prog. Phys.* **, 35** (1972) 717.

[8] C. Adamuscin, A. Z. Dubnickova, S. Dubnicka, R. Pekarik and P. Weisenpacher, *Eur. Phys. J.* **C28** (2003) 115.

[9] S. Dubnicka, A. Z. Dubnickova and P. Weisenpacher, *Eur. Phys. J.* **C32** (2003) 381.

[10] S. S. Schweber, *An introduction to relativistic quantum theory*, Harper and Row, New York, 1961.

[11] V. A. Matveev, R. M. Muradian and A. N. Tavkhelidze, *Nuovo Cim. Lett.* **7** (1973) 719.

[12] S. J. Brodsky and G. R. Farrar, *Phys. Rev. Lett.* **31** (1973) 1153.

[13] S. Dubnicka, A. Z. Dubnickova and P. Weisenpacher, *J. Phys.* **G29** (2003) 405.

[14] M. K. Jones et al., *Phys. Rev. Lett.* **84** (2000) 1398.

[15] O. Gayou et al., *Phys. Rev. Lett.* **88** (2002) 092301.

[16] V. Punjabi et al., *Phys. Rev.* **C71** (2005) 055202.

[17] A. I. Akhiezer and M. P. Rekalo, *Sov. J. Part. Nucl.* **4** (1974) 277.

[18] A. Afanasev, I. Akushevich and N. Merenkov, *Phys. Rev.* **D64** (2001) 113009.

[19] P. A. M. Guichon and M. Vanderhaeghen, *Phys. Rev. Lett.* **91** (2003) 142303.

[20] P. G. Blunden, W. Melnitchouk and J. A. Tjon, *Phys. Rev. Lett.* **91** (2003) 142304.

[21] S. Dubnicka, E. A. Kuraev, M. Secansky and A. Vinnikov, Polarization transfer measurements of proton form factors: Deformation by initial collinear photons, hep-ph/0507242, 2005.

[22] A. V. Afanasev, S. J. Brodsky, C. E. Carlson, Y.-C. Chen and M. Vanderhaeghen, *Phys. Rev.* **D72** (2005) 013008.

[23] E. Tomasi-Gustafsson and G. I. Gakh, *Phys. Rev.* **C72** (2005) 015209.

[24] Y. M. Bystritskiy, E. A. Kuraev and E. Tomasi-Gustafsson, *Phys. Rev.* **C75** (2007) 015207.

[25] C. Adamuscin, S. Dubnicka, A. Z. Dubnickova and P. Weisenpacher, *Prog. Part. Nucl. Phys.* **55** (2005) 228.

[26] A. Z. Dubnickova and S. Dubnicka, *ICTP Trieste* **IC-91-149** (1991) .

[27] A. P. Kobushkin and A. I. Syamtomov, *Phys. Atom. Nucl.* **58** (1995) 1477.

[28] E. Tomasi-Gustafsson, G. I. Gakh and C. Adamuscin, *Phys. Rev.* **C73** (2006) 045204.

[29] R. A. Gilman and F. Gross, *J. Phys.* **G28** (2002) R37.

[30] C. Adamuscin, L. Bimbot, S. Dubnicka, A. Z. Dubnickova and E. Tomasi-Gustafsson, Phenomenological insight into JLab proton polarization data puzzle by deuteron impulse approximation, hep-ph/0703066, 2007.

[31] N. Cabibbo and R. Gatto, *Phys. Rev.* **124** (1961) 1577.

[32] M. Lacombe et al., *Phys. Rev.* **C21** (1980) 861.

[33] F. Iachello, A. D. Jackson and A. Lande, *Phys. Lett.* **B43** (1973) 191.

[34] D. M. Nikolenko et al., *Phys. Rev. Lett.* **90** (2003) 072501.

[35] R. Barlow, Asymmetric errors, physics/0401042, 2004.

[36] S. J. Brodsky and J. R. Hiller, *Phys. Rev.* **D46** (1992) 2141.

[37] S. J. Brodsky, C.-R. Ji and G. P. Lepage, *Phys. Rev. Lett.* **51** (1983) 83.

[38] C. E. Carlson and F. Gross, *Phys. Rev.* **D36** (1987) 2060.

[39] C. Adamuscin, S. Dubnicka and A. Z. Dubnickova, Unitary and Analytic Model of the Deuteron Electromagnetic Structure, to be published.

[40] D. O. R. Eden, P. Landshoff and J. Polkinghorn, *The analytic S-matrix*, Cambridge Univ. Press, 1966.

[41] S. Dubnicka and O. Dumbrajs, *Phys. Rept.* **19** (1975) 141.

[42] http://root.cern.ch/.

[43] C. Adamuscin, E. Tomasi-Gustafsson, E. Santopinto, R. Bijker and F. Iachello, Two component model for the axial form factor of the nucleon, to be published.

[44] V. Bernard, L. Elouadrhiri and U. G. Meissner, *J. Phys.* **G28** (2002) R1.

[45] Y. Nambu and M. Yoshimura, *Phys. Rev. Lett.* **24** (1970) 25.

[46] G. Benfatto, F. Nicolo and G. C. Rossi, *Nuovo Cim.* **A14** (1973) 425.

[47] G. Furlan, N. Paver and C. Verzegnassi, *Nuovo Cim.* **A70** (1970) 247.

[48] N. Dombey and B. J. Read, *Nucl. Phys.* **B60** (1973) 65.

[49] P. Joos et al., *Phys. Lett.* **B62** (1976) 230.

[50] E. D. Bloom et al., *Phys. Rev. Lett.* **30** (1973) 1186.

[51] C. Adamuscin, E. A. Kuraev, E. Tomasi-Gustafsson and F. E. Maas, *Submitted to Phys. Rev. C* .

[52] M. P. Rekalo, *Sov. J. Nucl. Phys.* **1** (1965) 760.

[53] A. Z. Dubnickova, S. Dubnicka and M. P. Rekalo, *Z. Phys.* **C70** (1996) 473.

[54] H. H. Gutbrod, K. D. Gross, W. F. Henning and V. Metag, *Conceptual design report* Darmstadt GSI - (01/11,rec.Dec.) 708 p.

[55] H. W. L. Naus and J. H. Koch, *Phys. Rev.* **C36** (1987) 2459.

[56] T. Fuchs and S. Scherer, *Phys. Rev.* **C68** (2003) 055501.

[57] F. Iachello and Q. Wan, *Phys. Rev.* **C69** (2004) 055204.

[58] E. Tomasi-Gustafsson, F. Lacroix, C. Duterte and G. I. Gakh, *Eur. Phys. J.* **A24** (2005) 419.

[59] B. Aubert et al., *Phys. Rev.* **D73** (2006) 012005.

[60] E. Tomasi-Gustafsson and M. P. Rekalo, *Phys. Lett.* **B504** (2001) 291.

[61] C. Bruch, A. Khodjamirian and J. H. Kuhn, *Eur. Phys. J.* **C39** (2005) 41.

[62] E. A. Kuraev, C. Adamuscin, E. Tomasi-Gustafsson and F. Maas, Study of resonant processes for multi-pion production in $p\bar{p} \to \ell^+\ell^- n(\pi)$ π-annihilation, DAPNIA-06-450.

[63] G. I. Gakh, E. Tomasi-Gustafsson, C. Adamuscin, S. Dubnicka and A. Z. Dubnickova, *Phys. Rev.* **C74** (2006) 025202.

[64] M. P. R. A. I. Akhiezer, *Electrodynamics of Hadrons*, Naukova Dumka, Kiev, 1977.

[65] R. G. Arnold, C. E. Carlson and F. Gross, *Phys. Rev.* **C21** (1980) 1426.

[66] C. Adamuscin, G. I. Gakh and E. Tomasi-Gustafsson, Polarization effects in the reaction $e^+e^- \to \rho^+\rho^-$ and determination of the ρ-meson form factors in the time-like region, DAPNIA-06-469.